Semi-Inclusive Deep Inelastic Scattering in Wandzura-Wilczek-type approximation

S. Bastami^a **H. Avakian**^{c} **A. V. Efremov**^{d} **A. Kotzinian**^{e} **B. U. Musch**^{f} **B. Parsamyan**^{e} **A. Prokudin**^{b,c} **M. Schlegel**^{g} **P. Schweitzer**^{a,g} **W. Vogelsang**^{g}

^{a}*Department of Physics, University of Connecticut, Storrs, CT 06269, U.S.A.*

^{b}*Division of Science, Penn State Berks, Reading, PA 19610, USA*

^{c}*Thomas Jefferson National Accelerator Facility, Newport News, VA 23606, U.S.A.*

^{d}*Joint Institute for Nuclear Research, Dubna, 141980 Russia*

^{e}*Dipartimento di fisica teorica, Università degli studi di Torino, and Sezione dell'INFN di Torino, Via Pietro Giuria 1, 10125 Torino, Italy*

^{f}*Institut für Theoretische Physik, Universität Regensburg, 93040 Regensburg, Germany*

^{g}*Institute for Theoretical Physics, Universität Tübingen, D-72076 Tübingen, Germany*

  E-mail: `saman.bastami@uconn.edu`, `avakian@jlab.org`,
  `efremov@theor.jinr.ru`, `aram.kotzinian@cern.ch`, `bmusch@b-mu.de`,
  `bakur@cern.ch`, `prokudin@jlab.org`, `marc.schlegel@uni-tuebingen.de`,
  `peter.schweitzer@phys.uconn.edu`, `werner.vogelsang@uni-tuebingen.de`

ABSTRACT: We present the complete cross-section for pion production in Semi-Inclusive Deep Inelastic Scattering (SIDIS) in the Wandzura-Wilczek-type approximation up to power-suppressed $\mathcal{O}(1/Q^2)$ terms. We compute all twist-2 and twist-3 SIDIS structure functions and the corresponding asymmetries. We discuss the applicability of the Wandzura-Wilczek-type approximations on the basis of available data, and make predictions which can be tested by data from Jefferson Lab, COMPASS, HERMES, and the future EIC. The results of this paper can be readily used for phenomenology and for event generators for SIDIS, and will help to improve our understanding of the TMD theory beyond leading twist.

KEYWORDS: Wandzura-Wilczek approximation, semi-inclusive deep inelastic scattering, transverse momentum dependent distribution functions, spin and azimuthal asymmetries, leading and subleading twist

Contents

1 Introduction

A great deal of what is known about the quark-gluon structure of nucleon is due to studies of parton distribution functions (PDFs) in deeply inelastic reactions. Leading-twist PDFs tell us how likely it is to find an unpolarized parton (described by PDF $f_1^a(x)$, $a = q, \bar{q}, g$) or a longitudinally polarized parton (described by PDF $g_1^a(x)$, $a = q, \bar{q}, g$) in a fast-moving unpolarized or longitudinally polarized nucleon, which carries the fraction x of the nucleon momentum. This information depends on the "resolution (renormalization) scale" associated with the hard scale Q of the process. Although the PDFs $f_1^a(x)$ and $g_1^a(x)$ continue being the subject of intense research (small-x, large-x, helicity sea and gluon distributions) they can be considered as rather well-known, and the frontier has been extended in the last years to go beyond the one-dimensional picture offered by PDFs.

One way to do this consists in a systematic inclusion of transverse parton momenta $k_\perp$ whose effects manifest themselves in terms of transverse momenta of the reaction products in the final state. If these transverse momenta are much smaller than the hard scale Q of the process, the formal description is given in terms of transverse momentum dependent distribution functions (TMDs) and fragmentation functions (FFs) which are defined in terms of quark-quark correlators [1–4], and depend on two independent variables: the fraction x of nucleon momentum carried by parton, and intrinsic transverse momentum $k_\perp$ of the parton. Being a vector in the plane transverse with respect to the light-cone direction singled out by the hard momentum flow in the process, $k_\perp$ allows us to access novel information on the nucleon spin structure through correlations of $k_\perp$ with nucleon and/or parton spin. The latter is a well-defined concept for twist-2 TMDs interpreted in the infinite momentum frame or in lightcone quantization formalism.

One powerful tool to study TMDs are measurements of the SIDIS process. By exploring various possibilities for electron/muon beam and target polarizations unambiguous information can be accessed on the 8 leading-twist TMDs [2] and, if one assumes factorization, on certain linear combinations of the 16 subleading-twist TMDs [3, 4]. Complementary information can be obtained from the Drell-Yan process [5], and e^+e^- annihilation [6].

In QCD the TMDs are independent functions. Each TMD contains unique information on a different aspect of the nucleon structure. Twist-2 TMDs have partonic interpretations. Twist-3 TMDs give insights on quark-gluon correlations in the nucleon [7–9]. Besides positivity constraints [10] there is little model-independent information on TMDs. An important question with practical applications is: do useful *approximations* for TMDs exist? Experience from collinear PDFs encourages to explore this possibility: the twist-3 $g_T^a(x)$ and $h_L^a(x)$ can be expressed in terms of contributions from twist-2 $g_1^a(x)$ and $h_1^a(x)$, and additional quark-gluon-quark ($\bar{q}gq$) correlations or current quark mass terms [11, 12]. We shall refer to the latter generically as $\bar{q}gq$-terms, keeping in mind one deals in each case with matrix elements of different operators. The $\bar{q}gq$-correlations contain new insights on hadron structure which are worthwhile exploring for their own sake, see [13] on $g_T^a(x)$.

The striking observation is that the $\bar{q}gq$-terms in $g_T^a(x)$ and $h_L^a(x)$ are small: theoretical mechanisms predict this [14–17], and in the case of $g_T^a(x)$ data confirm or are compatible with these predictions [18, 19]. This approximation ("neglect of $\bar{q}gq$-terms") is commonly known as Wandzura-Wilczek (WW) approximation [11]. The possibility to apply this type of approximation also to TMDs has been explored in specific cases in [20–25]. In both cases, PDFs and TMDs, one basically assumes that the contributions from $\bar{q}gq$-terms can be neglected with respect to $\bar{q}q$-terms. But the nature of the omitted matrix elements is different, and in the context of TMDs one often prefers to speak about WW-type approximations.

In this work, after introducing the SIDIS process and defining TMDs and FFs (Sec. 2), we shall introduce the approximations, and review what is presently known about their reliability from experiment and theory (Sec. 3). We will show that under the assumption of the validity of these approximations it is possible to describe all leading and subleading SIDIS structure functions in terms of a basis of 6 TMDs and 2 FFs, and review what is presently known about these functions (Sec. 4). Using the latest available extractions of the 8 basis functions we will systematically apply the WW and/or WW-type approximations to SIDIS structure at leading (Sec. 6) and subleading (Sec. 7) twist. We will conclude with a critical discussion (Sec. 8).

This is the first study of all SIDIS structure functions up to twist-3 in a unique approach. Our results are of use for experiments prepared in the near-term (Jefferson Lab 12) or proposed in the long-term (Electron Ion Collider), and provide helpful input for Montecarlo event generators [26]. Our predictions will either be confirmed within the expected accuracy, implying the approximations work and calling for dedicated theoretical explanations why. Or they will fail in certain cases, calling for theoretical work to explain why in some cases $\bar{q}gq$-terms are sizable. In any case, our results will deepen our understanding.

2 The SIDIS process in terms of TMDs and FFs

In this section we review the description of the SIDIS process, define structure functions, PDFs, TMDs, FFs and recall how they describe the SIDIS structure functions.

2.1 The SIDIS process

The SIDIS process is sketched in Fig. 1. Here l and P are momenta of incoming lepton and nucleon, and l' and P_h are the momenta of the outgoing electron and produced hadron. The virtual photon momentum $q = l - l'$ selects a z-axis, and l' points in the direction of the x-axis from which azimuthal angles are counted. The relevant kinematic invariants are
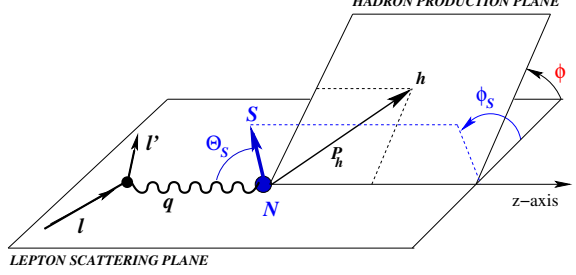
Figure 1. Kinematics of SIDIS process $lN \to l'hX$.

$$x = \frac{Q^2}{2\,P\cdot q}, \ \ y = \frac{P\cdot q}{P\cdot l}, \ \ z = \frac{P\cdot P_h}{P\cdot q}, \ \ Q^2 = -q^2. \tag{2.1}$$

In addition to x, y, z the cross section is also differential in the azimuthal angle ϕ_h of the produced hadron, the square of its momentum component P_{hT} perpendicular with respect to the virtual photon momentum, and the azimuthal angle ψ_l characterizing the overall orientation of the lepton scattering plane in the lab frame. Notice that $d\psi_l \simeq d\phi_S$ where ϕ_S is the azimuthal angle of the nucleon spin vector. It is convenient to define the unpolarized lepton – quark scattering cross section

$$\sigma_0 \equiv \frac{d\sigma}{dy} = \frac{4\pi\alpha_{em}^2}{x\,y\,Q^2}\left(1 - y + \frac{1}{2}y^2\right) \tag{2.2}$$

To leading order in $1/Q$ the SIDIS cross-section is given by

$$\frac{d^6\sigma_{\text{leading}}}{dx\,dy\,dz\,d\phi_S\,d\phi_h\,dP_{hT}^2} = \frac{\sigma_0}{4\pi}\,F_{UU}(x,z,P_{hT}^2)\Bigg\{ 1 + \cos(2\phi_h)\,p_1\,A_{UU}^{\cos(2\phi_h)}$$

$$+ S_L \sin(2\phi_h)\,p_1\,A_{UL}^{\sin(2\phi_h)} + \lambda\,S_L\,p_2\,A_{LL}$$

$$+ \lambda\,S_T \cos(\phi_h - \phi_S)\,p_2\,A_{LT}^{\cos(\phi_h - \phi_S)} + S_T \sin(\phi_h - \phi_S)\,A_{UT}^{\sin(\phi_h - \phi_S)}$$

$$+ S_T \sin(\phi_h + \phi_S)\,p_1\,A_{UT}^{\sin(\phi_h + \phi_S)} + S_T \sin(3\phi_h - \phi_S)\,p_1\,A_{UT}^{\sin(3\phi_h - \phi_S)} \Bigg\} \tag{2.3a}$$

where F_{UU} is the structure function due to transverse polarization of the virtual photon (sometimes denoted as $F_{UU,T}$), and we systematically neglect $1/Q^2$ corrections in kinematic factors and a structure function arising from longitudinal polarization of the virtual photon (sometimes denoted as $F_{UU,L}$). The structure functions (and asymmetries A) also depend on Q^2 via the scale dependence of TMDs and FFs, which we do not show in formulas throughout this work.

At subleading order one has

$$\frac{d^6\sigma_{\text{subleading}}}{dx\,dy\,dz\,d\phi_S\,d\phi_h\,dP_{hT}^2} = \frac{\sigma_0}{4\pi}\,F_{UU}(x,z,P_{hT}^2)\Bigg\{\cos(\phi_h)\,p_3\,A_{UU}^{\cos(\phi_h)}$$

$$+\lambda\sin(\phi_h)\,p_4\,A_{LU}^{\sin(\phi_h)} + S_L\sin(\phi_h)\,p_3\,A_{UL}^{\sin(\phi_h)} + S_T\sin(\phi_S)\,p_3\,A_{UT}^{\sin(\phi_S)}$$

$$+S_T\sin(2\phi_h-\phi_S)\,p_3\,A_{UT}^{\sin(2\phi_h-\phi_S)} + \lambda\,S_L\cos(\phi_h)\,p_4\,A_{LL}^{\cos(\phi_h)}$$

$$+\lambda\,S_T\cos(\phi_S)\,p_4\,A_{LT}^{\cos(\phi_S)} + \lambda\,S_T\cos(2\phi_h-\phi_S)\,p_4\,A_{LT}^{\cos(2\phi_h-\phi_S)}\Bigg\} \qquad (2.3b)$$

Neglecting $1/Q^2$ corrections, the kinematic prefactors p_i are given by

$$p_1 = \frac{1-y}{1-y+\frac{1}{2}y^2}\,, \quad p_2 = \frac{y(1-\frac{1}{2}y)}{1-y+\frac{1}{2}y^2}\,, \quad p_3 = \frac{(2-y)\sqrt{1-y}}{1-y+\frac{1}{2}y^2}\,, \quad p_4 = \frac{y\sqrt{1-y}}{1-y+\frac{1}{2}y^2}\,.$$
$$(2.4)$$

and the asymmetries are defined as

$$A_{XY}^{\text{weight}} \equiv A_{XY}^{\text{weight}}(x,z,P_{hT}) = \frac{F_{XY}^{\text{weight}}(x,z,P_{hT})}{F_{UU}(x,z,P_{hT})}\,. \qquad (2.5)$$

Hereby the first index $X = U(L)$ denotes the unpolarized beam (longitudinally polarized beam with helicity λ). The second index $Y = U(L,T)$ refers to the target which can be unpolarized (or longitudinally, transversely polarized with respect to virtual photon). The superscript "weight" indicates the azimuthal dependence with no index indicating an isotropic angular distribution of the produced hadrons.

Experimental collaborations often define asymmetries in terms of counts $N(\phi_h)$. This means the kinematic prefactors p_i and $1/(x\,y\,Q^2)$ are included in the numerators or denominators of the asymmetries which are averaged over y within experimental kinematics. We will call the corresponding asymmetries $A_{XY,\langle y\rangle}^{\text{weight}}$. For instance, in unpolarized case one has

$$N(\phi) = \frac{N_0}{2\pi}\left(1 + \cos\phi\,A_{UU,\langle y\rangle}^{\cos\phi_h} + +\cos 2\phi\,A_{UU,\langle y\rangle}^{\cos 2\phi_h}\right) \qquad (2.6)$$

where N_0 denotes the total ϕ_h-averaged) number of counts in the kinematic bin of interest. It would be preferable if asymmetries were analyzed with known kinematic prefactors divided out on event-by-event basis. One could then directly compare asymmetries A_{XY}^{weight} measured in different experiments and kinematics, and focus on effects of evolution or power suppression for twist-3. In practice, data analysis is easier with kinematic factors included. Data for such asymmetries $A_{XY,\langle y\rangle}^{\text{weight}}$ are more easily available. We will define and comment on the explicit expressions as needed.

For completeness we remark that after integrating the cross section over transverse hadron momenta one obtains

$$\frac{d^4\sigma_{\text{leading}}}{dx\,dy\,dz\,d\phi_S} = \frac{\sigma_0}{2\pi}\,F_{UU}(x,z)\Bigg\{1 + \lambda\,S_L\,p_2\,A_{LL}\Bigg\} \qquad (2.7a)$$

$$\frac{d^4\sigma_{\text{subleading}}}{dx\,dy\,dz\,d\phi_S} = \frac{\sigma_0}{2\pi}\,F_{UU}(x,z)\Bigg\{S_T\sin(\phi_S)\,p_3\,A_{UT}^{\sin(\phi_S)} + \lambda\,S_T\cos(\phi_S)\,p_4\,A_{LT}^{\cos(\phi_S)}\Bigg\} \qquad (2.7b)$$

where (and analog for the other structure functions)

$$F_{UU}(x, z) = \int d^2 P_{hT} \, F_{UU}(x, z, P_{hT}) \tag{2.8}$$

and the asymmetries are defined as

$$A_{XY}^{\text{weight}}(x, z) = \frac{F_{XY}^{\text{weight}}(x, z)}{F_{UU}(x, z)} \, . \tag{2.9}$$

The connection of "collinear" SIDIS structure functions in (2.7a, 2.7b) to those known from inclusive DIS is established by integrating over z and summing over hadrons as

$$\sum_h \int dz \, z \, F_{UU}(x, z) \quad \equiv \quad 2 \, x \, F_1(x) \, , \tag{2.10a}$$

$$\sum_h \int dz \, z \, F_{LL}(x, z) \quad \equiv \quad 2 \, x \, g_1(x) \, , \tag{2.10b}$$

$$\sum_h \int dz \, z \, F_{LT}^{\cos \phi_S}(x, z) \equiv - \gamma \, 2 \, x \left(g_1(x) + g_2(x) \right) , \tag{2.10c}$$

$$\sum_h \int dz \, z \, F_{UT}^{\sin \phi_S}(x, z) \quad = \quad 0 \, , \tag{2.10d}$$

where $\gamma = 2 M_N x / Q$ signals the twist-3 character of $F_{LT}^{\cos \phi_S}(x, z)$. We consequently neglect $1/Q^2$ effects, including the twist-4 DIS structure function $F_2(x)$. $F_{UT}^{\sin \phi_S}(x, z)$ has no DIS counterpart due to time reversal symmetry of strong interactions.

2.2 TMDs, FFs and structure functions

TMDs are defined in terms of light-front correlators

$$\Phi(x, \boldsymbol{k}_\perp)_{ij} = \int \frac{d\xi^- d^2 \boldsymbol{\xi}_\perp}{(2\pi)^3} \, e^{ik\xi} \, \langle N(P, S) | \bar{\psi}_j(0) \, \mathcal{W}_{(0, \infty)} \mathcal{W}_{(\infty, \xi)} \, \psi_i(\xi) | N(P, S) \rangle \Big|_{\substack{\xi^+ = 0 \\ k^+ = xP^+}} \tag{2.11}$$

where the symbolic Wilson-lines refer to the SIDIS process [27]. For a generic four-vector a^μ we define the light-cone coordinates $a^\mu = (a^+, a^-, a_\perp)$ with $a^\pm = (a^0 \pm a^3)/\sqrt{2}$. The light-cone direction is singled out by the virtual photon momentum and transverse vectors like $\boldsymbol{k}_\perp$ are perpendicular to it. In the virtual-photon–nucleon center-of-mass frame, nucleon and the partons inside it move in the $(+)$-lightcone direction, while the struck quark and the produced hadron move in $(-)$-light-cone direction. In the nucleon rest frame the polarization vector is given by $S = (0, \boldsymbol{S}_T, S_L)$ with $\boldsymbol{S}_T^2 + S_L^2 = 1$.

The 8 leading-twist TMDs [2] are projected out from the correlator (2.11) as follows (blue (online only): T-even, red (online only): T-odd; we suppress flavor and renormalization scale dependence)

$$\frac{1}{2}\,\mathrm{Tr}\left[\gamma^+\,\Phi(x,\boldsymbol{k}_\perp)\right] = f_1 - \frac{\varepsilon^{jk}k_\perp^j S_T^k}{M_N}\,f_{1T}^\perp\,, \tag{2.12a}$$

$$\frac{1}{2}\,\mathrm{Tr}\left[\gamma^+\gamma_5\,\Phi(x,\boldsymbol{k}_\perp)\right] = S_L\,g_1 + \frac{\boldsymbol{k}_\perp\cdot\boldsymbol{S}_T}{M_N}\,g_{1T}^\perp\,, \tag{2.12b}$$

$$\frac{1}{2}\,\mathrm{Tr}\left[i\sigma^{j+}\gamma_5\,\Phi(x,\boldsymbol{k}_\perp)\right] = S_T^j\,h_1 + S_L\,\frac{k_\perp^j}{M_N}\,h_{1L}^\perp + \frac{\kappa^{jk}S_T^k}{M_N^2}\,h_{1T}^\perp + \frac{\varepsilon^{jk}k_\perp^k}{M_N}\,h_1^\perp\,, \tag{2.12c}$$

and the 16 subleading twist TMDs [1, 4] are given by

$$\frac{1}{2}\mathrm{Tr}\left[1\,\Phi(x,\boldsymbol{k}_\perp)\right] = \frac{M_N}{P^+}\left[e - \frac{\varepsilon^{jk}k_\perp^j S_T^k}{M_N}\,e_T^\perp\right], \tag{2.12d}$$

$$\frac{1}{2}\mathrm{Tr}\left[i\gamma_5\Phi(x,\boldsymbol{k}_\perp)\right] = \frac{M_N}{P^+}\left[S_L e_L + \frac{\boldsymbol{k}_\perp\cdot\boldsymbol{S}_T}{M_N}\,e_T\right], \tag{2.12e}$$

$$\frac{1}{2}\mathrm{Tr}\left[\gamma^j\,\Phi(x,\boldsymbol{k}_\perp)\right] = \frac{M_N}{P^+}\left[\frac{k_\perp^j}{M_N}f^\perp + \varepsilon^{jk}S_T^k f_T + S_L\frac{\varepsilon^{jk}k_\perp^k}{M_N}f_L^\perp - \frac{\kappa^{jk}\varepsilon^{kl}S_T^l}{M_N^2}f_T^\perp\right], \tag{2.12f}$$

$$\frac{1}{2}\mathrm{Tr}\left[\gamma^j\gamma_5\Phi(x,\boldsymbol{k}_\perp)\right] = \frac{M_N}{P^+}\left[S_T^j\,g_T + S_L\frac{k_\perp^j}{M_N}g_L^\perp + \frac{\kappa^{jk}S_T^k}{M_N^2}g_T^\perp + \frac{\varepsilon^{jk}k_\perp^k}{M_N}g^\perp\right], \tag{2.12g}$$

$$\frac{1}{2}\mathrm{Tr}\left[i\,\sigma^{jk}\gamma_5\Phi(x,\boldsymbol{k}_\perp)\right] = \frac{M_N}{P^+}\left[\frac{S_T^j k_\perp^k - S_T^k k_\perp^j}{M_N}\,h_T^\perp - \varepsilon^{jk}\,h\right], \tag{2.12h}$$

$$\frac{1}{2}\mathrm{Tr}\left[i\,\sigma^{+-}\gamma_5\,\Phi(x,\boldsymbol{k}_\perp)\right] = \frac{M_N}{P^+}\left[S_L\,h_L + \frac{\boldsymbol{k}_\perp\cdot\boldsymbol{S}_T}{M_N}\,h_T\right]. \tag{2.12i}$$

where $\kappa^{jk}\equiv(k_\perp^j k_\perp^k - \frac{1}{2}\boldsymbol{k}_\perp^2\delta^{jk})$. The indices j,k,l refer to the plane transverse with respect to the light-cone, $\epsilon^{ij}\equiv\epsilon^{-+ij}$ and $\epsilon^{0123}=+1$. Dirac-structures not listed in (2.12a–2.12i) are twist-4 [3]. Integrating out transverse momenta in the correlator (2.11) leads to the 'usual' PDFs known from collinear kinematics [12, 28], namely at twist-2 level

$$\frac{1}{2}\,\mathrm{Tr}\left[\gamma^+\,\Phi(x)\right] = f_1\,, \tag{2.13a}$$

$$\frac{1}{2}\,\mathrm{Tr}\left[\gamma^+\gamma_5\,\Phi(x)\right] = S_L\,g_1\,, \tag{2.13b}$$

$$\frac{1}{2}\,\mathrm{Tr}\left[i\sigma^{j+}\gamma_5\,\Phi(x)\right] = S_T^j\,h_1\,, \tag{2.13c}$$

and at twist-3 level

$$\frac{1}{2}\,\mathrm{Tr}\left[1\,\Phi(x)\right] = \frac{M_N}{P^+}\,e\,, \tag{2.13d}$$

$$\frac{1}{2}\,\mathrm{Tr}\left[\gamma^j\gamma_5\,\Phi(x)\right] = \frac{M_N}{P^+}\,S_T^j\,g_T\,, \tag{2.13e}$$

$$\frac{1}{2}\,\mathrm{Tr}\left[i\,\sigma^{+-}\gamma_5\,\Phi(x)\right] = \frac{M_N}{P^+}\,S_L\,h_L\,. \tag{2.13f}$$

Other structures drop out either due to explicit $k_\perp$-dependence, or due to the sum rules [4]

$$\int d^2\boldsymbol{k}_\perp \, f_T^a(x, k_\perp^2) = \int d^2\boldsymbol{k}_\perp \, e_L^a(x, k_\perp^2) = \int d^2\boldsymbol{k}_\perp \, h^a(x, k_\perp^2) = 0 \qquad (2.14)$$

imposed by time reversal constraints.

The fragmentation functions are similarly defined in terms of the correlator

$$\Delta(z, \boldsymbol{P}_\perp)_{ij} = \sum_X \int \frac{d\xi^+ d^2\boldsymbol{\xi}_\perp}{2z(2\pi)^3} \, e^{ip\xi} \, \langle 0|\mathcal{W}_{(\infty,\xi)}\psi_i(\xi) \, |h, X\rangle \, \langle h, X|\bar\psi_j(0)\mathcal{W}_{(0,\infty)}|0\rangle \Big|_{\substack{\xi^-=0 \\ p^-=P_h^-/z \\ \boldsymbol{p}_\perp=-\boldsymbol{P}_\perp/z.}} \tag{2.15}$$

In this work we will consider only unpolarized final state hadrons. If the produced hadron moves fast in the $(-)$ light cone direction, the twist-2 FFs are projected out as

$$\frac{1}{2}\mathrm{Tr}\big[\gamma^- \Delta(z, \boldsymbol{P}_\perp)\big] = D_1 \,, \tag{2.16a}$$

$$\frac{1}{2}\mathrm{Tr}\big[i\sigma^{j-}\gamma_5\Delta(z, \boldsymbol{P}_\perp)\big] = \epsilon^{jk} \frac{P_\perp^k}{zm_h} H_1^\perp \,, \tag{2.16b}$$

and at twist-3 level

$$\frac{1}{2}\,\mathrm{Tr}\Big[\,1\,\Delta(z, \boldsymbol{P}_\perp)\Big] = \frac{M_h}{P_h^-}\,E \,, \tag{2.16c}$$

$$\frac{1}{2}\,\mathrm{Tr}\Big[\,\gamma^j\,\Delta(z, \boldsymbol{P}_\perp)\Big] = -\frac{P_\perp^j}{zP_h^-}\,D^\perp \,, \tag{2.16d}$$

$$\frac{1}{2}\,\mathrm{Tr}\Big[\gamma^j\gamma_5\,\Delta(z, \boldsymbol{P}_\perp)\Big] = \varepsilon^{jk} \frac{P_\perp^k}{zP_h^-}\,G^\perp \,, \tag{2.16e}$$

$$\frac{1}{2}\,\mathrm{Tr}\Big[i\,\sigma^{jk}\gamma_5\,\Delta(z, \boldsymbol{P}_\perp)\Big] = -\varepsilon^{jk} \frac{M_h}{P_h^-}\,H \,. \tag{2.16f}$$

Here besides scale and flavor dependence we also do not indicate the type of hadron h. Integration over transverse hadron momenta leaves us with $D_1(z)$, $E(z)$, $H(z)$ while the other structures drop out due to their $P_\perp$ dependence.

The structure functions in Eqs. (2.3a, 2.3b) are described in Bjorken limit at tree level in terms of convolutions of TMDs and FFs. We define the unit vector $\hat{\boldsymbol{h}} = \boldsymbol{P}_{hT}/P_{hT}$ and use the following convolution integrals (see Appendix B.1 for details)

$$\mathcal{C}\Big[\omega\, f\, D\Big] = x \sum_a e_a^2 \int d^2\boldsymbol{k}_\perp d^2\boldsymbol{P}_\perp \, \delta^{(2)}(z\boldsymbol{k}_\perp + \boldsymbol{P}_\perp - \boldsymbol{P}_{hT}) \, \omega \, f^a(x, k_\perp^2) \, D^a(z, \boldsymbol{P}_\perp^2) \,, \tag{2.17}$$

where ω is a weight function which in general depends on $\boldsymbol{k}_\perp$ and $\boldsymbol{P}_\perp$. The 8 leading-twist

structure functions are

$$F_{UU} = \mathcal{C}\left[\, \omega^{\{0\}}\, f_1 D_1 \,\right] \tag{2.18a}$$

$$F_{LL} = \mathcal{C}\left[\, \omega^{\{0\}}\, g_1 D_1 \,\right] \tag{2.18b}$$

$$F_{UT}^{\sin(\phi_h+\phi_S)} = \mathcal{C}\left[\, \omega_{\mathrm{A}}^{\{1\}}\, h_1 H_1^\perp \,\right] \tag{2.18c}$$

$$F_{UT}^{\sin(\phi_h-\phi_S)} = \mathcal{C}\left[\, -\omega_{\mathrm{B}}^{\{1\}}\, f_{1T}^\perp D_1 \,\right] \tag{2.18d}$$

$$F_{LT}^{\cos(\phi_h-\phi_S)} = \mathcal{C}\left[\, \omega_{\mathrm{B}}^{\{1\}}\, g_{1T}^\perp D_1 \,\right] \tag{2.18e}$$

$$F_{UU}^{\cos 2\phi_h} = \mathcal{C}\left[\, \omega_{\mathrm{AB}}^{\{2\}}\, h_1^\perp\, H_1^\perp \,\right] \tag{2.18f}$$

$$F_{UL}^{\sin 2\phi_h} = \mathcal{C}\left[\, \omega_{\mathrm{AB}}^{\{2\}}\, h_{1L}^\perp H_1^\perp \,\right] \tag{2.18g}$$

$$F_{UT}^{\sin(3\phi_h-\phi_S)} = \mathcal{C}\left[\, \omega^{\{3\}}\, h_{1T}^\perp H_1^\perp \,\right]. \tag{2.18h}$$

At subleading-twist we have the structure functions

$$F_{UU}^{\cos\phi_h} = \frac{2M}{Q}\,\mathcal{C}\left[\, \omega_{\mathrm{A}}^{\{1\}}\left(xh\,H_1^\perp + r_h\, f_1\,\frac{\tilde{D}^\perp}{z}\right) - \omega_{\mathrm{B}}^{\{1\}}\left(xf^\perp D_1 + r_h\, h_1^\perp\frac{\tilde{H}}{z}\right)\right] \tag{2.19a}$$

$$F_{LU}^{\sin\phi_h} = \frac{2M}{Q}\,\mathcal{C}\left[\, \omega_{\mathrm{A}}^{\{1\}}\left(x\,e\,H_1^\perp + r_h\, f_1\,\frac{\tilde{G}^\perp}{z}\right) + \omega_{\mathrm{B}}^{\{1\}}\left(xg^\perp D_1 + r_h\, h_1^\perp\frac{\tilde{E}}{z}\right)\right] \tag{2.19b}$$

$$F_{UL}^{\sin\phi_h} = \frac{2M}{Q}\,\mathcal{C}\left[\, \omega_{\mathrm{A}}^{\{1\}}\left(xh_L H_1^\perp + r_h\, g_1\,\frac{\tilde{G}^\perp}{z}\right) + \omega_{\mathrm{B}}^{\{1\}}\left(xf_L^\perp D_1 - r_h\, h_{1L}^\perp\frac{\tilde{H}}{z}\right)\right] \tag{2.19c}$$

$$F_{LL}^{\cos\phi_h} = \frac{2M}{Q}\,\mathcal{C}\left[-\omega_{\mathrm{A}}^{\{1\}}\left(xe_L H_1^\perp - r_h\, g_1\,\frac{\tilde{D}^\perp}{z}\right) - \omega_{\mathrm{B}}^{\{1\}}\left(xg_L^\perp D_1 + r_h\, h_{1L}^\perp\frac{\tilde{E}}{z}\right)\right] \tag{2.19d}$$

$$F_{UT}^{\sin\phi_S} = \frac{2M}{Q}\,\mathcal{C}\left[\, \omega^{\{0\}}\left(xf_T D_1 \,-\, r_h\, h_1\,\frac{\tilde{H}}{z}\right)\right.$$
$$\left. -\frac{\omega_{\mathrm{B}}^{\{2\}}}{2}\left(xh_T H_1^\perp + r_h\, g_{1T}^\perp\,\frac{\tilde{G}^\perp}{z} - xh_T^\perp H_1^\perp + r_h\, f_{1T}^\perp\,\frac{\tilde{D}^\perp}{z}\right)\right] \tag{2.19e}$$

$$F_{LT}^{\cos\phi_S} = \frac{2M}{Q}\,\mathcal{C}\left[-\omega^{\{0\}}\left(xg_T D_1 + r_h\, h_1\,\frac{\tilde{E}}{z}\right)\right.$$
$$\left. +\frac{\omega_{\mathrm{B}}^{\{2\}}}{2}\left(xe_T H_1^\perp - r_h\, g_{1T}^\perp\,\frac{\tilde{D}^\perp}{z} + xe_T^\perp H_1^\perp + r_h\, f_{1T}^\perp\,\frac{\tilde{G}^\perp}{z}\right)\right] \tag{2.19f}$$

$$F_{UT}^{\sin(2\phi_h-\phi_S)} = \frac{2M}{Q}\,\mathcal{C}\left[\, \frac{\omega_{\mathrm{AB}}^{\{2\}}}{2}\left(xh_T H_1^\perp + r_h\, g_{1T}^\perp\,\frac{\tilde{G}^\perp}{z} + xh_T^\perp H_1^\perp - r_h\, f_{1T}^\perp\,\frac{\tilde{D}^\perp}{z}\right)\right.$$
$$\left. +\omega_{\mathrm{C}}^{\{2\}}\left(xf_T^\perp D_1 - r_h\, h_{1T}^\perp\frac{\tilde{H}}{z}\right)\right] \tag{2.19g}$$

$$F_{LT}^{\cos(2\phi_h - \phi_S)} = \frac{2M}{Q} \mathcal{C}\left[-\frac{\omega_{AB}^{\{2\}}}{2}\left(xe_T H_1^\perp - r_h\, g_{1T}^\perp\, \frac{\tilde{D}^\perp}{z} - xe_T^\perp H_1^\perp - r_h\, f_{1T}^\perp\, \frac{\tilde{G}^\perp}{z} \right) \right.$$
$$\left. -\omega_C^{\{2\}}\left(xg_T^\perp D_1 + r_h\, h_{1T}^\perp\, \frac{\tilde{E}}{z} \right) \right] \tag{2.19h}$$

where $r_h = m_h/M_N$ and $F_{XY}^{\text{weight}} \equiv F_{XY}^{\text{weight}}(x, z, P_{hT})$. The weight functions are defined as

$$\omega^{\{0\}} = 1\,,$$
$$\omega_A^{\{1\}} = \frac{\hat{\boldsymbol{h}} \cdot \boldsymbol{P}_\perp}{zm_h}\,, \quad \omega_B^{\{1\}} = \frac{\hat{\boldsymbol{h}} \cdot \boldsymbol{k}_\perp}{M_N}\,,$$
$$\omega_A^{\{2\}} = \frac{2\left(\hat{\boldsymbol{h}} \cdot \boldsymbol{P}_\perp \right)\left(\hat{\boldsymbol{h}} \cdot \boldsymbol{k}_\perp \right)}{zM_N m_h}\,, \quad \omega_B^{\{2\}} = -\frac{\boldsymbol{P}_\perp \cdot \boldsymbol{k}_\perp}{zM_N m_h}\,, \quad \omega_C^{\{2\}} = \frac{2\left(\hat{\boldsymbol{h}} \cdot \boldsymbol{k}_\perp \right)^2 - \boldsymbol{k}_\perp^2}{2M_N^2}\,,$$
$$\omega^{\{3\}} = \frac{4\left(\hat{\boldsymbol{h}} \cdot \boldsymbol{P}_\perp \right)\left(\hat{\boldsymbol{h}} \cdot \boldsymbol{k}_\perp \right)^2 - 2\left(\hat{\boldsymbol{h}} \cdot \boldsymbol{k}_\perp \right)\left(\boldsymbol{k}_\perp \cdot \boldsymbol{P}_\perp \right) - \left(\hat{\boldsymbol{h}} \cdot \boldsymbol{P}_\perp \right)\boldsymbol{k}_\perp^2}{2zM_N^2 m_h}\,, \tag{2.20}$$

and $\omega_{AB}^{\{2\}} = \omega_A^{\{2\}} + \omega_B^{\{2\}}$. In $\omega_i^{\{n\}}$ the index $n = 0, 1, 2, 3$ indicates the (maximal) power $(P_{hT})^N$ with which the corresponding contribution scales, and index i (if any) distinguishes different types of contributions at the given order N. Notice that twist-3 structure functions in Eqs. (2.19a–2.19h) contain an explicit factor M/Q. We also recall that we neglect two structure functions due to longitudinal virtual photon polarization which contribute, in the TMD factorization framework, at order $\mathcal{O}(M^2/Q^2)$, one being $F_{UU,L}$ and the other contributing to the $\sin(\phi_h - \phi_S)$ angular distribution [4].

The structures surviving P_{hT}-integration of the SIDIS cross section in (2.7a, 2.7b) are associated with the trivial weights $\omega^{\{0\}}$ and expressed in terms of collinear PDFs and FFs as follows (here the sum rules (2.14) are used)

$$F_{UU}(x, z) = x \sum_a e_a^2\, f_1^a(x)\, D_1^a(z) \tag{2.21a}$$

$$F_{LL}(x, z) = x \sum_a e_a^2\, g_1^a(x)\, D_1^a(z) \tag{2.21b}$$

$$F_{LT}^{\cos\phi_S}(x, z) = -\frac{2M_N}{Q}\, x \sum_a e_a^2\left(x\, g_T^q(x) + r_h\, h_1^a(x)\frac{\tilde{E}^a(z)}{z} \right) \tag{2.21c}$$

$$F_{UT}^{\sin\phi_S}(x, z) = -\frac{2\, m_h}{Q}\, x \sum_a e_a^2\, h_1^a(x)\frac{\tilde{H}^a(z)}{z} \tag{2.21d}$$

Finally, using the sum rules for the T-odd FFs $\sum_h \int dz\, \tilde{E}^a(z) = 0$ and $\sum_h \int dz\, \tilde{H}^a(z) = 0$ we recover Eqs. (2.10a–2.10d) and obtain for the DIS structure functions

$$F_1(x) = \frac{1}{2}\sum_a e_a^2\, f_1^a(x) \tag{2.22a}$$

$$g_1(x) = \frac{1}{2}\sum_a e_a^2\, g_1^a(x) \tag{2.22b}$$

$$g_2(x) = \frac{1}{2}\sum_a e_a^2\, g_T^a(x)\, -\, g_1(x) \tag{2.22c}$$

Having established the notation we now define and discuss the approximations.

3 WW and WW-type approximations

In this section we will define the approximations and review what is known about them. The basic idea of the approximations is simple. One assumes that the contributions from $\bar{q}gq$-terms can be neglected with respect to $\bar{q}q$-terms with a useful accuracy,

$$\left|\frac{\langle\bar{q}gq\rangle}{\langle\bar{q}q\rangle}\right| \ll 1 \,. \tag{3.1}$$

3.1 WW approximation for PDFs

The WW approximation applies in principle to all twist-3 PDFs, Eqs. (2.13d, 2.13e, 2.13f). It was established first for $g_T^a(x)$ [11], and later for $h_L^a(x)$ [12]. The situation of $e^a(x)$ is somewhat special, see below and the review [29].

The origin of the approximations is as follows. The operators defining $g_T^a(x)$ and $h_L^a(x)$ can be decomposed by means of QCD equations of motion in twist-2 parts, and pure twist-3 (interaction dependent) $\bar{q}gq$-terms and current quark mass terms. We denote $\bar{q}gq$-terms and mass-terms collectively and symbolically by functions with a tilde. Such decompositions are possible because $g_T^a(x)$ and $h_L^a(x)$ are "twist-3" not according to the "strict QCD definition" (twist = mass dimension of associated local operator minus its spin). Rather they are classified according to the "working definition" [30] (a function is "twist t" if it contributes to cross sections suppressed by $(M/Q)^{t-2}$ with M a generic hadronic and Q the hard scale). The two definitions coincide for twist-2 quantities, but higher twist observables in general contain "contaminations" by leading twist.

In this way one obtains the decompositions and, if they apply, WW approximations [11, 12] (keep in mind here tilde terms contain pure twist-3 and current quark mass terms)

$$g_T^a(x) = \int_x^1 \frac{dy}{y}\, g_1^a(y) + \tilde{g}_T^a(x) \stackrel{\text{WW}}{\approx} \int_x^1 \frac{dy}{y}\, g_1^a(y) \,, \tag{3.2a}$$

$$h_L^a(x) = 2x\int_x^1 \frac{dy}{y^2}\, h_1^a(y) + \tilde{h}_L^a(x) \stackrel{\text{WW}}{\approx} 2x\int_x^1 \frac{dy}{y^2}\, h_1^a(y) \,, \tag{3.2b}$$

$$x\, e^a(x) = x\,\tilde{e}^a(x) \stackrel{\text{WW}}{\approx} 0 \tag{3.2c}$$

where we included $e^a(x)$ which ia a special case in the sense that it receives no twist-2 contribution. Notice that a prefactor of x is provided to cancel a $\delta(x)$-type singularity [29]. After introducing the WW-type approximations for TMDs and FFs, we will come back to (3.2a, 3.2b) and review the theoretical predictions and experimental data supporting them.

3.2 WW-type approximations for TMDs and FFs

Analog to WW approximations for PDFs discussed in Sec. 3.1, also certain TMDs and FFs can be decomposed in twist-2 contributions and tilde-terms. The latter may be assumed, in the spirit of (3.1), to be small. Hereby it is important to keep in mind that one deals with different types of ("unintegrated") $\bar{q}gq$-correlations, and we prefer to refer to them as WW-type approximations.

In the T-even case one obtains the following approximations, where the terms on the left-hand-side are twist-3, those on the right-hand-side (if any) are twist-2,

$$xe^q(x, k_\perp^2) \stackrel{\text{WW}-\text{type}}{\approx} 0, \tag{3.3a}$$

$$xf^{\perp q}(x, k_\perp^2) \stackrel{\text{WW}-\text{type}}{\approx} f_1^q(x, k_\perp^2), \tag{3.3b}$$

$$xg_L^{\perp q}(x, k_\perp^2) \stackrel{\text{WW}-\text{type}}{\approx} g_1^q(x, k_\perp^2), \tag{3.3c}$$

$$xg_T^{\perp q}(x, k_\perp^2) \stackrel{\text{WW}-\text{type}}{\approx} g_{1T}^{\perp q}(x, k_\perp^2), \tag{3.3d}$$

$$xg_T^q(x, k_\perp^2) \stackrel{\text{WW}-\text{type}}{\approx} g_{1T}^{\perp(1)q}(x, k_\perp^2), \tag{3.3e}$$

$$xh_L^q(x, k_\perp^2) \stackrel{\text{WW}-\text{type}}{\approx} -2\,h_{1L}^{\perp(1)q}(x, k_\perp^2), \tag{3.3f}$$

$$xh_T^q(x, k_\perp^2) \stackrel{\text{WW}-\text{type}}{\approx} -h_1^q(x, k_\perp^2) - h_{1T}^{\perp(1)}(x, k_\perp^2), \tag{3.3g}$$

$$xh_T^{\perp q}(x, k_\perp^2) \stackrel{\text{WW}-\text{type}}{\approx} h_1^q(x, k_\perp^2) - h_{1T}^{\perp(1)}(x, k_\perp^2). \tag{3.3h}$$

In the T-odd case one obtains the approximations

$$xe_L^q(x, k_\perp^2) \stackrel{\text{WW}-\text{type}}{\approx} 0, \tag{3.4a}$$

$$xe_T^q(x, k_\perp^2) \stackrel{\text{WW}-\text{type}}{\approx} 0, \tag{3.4b}$$

$$xe_T^{\perp q}(x, k_\perp^2) \stackrel{\text{WW}-\text{type}}{\approx} 0, \tag{3.4c}$$

$$xg^{\perp q}(x, k_\perp^2) \stackrel{\text{WW}-\text{type}}{\approx} 0, \tag{3.4d}$$

$$xf_L^{\perp q}(x, k_\perp^2) \stackrel{\text{WW}-\text{type}}{\approx} 0, \tag{3.4e}$$

$$xf_T^{\perp q}(x, k_\perp^2) \stackrel{\text{WW}-\text{type}}{\approx} f_{1T}^{\perp q}(x, k_\perp^2), \tag{3.4f}$$

$$xf_T^q(x, k_\perp^2) \stackrel{\text{WW}-\text{type}}{\approx} -f_{1T}^{\perp(1)q}(x, k_\perp^2), \tag{3.4g}$$

$$xh^q(x, k_\perp^2) \stackrel{\text{WW}-\text{type}}{\approx} -2\,h_1^{\perp(1)}(x, k_\perp^2), \tag{3.4h}$$

where the superscript "(1)" denotes transverse moments of TMDs defined generically as

$$f^{(1)}(x, k_\perp^2) = \frac{k_\perp^2}{2M^2}\, f(x, k_\perp^2)\,, \quad f^{(1)}(x) = \int d^2\boldsymbol{k}_\perp f^{(1)}(x, k_\perp^2)\,. \tag{3.5}$$

Two very useful WW-type approximations follow from combining the WW approximations (3.2a, 3.2b) with the WW-type approximations (3.3e, 3.3f). This yields [1, 23, 31]

$$g_{1T}^{\perp(1)a}(x) \stackrel{\text{WW}-\text{type}}{\approx} x \int_x^1 \frac{dy}{y}\, g_1^a(y)\,, \tag{3.6a}$$

$$h_{1L}^{\perp(1)a}(x) \stackrel{\text{WW}-\text{type}}{\approx} -x^2 \int_x^1 \frac{dy}{y^2}\, h_1^a(y)\,. \tag{3.6b}$$

Aspects and phenomenological applications of some of the above WW-type approximations were discussed in [1, 20–25, 31].

WW-relations for FFs are actually not needed: in Eqs. (2.18, 2.18) either twist-2 FFs D_1^a, $H_1^{\perp a}$ enter or tilde FFs, as a consequence of how the azimuthal angles are defined [4]. For completeness we quote the WW-type approximations for FFs [4]

$$E(z, P_\perp^2) \stackrel{\text{WW-type}}{\approx} 0 \,, \tag{3.7a}$$

$$G^\perp(z, P_\perp^2) \stackrel{\text{WW-type}}{\approx} 0 \,, \tag{3.7b}$$

$$D^\perp(z, P_\perp^2) \stackrel{\text{WW-type}}{\approx} z\, D_1(z, P_\perp^2) \,, \tag{3.7c}$$

$$H(z, P_\perp^2) \stackrel{\text{WW-type}}{\approx} -\frac{P_\perp^2}{z M_h^2}\, H_1^\perp(z, P_\perp^2) \,. \tag{3.7d}$$

Having introduced the WW- and WW-type approximations, we will review in the following what is currently known from theory and experiment about our approximations.

3.3 Predictions from instanton vacuum model

Insights on the relatve size of hadronic matrix elements, such as Eq. (3.1), require a non-perturbative approach. It is by no means obvious which small parameter in the strong interaction regime would allow to explain such results.

A powerful non-perturbative approach is provided by the instanton model of the QCD vacuum [32–34]. This semi-classical approach assumes that properties of the QCD vacuum are dominated by instantons and anti-instantons, topological non-perturbative gluon field configurations, which form a strongly interacting medium. The approach provides a natural mechanism for dynamical chiral symmetry breaking, the dominant feature of strong interactions in the nonperturbative regime. It was shown with variational and numerical methods that the strongly interacting instanton medium is dilute. The ratio of average instanton size ρ_{av} and average instanton separation R_{av} is a non-trivial small parameter, numerically $\rho_{\text{av}}/R_{\text{av}} \sim 1/3$ [32–34], which can be explored.

Applying the instanton vacuum model to studies of $g_T^a(x)$ and $h_L^a(x)$ it was predicted that matrix elements of the $\bar{q}gq$ operators defining $\tilde{g}_T^a(x)$ [14] and $\tilde{h}_L^a(x)$ [15] are strongly suppressed by powers of the small parameter $\rho_{\text{av}}/R_{\text{av}}$ with respect to contributions from the respective twist-2 parts which are of the order $(\rho_{\text{av}}/R_{\text{av}})^0$. Numerically it was found

$$\left| \frac{\langle \bar{q}gq \rangle}{\langle \bar{q}q \rangle} \right| \sim \left(\frac{\rho}{R} \right)^4 \log\left(\frac{\rho}{R} \right) \sim 10^{-2} \tag{3.8}$$

in these 2 cases. This result strongly supports the generic approximation in Eq. (3.1) with the instanton packing fraction providing the non-trivial small parameter justifying the neglect of tilde-terms. The instanton calculus has not yet been applied to $\tilde{e}^a(x)$.

Noteworthy, the instanton vacuum predictions for $\tilde{g}_T^a(x)$ were made before the advent of the first precise data on $g_2(x)$ which we discuss in the next section.
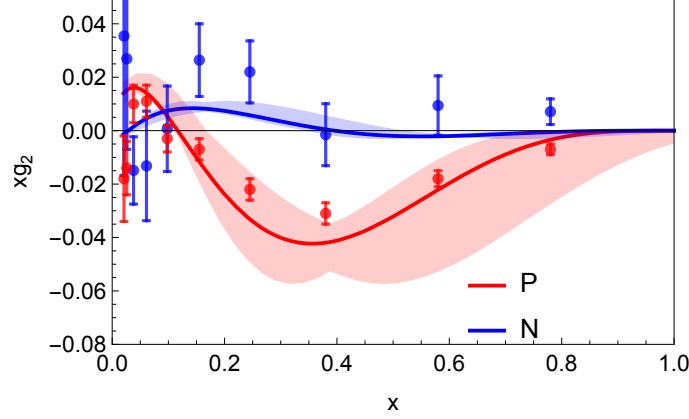
Figure 2. g_2 structure function in WW-approximation, Eq. (3.9), for proton (P) and neutron (N) targets. The data are from [18, 19]. The error band procedure is described in the text.

3.4 Tests of WW approximation in DIS experiments

The presently available phenomenological information on $g_T^a(x)$ is due to measurements of the structure function $g_2(x)$, Eq. (2.22c), in DIS off various transversely polarized targets. In the WW-approximation (3.2a) one can write $g_2(x)$ as a total derivative expressed in terms of the experimentally well known twist-2 structure function $g_1(x)$ as follows

$$g_2(x) \overset{\text{WW}}{\approx} g_2(x)_{\text{WW}} \equiv \frac{d}{dx}\left[\frac{x}{2}\int_x^1 \frac{dy}{y}\, g_1(y)\right]. \tag{3.9}$$

Data support (3.9) to a good accuracy [18, 19], although especially at smaller x more stringent tests are not yet possible. Overall it has been estimated that the WW approximation for $g_2(x)$ and $g_T^a(x)$ works with an accuracy of about 40 % or better [35].

We present calculations of $g_2(x)_{WW}$ in Fig. 2. How well does the WW approximation describe data if we allow for a theoretical "error band" of about 40 % as deduced in [35]? In order to investigate this question, we split this uncertainty in two parts, $\varepsilon_1 = \pm 20\,\%$ and $\varepsilon_2(x) = \pm 20\,\%(1-x)^\epsilon$ with a small $\epsilon > 0$, and estimate the impact of this uncertainty as

$$g_2(x)_{\text{WW}} = (1 \pm \varepsilon_1)\frac{d}{dx}\left[x\int_x^1 \frac{dy}{y}\left(\frac{1}{2}\sum_a e_a^2\, g_1^a(y(1 \pm \varepsilon_2))\right)\right]. \tag{3.10}$$

The effect of ε_1 is to change the magnitude of $g_2(x)_{\text{WW}}$, ε_2 varies the position of its zero. The x-dependence of ε_2 preserves $\lim_{x\to 1} g_2(x) = 0$; we use $\epsilon = 0.05$ which yields $\varepsilon_2 \approx 20\,\%$ up to the highest measured x-bin. The good agreement of $g_2(x)_{\text{WW}}$ with data is encouraging, and in line with theory predictions [14]. Our estimate with the splitted uncertainties $\varepsilon_{1,2}$ may overestimate in certain x-bins the 40 %-"error band" estimated in [35]. This however helps us to display a conservative estimate of possible uncertainties.

Presently $h_L^a(x)$ is unknown. With phenomenological information on $h_1^a(x)$ [36–38], the WW approximation (3.2b) for $h_L^a(x)$ could be tested experimentally in Drell-Yan [39].

3.5 Tests in lattice QCD

The lowest Mellin moments of the PDF $g_T^q(x)$ were studied in lattice QCD in the quenched approximation [16] and with $N_f = 2$ flavors of light dynamical quarks [17]. The obtained results were compatible with a small $\tilde{g}_T^q(x)$. We are not aware of lattice QCD studies related to the PDF $h_L^a(x)$, and turn now our attention to TMD studies in lattice QCD.

After first exploratory investigations of TMDs on the lattice [40, 41], recent years have witnessed considerable progress and improvements with regard to rigor, realism and methodology [42–45]. However, numerical results from recent calculations are only available for a subset of observables, and the quantities calculated are not in a form that lends itself to straighforward tests of the WW-type relations as presented in this paper. Details about recent works and future perspectives are discussed at the end of this section.

For the time being, we content ourselves with rather crude comparisons based on the data published in Refs. [40, 41]. These early works explored all nucleon and quark polarizations, but they used a gauge link that does not incorporate the final or initial state interactions present in SIDIS or Drell-Yan experiments. In other words, the transverse momentum dependent quantities computed in [40, 41] are not precisely the TMDs measurable in experiment. More caveats will be discussed along the way.

Let us now translate the approximations (3.6a, 3.6b) into expressions for which we have a chance to compare them with available lattice data. For that we multiply the Eqs. (3.6a, 3.6b) by x^N with $N = 0, 1, 2, \ldots$ and integrate over $x \in [-1, 1]$ which yields

$$\int_{-1}^{1} dx \; x^N g_{1T}^{\perp(1)q}(x) \overset{\text{WW−type}}{\approx} \frac{1}{N+2} \int_{-1}^{1} dx \; x^{N+1} g_1^q(x) \;, \tag{3.11}$$

$$\int_{-1}^{1} dx \; x^N h_{1L}^{\perp(1)q}(x) \overset{\text{WW−type}}{\approx} -\frac{1}{N+3} \int_{-1}^{1} dx \; x^{N+1} h_1^q(x) \;. \tag{3.12}$$

with the understanding that negative x refer to antiquark distributions $g_1^{\bar{q}}(x) = + g_1^q(-x)$, $h_1^{\bar{q}}(x) = -h_1^q(-x)$, $g_{1T}^{\perp(1)\bar{q}}(x) = -g_{1T}^{\perp(1)q}(-x)$, $h_{1L}^{\perp(1)\bar{q}}(x) = +h_{1L}^{\perp(1)q}(-x)$ depending on C-parity of the involved operators [1]. The right hand sides of Eqs. (3.11, 3.12) are x-moments of parton distributions, and those can be obtained from lattice QCD using well-established methods based on operator product expansion. The left hand sides are moments of TMDs in x and $\boldsymbol{k}_\perp$. We have to keep in mind that TMDs diverge for large $\boldsymbol{k}_\perp$. Therefore, without regularizing these divergences in a scheme suitable for the comparison of left and right hand side, a test of the above relations is meaningless, even before we get to address the issues of lattice calculations. Let us not give up at this point and take a look at the lattice observables of Ref. [41]. Here, the TMDs are obtained from amplitudes $\tilde{A}_i(l^2, \ldots)$ in Fourier space, where $\boldsymbol{k}_\perp$ is encoded in the Fourier conjugate variable $\boldsymbol{\ell}_\perp$, which is the transverse displacement of quark operators in the correlator evaluated on the lattice. In Fourier-space, the aforementioned divergent behavior for large $\boldsymbol{k}_\perp$ translates into strong lattice scale and scheme dependences at short distances $\boldsymbol{\ell}_\perp$ between the quark operators. The $\boldsymbol{k}_\perp$ integrals needed for the left hand sides of Eqs. (3.11, 3.12) correspond to the amplitudes at $\boldsymbol{\ell}_\perp = 0$, where scheme and scale-dependence is greatest. In Ref. [41] Gaussian fits have been performed to the amplitudes *excluding* data at short quark separations $\boldsymbol{\ell}_\perp$. The Gaussians

describe the long range data quite well and bridge the gap at short distances $\boldsymbol{\ell}_\perp$. Taking the Gaussian fit at $\boldsymbol{\ell}_\perp = 0$, we get a value which is (presumably) largely lattice scheme and scale independent. We have thus swept the problem of divergences under the rug. The Gaussian fit acts as a crude regularization of the divergences that appear in TMDs at large $\boldsymbol{k}_\perp$ and manifest themselves as short range artefacts on the lattice. Casting this line of thought into Mathematics, we get

$$\int_{-1}^{1} dx \, g_{1T}^{\perp(1)q}(x) = \int_{-1}^{1} dx \int d^2\boldsymbol{k}_\perp \frac{k_\perp^2}{2M^2} g_{1T}^{\perp q}(x, k_\perp) = -2\tilde{A}_{7,q}(\ell = 0) \overset{\text{Gaussian}}{=} -c_{7,q} \quad (3.13)$$

$$\int_{-1}^{1} dx \, h_{1L}^{\perp(1)q}(x) = \int_{-1}^{1} dx \int d^2\boldsymbol{k}_\perp \frac{k_\perp^2}{2M^2} h_{1T}^{\perp q}(x, k_\perp) = -2\tilde{A}_{10,q}(\ell = 0) \overset{\text{Gaussian}}{=} -c_{10,q} \quad (3.14)$$

We have thus expressed the left hand side of Eqs. (3.11, 3.12) in terms of amplitudes $c_{7,q}$ and $c_{10,q}$ of the Gaussian fits on the lattice. Before quoting numbers, a few more comments are in order. The overall multiplicative renormalization had been fixed by setting the Gaussian integral $c_{2,u-d}$ of the unpolarized TMD f_1 in the isovector channel (u-d) to the nucleon quark content, namely, to 1. The validity the assumption that renormalization is mutliplicative and flavor-independent for the non-local lattice operators is under investigation [46]. The gauge link that goes into the evaluation of the quark-quark correlator introduces a power divergence that has to be subtracted. The subtraction scheme that was chosen on the lattice is not known to have a clear relation to a "real world" subtraction scheme designed for experimental TMDs and the corresponding gauge link geometry. The gauge link renormalization mainly influences the width of the Gaussian fits; the amplitudes are only slightly affected, so it may not play a big role for our discussion. Altogether, the significance of our numerical "tests" of WW-relations should be taken with a grain of salt.

For the test of Eq. (3.11), we use the numbers $\int dx \, g_{1T}^{\perp(1)u}(x) \overset{\text{Gaussian}}{=} -c_{7,u} = 0.1041(85)$ and $\int dx \, g_{1T}^{\perp(1)d}(x) \overset{\text{Gaussian}}{=} -c_{10,d} = -0.0232(42)$ from [41]. Lattice data for $\int dx \, x^N g_1^q(x)$ [47, 48] and $\int dx \, x^N h_1^q(x)$ [49] are available for $N = 0, 1, 2, 3$. These values have been computed using (quasi-) local operators which have been renormalized to the $\overline{MS}$ scheme at the scale $\mu^2 = 4\,\text{GeV}^2$. According to [48] (data set 4: with $am_{u,d} = 0.020$ with $m_\pi \approx 500\,\text{MeV}$) one has $\int dx \, x \, g_1^{u-d}(x) = 0.257(10)$ and $\int dx \, x \, g_1^{u+d}(x) = 0.159(14)$. Decomposing the results from [48] into individual flavors, and inserting them into Eq. (3.11) we obtain

$$\underbrace{\int dx \, g_{1T}^{\perp(1)u}(x)}_{=0.1041(85) \text{ Ref. [41]}} \overset{!}{\approx} \underbrace{\frac{1}{2} \int dx \, x \, g_1^u(x)}_{=0.104(9) \text{ Ref. [48]}} \quad ,$$

$$\underbrace{\int dx \, g_{1T}^{\perp(1)d}(x)}_{=-0.0232(42) \text{ Ref. [41]}} \overset{!}{\approx} \underbrace{\frac{1}{2} \int dx \, x \, g_1^u(x)}_{=-0.025(9) \text{ Ref. [48]}} \quad , \quad (3.15)$$

which confirms the approximation (3.11) for $N = 0$ within the statistical uncertainties of the lattice calculations. In order to test (3.12) we use $\int dx \, h_{1L}^{\perp(1)u}(x) = -0.0931(73)$ and $\int dx \, h_{1L}^{\perp(1)d}(x) = 0.0130(40)$ from [40] and the lattice data $\int dx \, x \, h_1^u(x) = 0.28(1)$ and

$\int dx\, x\, h_1^d(x) = -0.054(4)$ from QCDSF [49].[1] Inserting these numbers into (3.12) for the case $N = 0$ we obtain

$$\underbrace{\int dx\, h_{1L}^{\perp(1)u}(x)}_{=-0.0931(73)\ \text{Ref. [40]}} \overset{!}{\approx} \underbrace{-\frac{1}{3}\int dx\, x\, g_1^u(x)}_{=-0.093(3)\ \text{Ref. [48]}} \;,$$

$$\underbrace{\int dx\, h_{1L}^{\perp(1)d}(x)}_{=0.0130(40)\ \text{Ref. [40]}} \overset{!}{\approx} \underbrace{-\frac{1}{3}\int dx\, x\, h_1^u(x)}_{=0.018(1)\ \text{Ref. [48]}} \;. \tag{3.16}$$

which again confirms the WW-type approximation within the statistical uncertainties of the lattice calculations.

Several more comments are in order concerning the, at first glance, remarkably good confirmation of the WW-type approximations by lattice data in Eqs. (3.15, 3.16).

First, the relations refer to lattice parameters corresponding to pion masses of 500 MeV. We do not need to worry about that too much. The lattice results do provide a valid test of the approximations in a "hadronic world" with somewhat heavier pions and nucleons. All that matters in our context is that the relative size of $\bar{q}gq$-matrix elements is small with respect to $\bar{q}q$-matrix elements.

Second, we have to revisit carefully which approximations the above lattice calculations actually test. As mentioned above, in the lattice study [48] a specific choice for the path of the gauge link was chosen, which is actually different from the paths required in SIDIS or DY. With the path choice of [48] there are effectively only (T-even) A_i amplitudes, the B_i amplitudes are absent. Therefore, see [24, 25] and Sec. 3.6, the test (3.15) of the WW-type approximation (3.11) actually constitutes a test of the WW-approximation (3.2a) and confirms earlier lattice work [16, 17]. Similarly, the test (3.16) of the WW-type approximation (3.12) actually constitutes a test of the WW-approximation (3.2b). The latter however has not been reported previously in literature, and is a new result.

Third, to be precise: (3.15, 3.16) test the first Mellin moments of the WW approximations (3.2a, 3.2b), which corresponds to the Burkardt-Cottingham sum rule for $g_T^a(x)$ and an analog sum rule for $h_L^a(x)$, see [30] and references there in. In view of the long debate on the validity of those sum rules [29, 50, 51], this is in an interesting result in itself.

It is important to stress that in view of the pioneering and exploratory status of the TMD lattice calculations [48], this is already a remarkable and very interesting result. Thus, apart from the instanton calculus [15] also lattice data provide support for the validity of the WW approximation (3.2b). At the same time, however, we also have to admit that we do not really reach our goal of testing the WW-type approximations on the lattice. With the presently available lattice data this is not yet possible. Future lattice data on higher Mellin moments will provide further insights. Meanwhile we may try to gain insights into the quality of WW-type approximations from experiment.

---

[1] These numbers are read off from a figure in [49], and were computed on a different lattice. We interpolate them to a common value of the pion mass $m_\pi \approx 500$ MeV, and estimate the error conservatively in order to take systematic effects into account due to the use of a different lattice.

3.6 Tests in models

Effective approaches and models such as bag [12, 52–54], spectator [55], chiral quark-soliton [56], or light-cone constituent [57, 58] models support the approximations (3.2a, 3.2b) for PDFs within an accuracy of $(10-30)\,\%$ at low hadronic scale below $1\,\mathrm{GeV}$.

Turning to TMDs, we recall that in models without gluon degrees of freedom certain relations among TMDs hold, the so-called quark model Lorentz-invariance relations (qLIRs). Initially thought to be exact [1, 31] qLIRs were shown in models with gluons [59, 60] and in QCD [61] to be invalid. They originate from decomposing the (completely unintegrated) quark correlator in terms of Lorentz-invariant amplitudes, and TMDs are certain integrals over those amplitudes. When gluons are absent, the correlator consists of 12 amplitudes [1, 31], i.e. fewer amplitudes than TMDs which implies relations, qLIRs. In QCD the correct Lorentz decomposition requires the consideration of gauge links. This generates further amplitudes. As a result one has as many amplitudes as TMDs and no relations exist [61]. However, qLIRs "hold" in QCD in the WW-type approximation [24]. In models without gluon degrees of freedom they are exact [24, 25, 54, 55].

The bag, spectator and light-cone constituent quark models support the approximations (3.6a, 3.6b) within an accuracy of $(10-30)\,\%$ [54, 55, 57, 58]. The spectator and bag model support WW-type approximations within $(10-30)\,\%$ [54]. As they are defined in terms of quark bilinear expressions (2.11) it is possible to evaluate twist-3 functions in quark models [12]. The tilde-terms arise due to the different model interactions, and it is important to discuss critically how realistically they describe the $\bar{q}gq$-terms of QCD [62, 63].

In the covariant parton model with intrinsic 3D-symmetric parton orbital motion [64] quarks are free, $\bar{q}gq$ correlations absent, and all WW and WW-type relations exact [65, 66]. The phenomenological success of this approach [64] may hint at a general smallness of $\bar{q}gq$ terms, although many of the predictions from this model have yet to be tested [65].

Let us finally discuss quark-target models, where gluon degrees of freedom are included and WW(-type) approximations badly violated [59, 60, 67, 68]. This is natural in this class of models for two reasons. First, quark-mass terms are of $\mathcal{O}(m_q/M_N)$ and negligible in the nucleon case, but of $\mathcal{O}(100\,\%)$ in a quark target where m_q plays also the role of M_N. Second, even if one refrains from mass terms the approximations are spoiled by gluon radiation, see for instance [69] in the context of (3.2a). This means that perturbative QCD does not support the WW-approximation: they are certainly not preserved by evolution. However, scaling violations *per se* do not need to be large. What is crucial in this context are dynamical reasons for the smallness of the *matrix elements* of $\bar{q}gq$-operators. This requires the consideration of chiral symmetry breaking effects reflected in the hadronic spectrum, as considered in the instanton vacuum model [14, 15] but out of scope in quark-target models.

We are not aware of systematic tests of WW-type approximations for FFs. One information worth mentioning in this context is that in spectator models [55] tilde-contributions to FFs are proportional to the offshellness of partons [62, 63]. This natural feature may indicate that in the region dominated by effects of small P_T tilde-terms might be small. On the other hand, quarks have sizable constituent masses of the order of few hundred MeV in spectator models and the mass-terms are not small. The applicability of WW-type

approximations to FFs remains the least tested point in our approach.

3.7 Basis functions & limitations of WW-type approximations

The leading-twist 6 TMDs f_1^a, $f_{1T}^{\perp a}$, g_1^a, h_1^a, $h_1^{\perp a}$, $h_{1T}^{\perp a}$ and 2 FFs D_1^a, $H_1^{\perp a}$ provide a basis. Below we shall see that, under the assumption of the validity of WW-type approximations, it is possible to express all SIDIS structure in terms of the basis functions. Notice that SIDIS alone is of course not sufficient to determine the basis functions uniquely: the 8 basis functions appear in 6 SIDIS structure functions. It is crucial to take advantage of other processes: Drell-Yan for PDFs and TMDs and hadron production in e^+e^- annihilation for FFs, though other processes play also important roles.

The basis functions allow us to describe in WW-type approximation all other TMDs, and experiments will decide how well the approximations work. In two instances, however, we know in advance of limitations, namely in the description of T-odd TMDs which appear in the decomposition of the correlator (2.11) with no prefactor of $k_\perp$. There are three cases: $f_T^a(x, k_\perp)$, $h^a(x, k_\perp)$, $e_L^a(x, k_\perp)$. Such TMDs in principle survive integration of the correlator over $k_\perp$ and would have PDF counterparts if there were not the sum rules in Eq. (2.14). These sum rules arise because hypothetical PDF versions of T-odd TMDs vanish: they have a simple straight gauge link along the lightcone, and such objects vanish due to parity and time-reversal symmetry of strong interactions. This argument does not apply to other T-odd TMDs because they drop out from the $k_\perp$-integrate correlator due to explicit factors of e.g. $k_\perp^j$ in the case of the Sivers function.

Let us first discuss the case of $f_T^a(x, k_\perp)$. Taking the WW-type approximation (3.4g) literally, implies $x \int d^2 k_\perp f_T^a(x, k_\perp) = -f_{1T}^{\perp(1)a}(x) \neq 0$ at variance with the sum rule (2.14). We have $x f_T^a(x, k_\perp) = x \tilde{f}_T^a(x, k_\perp) - f_{1T}^{\perp(1)a}(x, k_\perp)$ from QCD equations of motion [4] which yields (3.4g). The point is of course that in this case it is essential to keep the tilde-function. The situation for the chirally and T-odd twist-3 TMD $h^a(x, k_\perp)$ is completely analog. The third function in (2.14) is $e_L^a(x, k_\perp)$ and causes no issues since $e_L^a(x, k_\perp) = \tilde{e}_L^a(x, k_\perp) \approx 0$ in WW-type approximation.

Does this mean WW-type approximations fail for $f_T^a(x, k_\perp)$ and $h^a(x, k_\perp)$? Not necessarily. One has to keep in mind the formal character of the sum rules (2.14) which include integration in the large-$k_\perp$ region where the TMD description does not apply. Thus, issues with the sum rules (2.14) do not need to exclude the possibility that the WW-type approximations for $f_T^a(x, k_\perp)$ and $h^a(x, k_\perp)$ in (3.4g, 3.4h) may work at small $k_\perp$ where we use them in our TMD approach. This would mean the UV region is essential to realize the sum rules (2.14). Alternatively, one could also envision the sum rules (2.14) to be sensitive to the IR region through gluonic or fermionic pole contributions manifest in tilde-terms.

At the present stage too little is known in the theory of subleading twist TMDs. Below in Sec. 7.6 and 7.7 we will discuss how one could deal with the TMDs $f_T^a(x, k_\perp)$ and $h^a(x, k_\perp)$ phenomenologically. For now let us keep in mind that one has to keep a vigilant eye on all WW-type approximations, and especially on those for $f_T^a(x, k_\perp)$ and $h^a(x, k_\perp)$.

4   SIDIS in WW-type approximation

In this section we consequently apply the WW- and WW-type approximation to SIDIS.

4.1   Leading structure functions amenable to WW-type approximations

The WW- and WW-type approximations are useful for the following two leading-twist structure functions

$$F_{LT}^{\cos(\phi_h-\phi_S)} \overset{\mathrm{WW}}{=} \mathcal{C}\left[\omega_{\mathrm{B}}^{\{1\}}\, g_{1T}^{\perp} D_1\right]\Bigg|_{\substack{g_{1T}^{\perp a} \to g_1^a \\ \text{Eq. (3.6a)}}} \tag{4.1a}$$

$$F_{UL}^{\sin 2\phi_h} \overset{\mathrm{WW}}{=} \mathcal{C}\left[\omega_{\mathrm{AB}}^{\{2\}}\, h_{1L}^{\perp} H_1^{\perp}\right]\Bigg|_{\substack{h_{1L}^{\perp a} \to h_1^a \\ \text{Eq. (3.6b)}}} \tag{4.1b}$$

4.2   Subleading structure functions in WW-type approximations

In the case of the subleading twist structure functions the WW-type approximations in Eqs. (3.3a–3.4h) lead to considerable simplifications. We obtain the approximations

$$F_{LU}^{\sin\phi_h} \overset{\mathrm{WW}}{=} 0\,, \tag{4.2a}$$

$$F_{LT}^{\cos\phi_S} \overset{\mathrm{WW}}{=} \frac{2M}{Q}\mathcal{C}\left[-\omega^{\{0\}}\, x\, g_T D_1\right]\Bigg|_{\substack{g_T^a \to g_1^a \\ \text{Eq. (3.2a)}}}\,, \tag{4.2b}$$

$$F_{LL}^{\cos\phi_h} \overset{\mathrm{WW}}{=} \frac{2M}{Q}\mathcal{C}\left[-\omega_{\mathrm{B}}^{\{1\}}\, x g_L^{\perp} D_1\right]\Bigg|_{\substack{g_L^{\perp a} \to g_1^a \\ \text{Eq. (3.3c)}}}\,, \tag{4.2c}$$

$$F_{LT}^{\cos(2\phi_h-\phi_S)} \overset{\mathrm{WW}}{=} \frac{2M}{Q}\mathcal{C}\left[-\omega_{\mathrm{C}}^{\{2\}}\, x g_T^{\perp} D_1\right]\Bigg|_{\substack{g_T^{\perp a} \to g_1^a \\ \text{Eqs. (3.3d, 3.6a)}}}\,, \tag{4.2d}$$

$$F_{UL}^{\sin\phi_h} \overset{\mathrm{WW}}{=} \frac{2M}{Q}\mathcal{C}\left[\ \omega_{\mathrm{A}}^{\{1\}}\, x\, h_L H_1^{\perp}\right]\Bigg|_{\substack{h_L^a \to h_{1L}^{\perp a} \\ \text{with Eq. (3.3f)}}}\,, \tag{4.2e}$$

$$F_{UU}^{\cos\phi_h} \overset{\mathrm{WW}}{=} \frac{2M}{Q}\mathcal{C}\left[\ \omega_{\mathrm{A}}^{\{1\}}\, x\, h\, H_1^{\perp} - \omega_{\mathrm{B}}^{\{1\}}\, x\, f^{\perp} D_1\right]\Bigg|_{\substack{f^{\perp a} \to f_1^a,\ h^a \to h_1^{\perp a} \\ \text{with Eqs. (3.3b, 3.4h)}}}\,, \tag{4.2f}$$

$$F_{UT}^{\sin\phi_S} \overset{\mathrm{WW}}{=} \frac{2M}{Q}\mathcal{C}\left[\ \omega^{\{0\}}\, x\, f_T D_1 - \frac{\omega_{\mathrm{B}}^{\{2\}}}{2}\left(xh_T - xh_T^{\perp}\right)H_1^{\perp}\right]\Bigg|_{\substack{f_T^a \to f_{1T}^{\perp a}, \\ h_T^a - h_T^{\perp a} \to h_1^a \\ (3.4g,\ 3.3g,\ 3.3h)}}\,, \tag{4.2g}$$

$$F_{UT}^{\sin(2\phi_h-\phi_S)} \overset{\mathrm{WW}}{=} \frac{2M}{Q}\mathcal{C}\left[\omega_{\mathrm{C}}^{\{2\}}\, x\, f_T^{\perp} D_1 + \frac{\omega_{\mathrm{AB}}^{\{2\}}}{2} x(h_T + h_T^{\perp})H_1^{\perp}\right]\Bigg|_{\substack{f_T^{\perp a} \to f_{1T}^{\perp a}, \\ (h_T^a + h_T^{\perp a}) \to h_{1T}^{\perp a} \\ \text{with (3.4f, 3.3g, 3.3h)}}}\,. \tag{4.2h}$$

4.3 Phenomenological information on basis functions

We have seen that the following 6 TMDs and 2 FFs provide a basis (Sec. 3) and allow us to express all SIDIS structure functions (Sec. 4) in WW-type approximation:

$$\text{basis:} \quad f_1^a, \ f_{1T}^{\perp a}, \ g_1^a, \ h_1^a, \ h_1^{\perp a}, \ h_{1T}^{\perp a}; \ D_1^a, \ H_1^{\perp a}. \tag{4.3}$$

Phenomenological information is available for all basis functions at least to some extent. In Fig. 3 we present plots of the basis functions, and refer to App. A for details. The four functions f_1^a, g_1^a, h_1^a, D_1^a are related to twist-2 collinear functions. All collinear functions are calculated at $Q^2 = 2.4$ (GeV^2). Collinear $f_1(x)$ are from Ref. [70], $g_1(x)$ are from
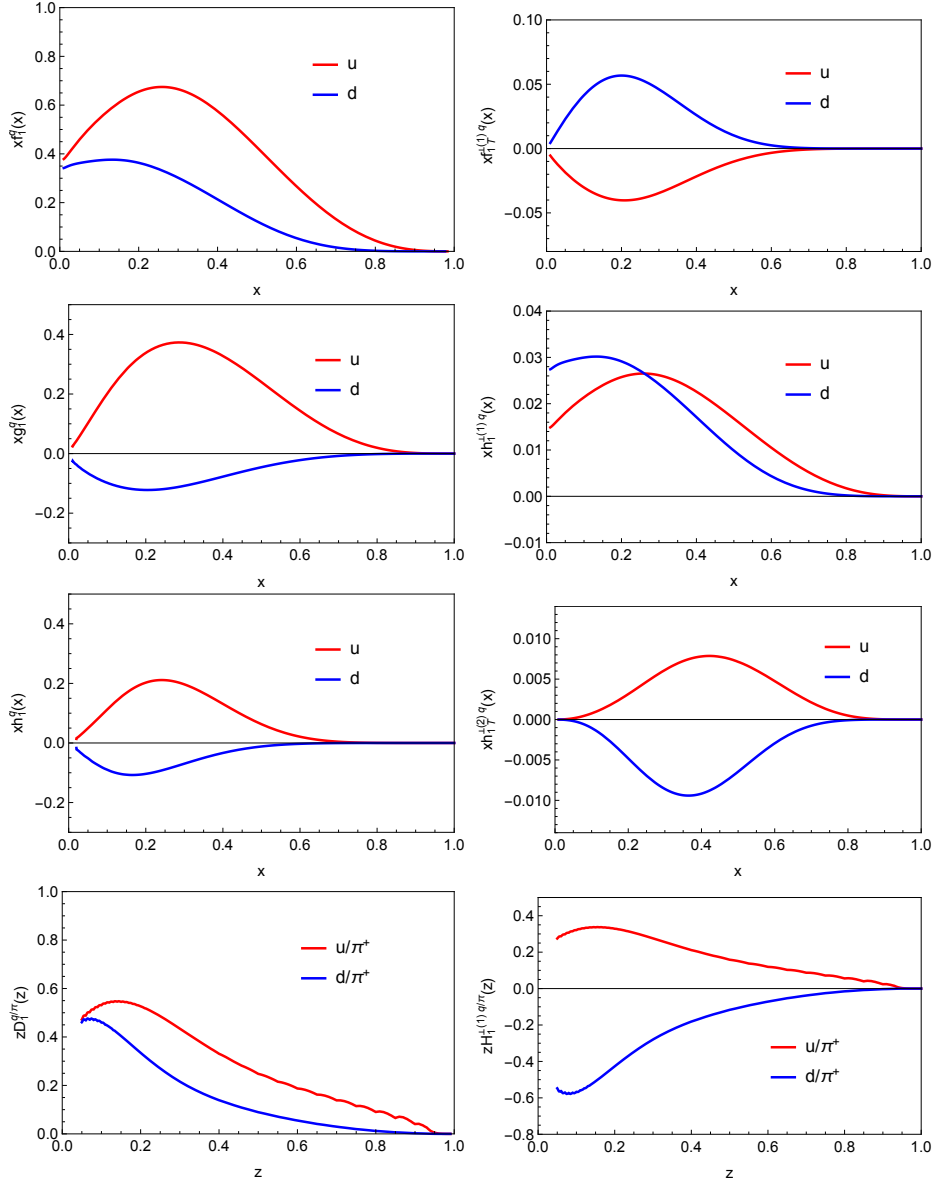
Figure 3. The basis functions f_1^a, g_1^a, h_1^a, $f_{1T}^{\perp a}$, $h_1^{\perp a}$, $h_{1T}^{\perp a}$; D_1^a, $H_1^{\perp a}$. For details see App. A.

Ref. [71], and $D_1(z)$ are from Ref. [72].The other four $f_{1T}^{\perp a}$, $h_1^{\perp a}$, $H_1^{\perp a}$ have no collinear counterparts, and we consider their (1)-moments, while for $h_{1T}^{\perp a}$ we consider the (2)-moment, such that parametrizations of TMD functions read

$$f_1^a(x, k_\perp^2) = f_1^a(x) \frac{e^{-k_\perp^2/\langle k_\perp^2\rangle_{f_1}}}{\pi \langle k_\perp^2\rangle_{f_1}} , \tag{4.4a}$$

$$D_1^a(z, P_\perp^2) = D_1^a(z) \frac{e^{-P_\perp^2/\langle P_\perp^2\rangle_{D_1}}}{\pi \langle P_\perp^2\rangle_{D_1}} , \tag{4.4b}$$

$$g_1^a(x, k_\perp^2) = g_1^a(x) \frac{e^{-k_\perp^2/\langle k_\perp^2\rangle_{g_1}}}{\pi \langle k_\perp^2\rangle_{g_1}} , \tag{4.4c}$$

$$f_{1T}^{\perp q}(x, k_\perp^2) = f_{1T}^{\perp(1)q}(x) \frac{2M^2}{\pi \langle k_\perp^2\rangle_{f_{1T}^\perp}^2} e^{-k_\perp^2/\langle k_\perp^2\rangle_{f_{1T}^\perp}} , \tag{4.4d}$$

$$h_1^q(x, k_\perp^2) = h_1^q(x) \frac{e^{-k_\perp^2/\langle k_\perp^2\rangle_{h_1}}}{\pi \langle k_\perp^2\rangle_{h_1}} , \tag{4.4e}$$

$$H_1^\perp(z, P_\perp^2) = H_1^{\perp(1)}(z) \frac{2z^2 m_h^2}{\pi \langle P_\perp^2\rangle_{H_1^\perp}^2} e^{-P_\perp^2/\langle P_\perp^2\rangle_{H_1^\perp}} , \tag{4.4f}$$

$$h_1^{\perp q}(x, k_\perp^2) = h_1^{\perp(1)q}(x) \frac{2M^2}{\pi \langle k_\perp^2\rangle_{h_1^\perp}^2} e^{-k_\perp^2/\langle k_\perp^2\rangle_{h_1^\perp}} , \tag{4.4g}$$

$$h_{1T}^{\perp q}(x, k_\perp^2) = h_{1T}^{\perp(2)q}(x) \frac{2M^4}{\pi \langle k_\perp^2\rangle_{h_{1T}^\perp}^3} e^{-k_\perp^2/\langle k_\perp^2\rangle_{h_{1T}^\perp}} , \tag{4.4h}$$

see App. A for details.

5 Leading twist asymmetries and basis functions

In this section we review how the basis functions describe available SIDIS data. This is of importance to asses the reliability of the predictions presented in the next sections.

5.1 Gauss Ansatz and F_{UU} structure function

Throughout this work we use the so-called Gauss Ansatz for the transverse momentum dependent distribution and fragmentation functions. This Ansatz is popular not only because it considerably simplifies the calculations. In fact, all convolution integrals of the type (2.17) can be solved analytically with this Ansatz. Far more important is the fact that it works phenomenologically with a good accuracy in many practical applications [73–78]. It should be kept in mind that the Gauss Ansatz can, of course, be only a rough approximation. For instance, it is not consistent with general matching expectations when $k_\perp$ becomes large [79]. Nevertheless, if one limits oneself to work in a region where the transverse momenta (of hadrons produced in SIDIS, dileptons produced in the Drell-Yan process, etc) are small with respect to the hard scale in the process, then the Ansatz works quantitatively very well. The most recent and detailed tests were reported in [76], where the Gauss Ansatz was shown to describe the most recent SIDIS data. No deviations could

be observed within the error bars of the data provided one takes into account the broadening of the Gaussian widths with increasing energy [76] according with expectations from QCD [80]. Remarkably, the Gauss Ansatz is approximately compatible with the $k_\perp$-shapes obtained from evolution [80] or fits to high-energy Tevatron data on weak-boson production [81]. On the other end, effective models at low [54, 57] and intermediate [66] energies also support it approximately.

The Gaussian Ansatz for the unpolarized TMD and unpolarized FF is given by

$$f_1^a(x, k_\perp^2) = f_1^a(x) \, \frac{e^{-k_\perp^2/\langle k_\perp^2 \rangle_{f_1}}}{\pi \langle k_\perp^2 \rangle_{f_1}} \;, \quad D_1^a(z, P_\perp^2) = D_1^a(z) \, \frac{e^{-P_\perp^2/\langle P_\perp^2 \rangle_{D_1}}}{\pi \langle P_\perp^2 \rangle_{D_1}} \;. \tag{5.1}$$

The parameters $\langle k_\perp^2 \rangle_{f_1}$ and $\langle P_\perp^2 \rangle_{D_1}$ can be assumed to be flavor- and x- or z-dependent, as present data do not allow us to constrain too many parameters, see App. A.1 for a review. This assumption can be relaxed, e.g. theoretical studies in chiral effective field theories predict a strong flavor-dependence in the $k_\perp$-behavior of sea and valence quark TMDs [82].

The structure function F_{UU} needed for our analysis reads

$$F_{UU}(x, z, P_{hT}) = x \sum_q e_q^2 \, f_1^q(x) \, D_1^q(z) \, \mathcal{G}(P_{hT}) \,, \tag{5.2a}$$

$$F_{UU}(x, z) \equiv \int d^2 P_{hT} \, F_{UU}(x, z, P_{hT}) = x \sum_q e_q^2 \, f_1^q(x) \, D_1^q(z) \,, \tag{5.2b}$$

where we introduce the notation $\mathcal{G}(P_{hT})$, which is defined as

$$\mathcal{G}(P_{hT}) = \frac{\exp(-P_{hT}^2/\lambda)}{\pi \, \lambda} \,, \quad \lambda = z^2 \, \langle k_\perp^2 \rangle_{f_1} + \langle P_\perp^2 \rangle_{D_1} \,, \tag{5.3}$$

with the understanding that the convenient abbreviation λ is expressed in terms of the Gaussian widths of the *preceding* TMD and FF. Notice that $\mathcal{G}(P_{hT}) \equiv \mathcal{G}(x, z, P_{hT})$ and that in general $\mathcal{G}(P_{hT})$ appears under the flavor sum due to a possible flavor-dependence of the involved Gaussian widths. The normalization $\int d^2 P_{hT} \, \mathcal{G}(P_{hT}) = 1$ correctly connects the structure function $F_{UU}(x, z, P_{hT})$ in (5.2a) with its P_{hT}-integrated counterpart (5.2b). In our effective description this is step is trivial. In QCD the connection of TMDs to PDFs is far more subtle [83]. Fig. 4 illustrates how the Gauss Ansatz describes selected SIDIS data. In Fig. 4 (b) we plot HERMES multiplicity [84]

$$M_n^h(x, z, P_{hT}) \equiv 2\pi P_{hT} \frac{F_{UU}(x, z, P_{hT})}{x \sum_q e_q^2 \, f_1^q(x)} \tag{5.4}$$

at $\langle Q^2 \rangle = 2.87 \, \text{GeV}^2$, $\langle x \rangle = 0.15$, $\langle z \rangle = 0.22$ for π^+ production on the proton target. In Fig. 4 (c) we plot COMPASS multiplicity [85]

$$n^h(x, z, P_{hT}) \equiv \pi \frac{F_{UU}(x, z, P_{hT})}{x \sum_q e_q^2 \, f_1^q(x)} \tag{5.5}$$

at $\langle Q^2 \rangle = 20 \, \text{GeV}^2$, $\langle x \rangle = 0.15$, $\langle z \rangle = 0.2$ for h^+ production on the deuterium target.

To streamline the presentation we refer to the comprehensive Appendix on the used parametrizations (App. A), and for technical details on the Gauss Ansatz (App. B).
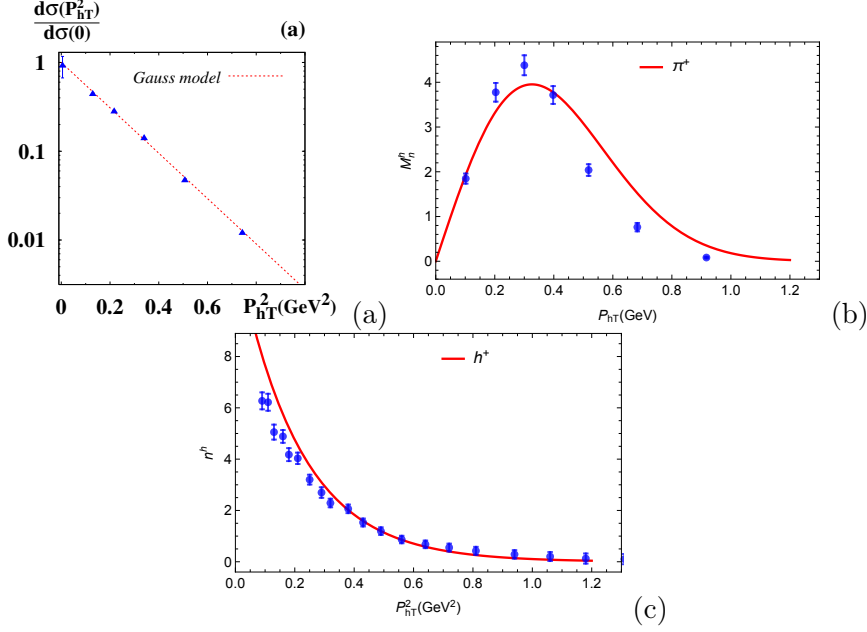
Figure 4. Examples of the description of transverse momenta of hadrons in unpolarized SIDIS. (a) Differential cross section at $\langle Q^2 \rangle = 2.37\,\text{GeV}^2$, $\langle x \rangle = 0.24$, $\langle z \rangle = 0.30$ measured at JLab with a 5.75 GeV beam [86]. Theoretical curve from Gauss model following Ref. [76]. (b) Example for HERMES multiplicities [84] at $\langle Q^2 \rangle = 2.87\,\text{GeV}^2$, $\langle x \rangle = 0.15$, $\langle z \rangle = 0.22$. (b) Example for COMPASS multiplicities [85] at $\langle Q^2 \rangle = 20\,\text{GeV}^2$, $\langle x \rangle = 0.15$, $\langle z \rangle = 0.2$.

5.2   Leading twist A_{LL}: first test of intrinsic $k_\perp$ beyond unpolarized case

In this Section we discuss the leading twist double spin asymmetry $A_{LL} \propto g_1^a D_1^a$ which does not require a WW-type approximation but is important for two reasons. First, we review one of our "basis functions" $g_1^a(x)$, and similarly we will review below also other "basis functions." Second, throughout this work we use the Gaussian Ansatz demonstrated to provide good services in unpolarized case [73–78]. However, nothing is known about the applicability of the Gaussian Ansatz in polarized case. The JLab data [87] on $A_{LL}(P_{hT})$ put us in the position to conduct a first "test" of our understanding of the $k_\perp$-behavior of polarized partons. To have an "informed idea" about the Gaussian width of $g_1(x, k_\perp)$ we will explore information from the exploratory lattice QCD study of TMDs [40].

We assume Gaussian form for $g_1^a(x, k_\perp^2)$

$$g_1^a(x, k_\perp^2) = g_1^a(x)\, \frac{e^{-k_\perp^2/\langle k_\perp^2 \rangle_{g_1}}}{\pi \langle k_\perp^2 \rangle_{g_1}}\ , \tag{5.6}$$

and resort to the lattice QCD results [40] to gain an estimate on width $\langle k_\perp^2 \rangle_{g_1}$, see App. A.2.

With $\lambda = z^2 \langle k_\perp^2 \rangle_{g_1} + \langle P_\perp^2 \rangle_{D_1}$ implicit in $\mathcal{G}(P_{hT})$, the structure function F_{LL} reads

$$F_{LL}(x, z, P_{hT}) = x \sum_q e_q^2\, g_1^q(x)\, D_1^q(z)\, \mathcal{G}(P_{hT})\,, \tag{5.7a}$$

$$F_{LL}(x, z) = x \sum_q e_q^2\, g_1^q(x)\, D_1^q(z)\,, \tag{5.7b}$$
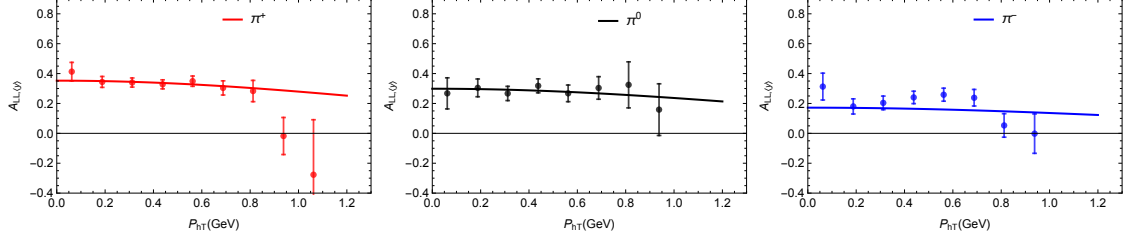
Figure 5. $A_{LL,\langle y \rangle}$ asymmetry compared with Jefferson Lab experimental results Ref. [87] for π^+ (left panel) and π^- (right panel). Solid lines are computations with mean values of kinematic variables $\langle x \rangle = 0.25$, $\langle z \rangle = 0.5$, $\langle Q^2 \rangle = 1.7$ GeV^2.

The first experimental results on the P_{hT}-dependence of $A_{LL} = F_{LL}/F_{UU}$ were presented by Jefferson Lab [87]. The definition of the asymmetry in [87] was

$$A_{LL,\langle y \rangle}(x, z, P_{hT}) = \langle p_2 \, A_{LL}(x, z, P_{hT}) \rangle \; = \; \frac{\langle y(2 - y) \, F_{LL}(x, z, P_{hT}) \rangle}{\langle (1 + (1 - y)^2) \, F_{UU}(x, z, P_{hT}) \rangle} \tag{5.8}$$

where $p_2 = y(2-y)/(1+(1-y)^2)$ and averaging (separately in numerator and denominator) over the kinematics of [87] is implied. We compare our results for $A_{LL,\langle y \rangle}(P_{hT})$ to Jefferson Lab data [87] in Fig. 5.

In our approach we use lattice results from [40] to constrain the Gaussian width $\langle k_\perp^2 \rangle_{g_1}$, see App. A.2. All other ingredients in (5.8) are known and tested through other observables, see Sec. 5.1. Therefore Fig. 5 provides several important tests. First, the Jefferson Lab data [87] is compatible with the Gauss Ansatz within error bars. Second, the lattice QCD results in the way we use them in App. A.2 give an appropriate description of these data.[2]

Encouraged by these findings we will use lattice predictions from Ref. [40] below also for the Gaussian widths of $g_{1T}^{\perp(1)a}$ and $h_{1L}^{\perp(1)a}$. Of course, at this point one could argue that the WW- and WW-type approximations (3.6a, 3.6a) also dictate that $g_{1T}^\perp$ and $h_{1L}^\perp$ have the same Gaussian widths as g_1 and h_1. In fact, the lattice results for the respective widths are numerically similar, which can be interpreted as yet another argument in favor of the usefulness of the approximations. The practical predictions depend only weakly on the choice of parameters.

---

[2] Another important test was already presented in [87]: the P_{hT}-integrated ("collinear") asymmetry (5.7b) is compatible with data from other experiments and with theoretical results obtained from parametrizations of $f_1^a(x)$, $g_1^a(x)$, $D_1^a(z)$. This shows that even at the moderate beam energies of the pre-12GeV era one was indeed already probing DIS at Jefferson Lab, at least to a very good approximation [87].

5.3 Leading twist $A_{UT}^{\sin(\phi_h - \phi_S)}$ Sivers asymmetry

The $F_{UT}^{\sin(\phi_h - \phi_S)}$ modulation of SIDIS cross section is related to the Sivers function [88], which describes the number density of unpolarized quarks inside a transversely polarized proton, has so far received the widest attention, from both phenomenological and experimental points of view.

The Sivers function $f_{1T}^{\perp}$ is related to initial and final state interactions of the struck quark and the rest of the nucleon and could not exist without the contribution of the orbital angular momentum of partons to the spin of the nucleon. As such it encodes the correlation between the partonic intrinsic motion and the transverse spin of the nucleon, and it generates a dipole deformation in momentum space.

Over the years, the Sivers function has been extracted from SIDIS data by several groups, with consistent results [74, 89–95].

The structure function $F_{UT}^{\sin(\phi_h - \phi_S)}$ reads

$$F_{UT}^{\sin(\phi_h - \phi_S)}(x, z, P_{hT}) = -x \sum_q e_q^2 \, f_{1T}^{\perp(1)q}(x) \, D_1^q(z) \, b_{\mathrm{B}}^{(1)} \left(\frac{z P_{hT}}{\lambda} \right) \mathcal{G}(P_{hT}), \quad (5.9\text{a})$$

$$F_{UT}^{\sin(\phi_h - \phi_S)}(x, z, \langle P_{hT} \rangle) = -x \sum_q e_q^2 \, f_{1T}^{\perp(1)q}(x) \, D_1^q(z) \, c_{\mathrm{B}}^{(1)} \left(\frac{z}{\lambda^{1/2}} \right), \quad (5.9\text{b})$$

where $\lambda = z^2 \langle k_\perp^2 \rangle_{f_{1T}^\perp} + \langle P_\perp^2 \rangle_{D_1}$ and $b_{\mathrm{B}}^{(1)} = 2 M_N$ and $c_{\mathrm{B}}^{(1)} = \sqrt{\pi} \, M_N$, see App. B.3 for details.

Notice that integrating structure functions over P_{hT} is different from integrating the cross section over P_{hT} where azimuthal hadron modulations drop out. Only if the relevant weight is $\omega^{\{0\}}$ we obtain "collinear structure functions:" $F_{UU}(x, z)$, $F_{LL}(x, z)$ in Secs. 5.1, 5.2 and below in Secs. 7.2, 7.6. In all other cases, despite integration over P_{hT}, we end up always with true convoluted TMDs (here within Gauss model). We stress this important point by displaying the dependence of the structure functions on the mean hadron momenta, for instance $F_{UT}^{\sin(\phi_h - \phi_S)}(x, z, \langle P_{hT} \rangle) = \int d^2 P_{hT} F_{UT}^{\sin(\phi_h - \phi_S)}(x, z, P_{hT})$ in (5.9b).

The asymmetries $A_{UT}^{\sin(\phi_h - \phi_S)} = F_{UT}^{\sin(\phi_h - \phi_S)}/F_{UU}$ and comparison to HERMES data [96] are plotted in Fig. 6.
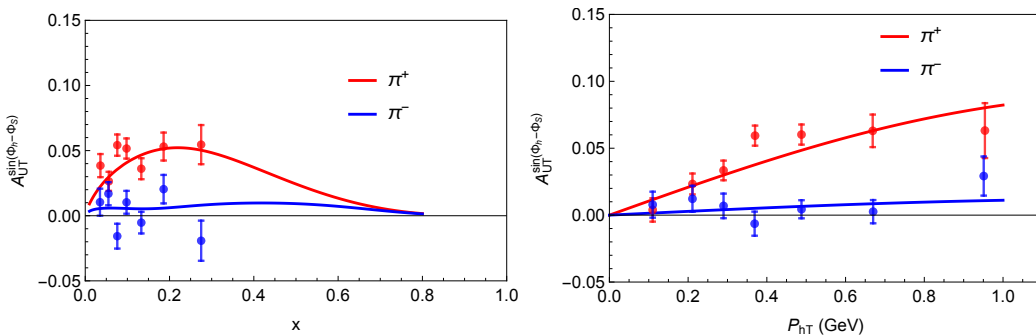
Figure 6. Comparison of calculation of $A_{UT}^{\sin(\phi_h - \phi_S)}$ using fit results of Ref. [97] as a function of x (left panel), and as a function of P_{hT} (right panel) at $\langle x \rangle = 0.15$, $\langle z \rangle = 0.34$, $\langle Q^2 \rangle = 2.4$ GeV^2 and HERMES data [96].

5.4 Leading twist $A_{UT}^{\sin(\phi_h+\phi_S)}$ Collins asymmetry

The $F_{UT}^{\sin(\phi_h+\phi_S)}$ modulation of the SIDIS cross section is due to convolution of the transversity distribution h_1, which is the only source of information on the tensor charge of the nucleon, and the Collins FF $H_1^\perp$, that decodes the fundamental correlation between the transverse spin of a fragmenting quark and the transverse momentum of the final produced hadron.

There are many extractions of h_1 and $H_1^\perp$ from a combined fit of SIDIS and e^+e^- data, for instance those of Refs. [98–100].
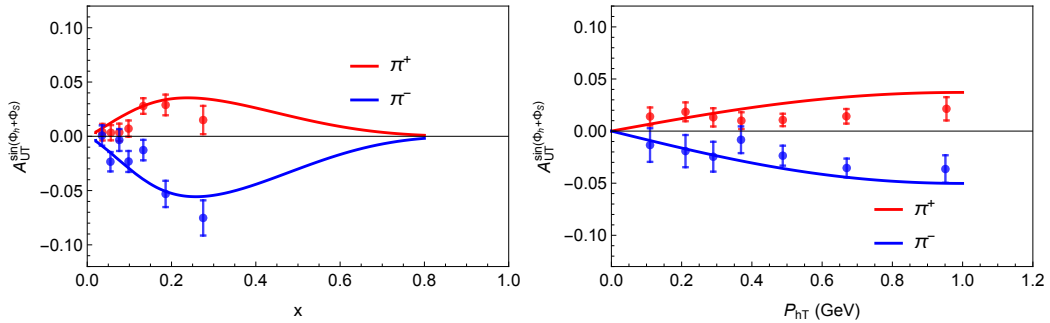
The structure function $F_{UT}^{\sin(\phi_h+\phi_S)}$ reads

$$F_{UT}^{\sin(\phi_h+\phi_S)}(x, z, P_{hT}) = x \sum_q e_q^2\, h_1^q(x)\, H_1^{\perp(1)q}(z)\, b_{\mathrm{A}}^{(1)} \left(\frac{z P_{hT}}{\lambda} \right) \mathcal{G}(P_{hT}), \quad (5.10\text{a})$$

$$F_{UT}^{\sin(\phi_h+\phi_S)}(x, z, \langle P_{hT}\rangle) = x \sum_q e_q^2\, h_1^q(x)\, H_1^{\perp(1)q}(z)\, c_{\mathrm{A}}^{(1)} \left(\frac{z}{\lambda^{1/2}} \right), \quad (5.10\text{b})$$

where $\lambda = z^2 \langle k_\perp^2 \rangle_{h_1} + \langle P_\perp^2 \rangle_{H_1^\perp}$ and $b_{\mathrm{A}}^{(1)} = 2m_h$ and $c_{\mathrm{A}}^{(1)} = \sqrt{\pi}\, m_h$, see App. B.3 for details.

The asymmetries $A_{UT}^{\sin(\phi_h+\phi_S)} = F_{UT}^{\sin(\phi_h+\phi_S)}/F_{UU}$ and comparison to HERMES data [101] are plotted in Fig. 7.

Figure 7. Comparison of calculation of $A_{UT}^{\sin(\phi_h+\phi_S)}$ using fit results of Ref. [98] as a function of x (left panel), and as a function of P_{hT} (right panel) at $\langle x \rangle = 0.15$, $\langle z \rangle = 0.34$, $\langle Q^2 \rangle = 2.4$ GeV^2 and HERMES data [96].

## 5.5 Leading twist $A_{UU}^{\cos(2\phi_h)}$ Boer-Mulders asymmetry

The structure function $F_{UU}^{\cos(2\phi_h)}$ reads

$$F_{UU}^{\cos(2\phi_h)}(x, z, P_{hT}) = x \sum_q e_q^2\, h_1^{\perp(1)q}(x)\, H_1^{\perp(1)q}(z)\, b_{\mathrm{AB}}^{(2)} \left(\frac{z P_{hT}}{\lambda} \right)^2 \mathcal{G}(P_{hT}), \quad (5.11\mathrm{a})$$

$$F_{UU}^{\cos 2\phi_h}(x, z, \langle P_{hT} \rangle) = x \sum_q e_q^2\, h_1^{\perp(1)q}(x)\, H_1^{\perp(1)q}(z)\, c_{\mathrm{AB}}^{(2)} \left(\frac{z}{\lambda^{1/2}} \right)^2, \quad (5.11\mathrm{b})$$

where $\lambda = z^2 \langle k_\perp^2 \rangle_{h_1^\perp} + \langle P_\perp^2 \rangle_{H_1^\perp}$ and $b_{\mathrm{AB}}^{(2)} = 4 M_N m_h$ and $c_{\mathrm{AB}}^{(2)} = 4 M_N m_h$, see App. B.3.

Asymmetries $A_{UU}^{\cos(2\phi_h)} = F_{UU}^{\cos(2\phi_h)} / F_{UU}$ for HERMES are plotted in Fig. 8. In the Fig. 8 we plot only the Boer-Mulders contribution to $A_{UU}^{\cos(2\phi_h)}$ which does not describe the data accurately. In fact, it is suspected that this observable receives a significant contribution from the Cahn effect [104], a term of higher twist character of the type $\langle P_{hT}^2 \rangle / Q^2$ which is not negligible in fixed target experiments [76]. This contribution was estimated and corrected for in the phenomenological works [102, 105, 106] which was of importance to obtain a picture of the Boer-Mulders function undistorted from Cahn effect. The point is that this substantial twist-4 contamination can be estimated phenomenologically, even though there is no rigorous theoretical basis for the description of such power-suppressed terms. In this work we consistently neglect power-suppressed contributions of order $1/Q^2$, and do so also in Fig. 8. Nevertheless we of course use the parametrizations of [102, 105, 106] offering the best currently available parametrizations for $h_1^\perp$ which were corrected for Cahn effect as good as it is possible at the current stage of art. It is unknown whether other asymmetries could be similarly effected by such type of power-corrections. This is an important point to be kept in mind as the lesson from Fig. 8 shows.
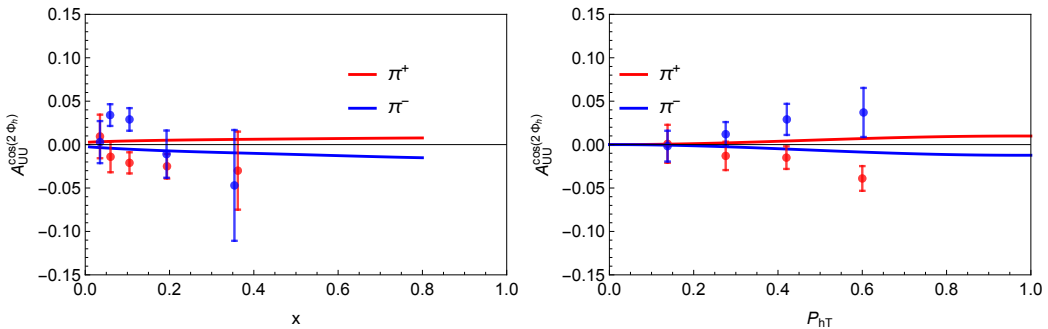
Figure 8. Comparison of calculation of $A_{UU}^{\cos(2\phi_h)}$ using fit results of Ref. [102] as a function of x (left panel), and as a function of P_{hT} (right panel) at $\langle x \rangle = 0.15$, $\langle z \rangle = 0.34$, $\langle Q^2 \rangle = 2.4$ GeV^2 and HERMES data [103].

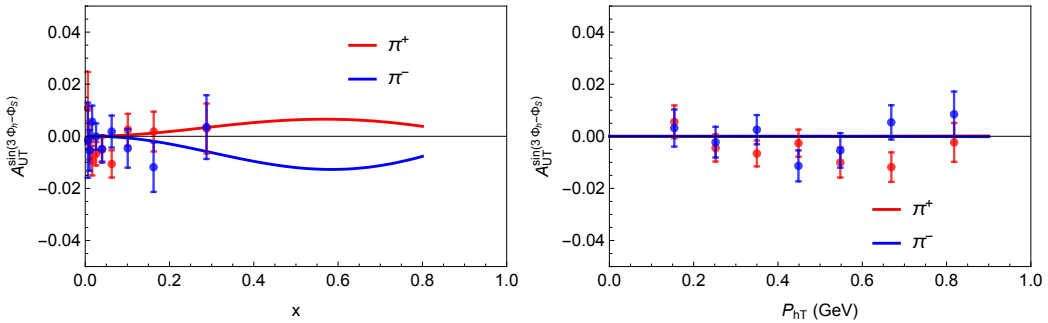## 5.6 Leading twist $A_{UT}^{\sin(3\phi_h-\phi_S)}$ asymmetry

The structure function $F_{UT}^{\sin(3\phi_h-\phi_S)}$ reads

$$F_{UT}^{\sin(3\phi_h-\phi_S)}(x,z,P_{hT}) = x\sum_q e_q^2\, h_{1T}^{\perp(2)q}(x)\, H_1^{\perp(1)q}(z)\, b^{(3)}\left(\frac{zP_{hT}}{\lambda}\right)^3 \mathcal{G}(P_{hT})\,, \quad (5.12a)$$

$$F_{UT}^{\sin(3\phi_h-\phi_S)}(x,z,\langle P_{hT}\rangle) = x\sum_q e_q^2\, h_{1T}^{\perp(2)q}(x)\, H_1^{\perp(1)q}(z)\, c^{(3)}\left(\frac{z}{\lambda^{1/2}}\right)^3\,, \quad (5.12b)$$

where $\lambda = z^2\langle k_\perp^2\rangle_{h_{1T}^\perp} + \langle P_\perp^2\rangle_{H_1^\perp}$ and $b^{(3)} = 2M_N^2 m_h$ and $c^{(3)} = 3/2\sqrt{\pi}\,M_N^2 m_h$, see App. B.3.

Asymmetries $A_{UT}^{\sin(3\phi_h-\phi_S)} = F_{UT}^{\sin(3\phi_h-\phi_S)}/F_{UU}$ for COMPASS data [107] are plotted in Fig. 9. Clearly, the pretzelosity TMD is the least known of the basis TMDs. Nevertheless it is of fundamental importance, as it provides one of the basis functions in our approach. It is so difficult to access it experimentally, because its contribution to the SIDIS cross section is proportional to P_{hT}^3, the TMD approach requires us to necessarily operate at $P_{hT} \ll Q$, and so far only moderate values of Q could be achieved in the fixed target experiments. A notable exception is COMPASS where the largest x-bins (where Q^2 is largest) bear the best hints on this TMD, see Fig. 9. Future high luminosity data from Jefferson Lab 12 are expected to significantly improve our knowledge of this TMD.

Figure 9. Comparison of calculation of $A_{UT}^{\sin(3\phi_h-\phi_S)}$ using fit results of Ref. [108] as a function of x (left panel), and as a function of P_{hT} (right panel) at $\langle x\rangle = 0.15$, $\langle z\rangle = 0.34$, $\langle Q^2\rangle = 2.4$ GeV^2 and preliminary COMPASS data [107].

6 Leading twist asymmetries in WW-type approximation

Two out of the 8 leading-twist structure functions can be described in the WW-type approximation thanks to the relations (3.6a, 3.6b) which allow us to express $g_{1T}^{\perp(1)q}(x)$ and $h_{1L}^{\perp(1)q}(x)$ on the basis of available information on $g_1^q(x)$ and $h_1^a(x)$, see Fig. 10. In this section we discuss the associated asymmetries.
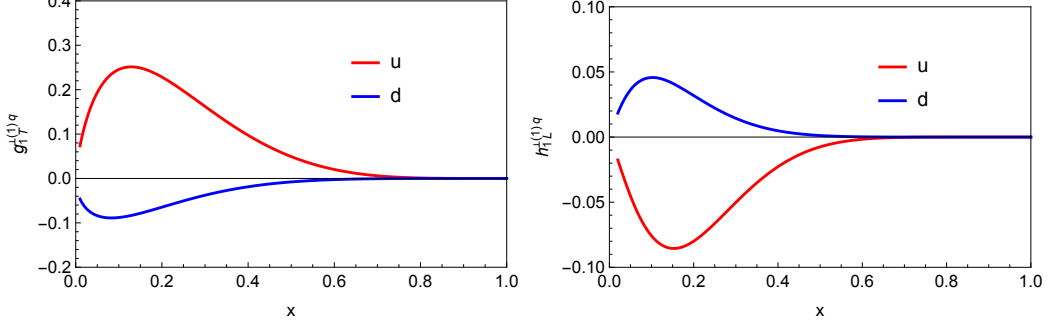
Figure 10. $g_{1T}^{\perp(1)q}(x)$ (left panel) and $h_{1L}^{\perp(1)q}(x)$ distributions (right panel) for u- and d-flavor.

6.1 Leading twist $A_{LT}^{\cos(\phi_h-\phi_S)}$

We assume for $g_{1T}^\perp$ the Gaussian Ansatz as follows [22]

$$g_{1T}^{\perp q}(x,k_\perp^2) = g_{1T}^{\perp(1)q}(x)\, \frac{2M^2}{\pi \langle k_\perp^2 \rangle_{g_{1T}^\perp}^2}\, e^{-k_\perp^2/\langle k_\perp^2 \rangle_{g_{1T}^\perp}}\ , \tag{6.1}$$

and evaluate $g_{1T}^{\perp(1)q}(x)$ using Eq. (3.6a) which yields the result shown in Fig. 10. For our numerical estimates we use $\langle k_\perp^2 \rangle_{g_{1T}^\perp} = \langle k_\perp^2 \rangle_{g_1}$ which is supported by lattice results [40].

In the Gauss Ansatz the structure function $F_{LT}^{\cos(\phi_h-\phi_S)}$ has the form

$$F_{LT}^{\cos(\phi_h-\phi_S)}(x,z,P_{hT}) = x \sum_q e_q^2\, g_{1T}^{\perp(1)q}(x)\, D_1^q(z)\, b_{\rm B}^{(1)}\left(\frac{zP_{hT}}{\lambda}\right) \mathcal{G}(P_{hT}) \tag{6.2a}$$

$$F_{LT}^{\cos(\phi_h-\phi_S)}(x,z,\langle P_{hT} \rangle) = x \sum_q e_q^2\, g_{1T}^{\perp(1)q}(x)\, D_1^q(z)\, c_{\rm B}^{(1)}\left(\frac{z}{\lambda^{1/2}}\right) \tag{6.2b}$$

where $\lambda = z^2 \langle k_\perp^2 \rangle_{g_{1T}^\perp} + \langle P_\perp^2 \rangle_{D_1}$, $b_{\rm B}^{(1)} = 2M_N$, $c_{\rm B}^{(1)} = \sqrt{\pi}\, M_N$, see App. B.3 for details. The $g_{1T}^{\perp q}$ and the Sivers function $f_{1T}^{\perp q}$ are both constrained by the positivity bound [10]

$$\frac{k_\perp^2}{M^2}\left((g_{1T}^{\perp q}(x,k_\perp^2))^2 + (f_{1T}^{\perp q}(x,k_\perp^2))^2 \right) \le (f_1^q(x,k_\perp^2))^2 \tag{6.3}$$

so that using our Gaussian parametrizations from Eqs. (5.1,6.1,A.5) one has

$$\frac{(f_1^q(x))^2}{16\pi M^2} - \frac{(f_{1T}^{\perp q}(x))^2}{4\pi \langle k_\perp^2 \rangle_{f_{1T}^\perp}} - \frac{(g_{1T}^{\perp q}(x))^2}{4\pi \langle k_\perp^2 \rangle_{g_{1T}^\perp}} \ge 0 \tag{6.4}$$

see Fig. 11 where RHS of this equation multiplied by $16\pi M^2$ is shown.

The asymmetry $A_{LT}^{\cos(\phi_h-\phi_S)}$ as a function of x for COMPASS is plotted in Fig. 12.
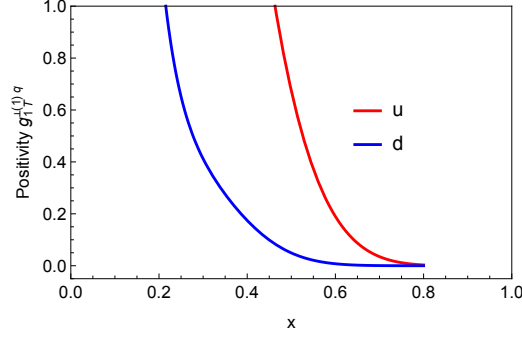
Figure 11. LHS of Eq. (6.4).
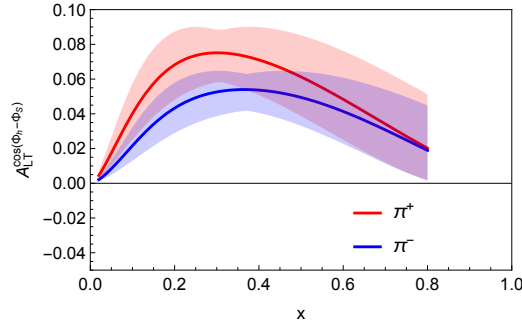
Figure 12. $A_{LT}^{\cos(\phi_h-\phi_S)}$ as a function of x at typical kinematics of COMPASS, $\langle x \rangle = 0.05$, $\langle z \rangle = 0.36$, $\langle Q^2 \rangle = 2.4$ GeV^2.

Can we compare here to COMPASS data from [109]?

6.2 Leading twist $A_{UL}^{\sin 2\phi_h}$ Kotzinian-Mulders asymmetry

We assume Gaussian form for Kotzinian-Mulders function $h_{1L}^{\perp a}$:

$$h_{1L}^{\perp a}(x, k_\perp^2) = h_{1L}^{\perp(1)a}(x) \frac{2M^2}{\pi \langle k_\perp^2 \rangle_{h_{1L}^\perp}^2} e^{-k_\perp^2 / \langle k_\perp^2 \rangle_{h_{1L}^\perp}^2} , \tag{6.5}$$

We will use WW-type approximation from Eq. (3.6b) for calculation of $h_{1L}^{\perp(1)a}(x)$ and for the estimates of the asymmetry $\langle k_\perp^2 \rangle_{h_{1L}^\perp} = \langle k_\perp^2 \rangle_{h_1} = 0.25$ (GeV^2). Notice that the Kotzinian-Mulders function and $h_{1L}^{\perp q}$ obey the positivity bound [10]

$$\frac{k_\perp^2}{M^2} \left((h_{1L}^{\perp q}(x, k_\perp^2))^2 + (h_1^{\perp q}(x, k_\perp^2))^2 \right) \leq (f_1^q(x, k_\perp^2))^2 . \tag{6.6}$$

so that using our Gaussian parametrizations from Eqs. (5.1,6.5,A.18) one has

$$\frac{(f_1^q(x))^2}{16\pi M^2} - \frac{(h_1^{\perp q}(x))^2}{4\pi \langle k_\perp^2 \rangle_{h_1^\perp}} - \frac{(h_{1L}^{\perp q}(x))^2}{4\pi \langle k_\perp^2 \rangle_{h_{1TL}^\perp}} \geq 0 \tag{6.7}$$

which, multiplied by $16\pi M^2$, is plotted in Fig. 13. Notice that for d-quark the positivity is violated that may be due to the big Boer-Mulders d-quark function from Ref. [102]. As far

as determination of the size of Boer-Mulders functions is far from ideal, we cautiously keep the present result. Future determinations of Boer-Mulders functions will help to clarify the issue of positivity constraints.

The structure function $F_{UL}^{\sin(2\phi_h)}$ reads

$$F_{UL}^{\sin(2\phi_h)}(x, z, P_{hT}) = x \sum_q e_q^2\, h_{1L}^{\perp(1)q}(x)\, H_1^{\perp(1)q/h}(z) \left(\frac{z P_{hT}}{\lambda}\right)^2 b_{AB}^{(2)}\, \mathcal{G}(P_{hT}), \quad (6.8a)$$

$$F_{UL}^{\sin(2\phi_h)}(x, z, \langle P_{hT}\rangle) = x \sum_q e_q^2\, h_{1L}^{\perp(1)q}(x)\, H_1^{\perp(1)q/h}(z) \left(\frac{z}{\lambda^{1/2}}\right)^2 c_{AB}^{(2)}, \qquad (6.8b)$$

where $\lambda = z^2 \langle k_\perp^2 \rangle_{h_{1L}^\perp} + \langle P_\perp^2 \rangle_{H_1^\perp}$ and $b_{AB}^{(2)} = c_{AB}^{(2)} = 4 M_N m_h$, see App. B.3 for details.

Resulting distributions $h_{1L}^{\perp(1)q}(x)$ are plotted in Fig. 10. The asymmetries $A_{UL}^{\sin(2\phi_h)} = F_{UL}^{\sin(2\phi_h)}/F_{UU}$ for Jefferson Lab 12 GeV are plotted in Fig. 14.
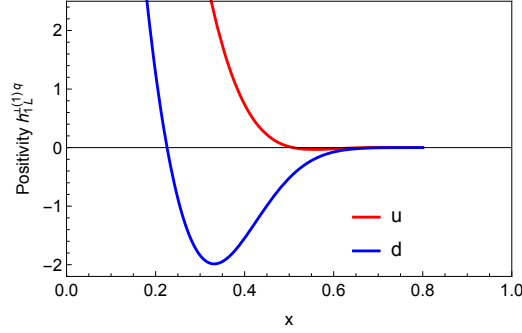
Figure 13. LHS of Eq. (6.7).
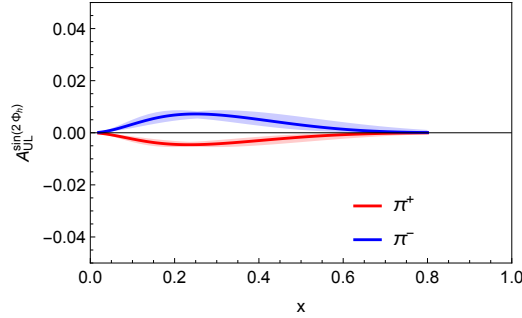
Figure 14. $A_{UL}^{\sin(2\phi_h)}$ as a function of x at typical kinematics of COMPASS, $\langle x \rangle = 0.05$, $\langle z \rangle = 0.36$, $\langle Q^2 \rangle = 2.4$ GeV^2.

7 Subleading twist asymmetries in WW-type approximation

The WW-type approximations are useful for all 8 subleading-twist observables, as shown in Sec. 4.2. In view of the complex structure of subleading-twist structure functions, WW-type approximations might be particularly useful for the interpretation of twist-3 observables.

7.1 Subleading twist $A_{LU}^{\sin \phi_h}$

We start our discussion with the structure function $F_{LU}^{\sin \phi_h}$, Eq. (2.19b), containing 4 terms: 2 are proportional to pure twist-3 fragmentation functions $\tilde{G}^{\perp a}$ and $\tilde{E}^a$ and neglected; the other 2 terms are proportional to the twist-3 TMDs e^a and $g^{\perp a}$ which also turn out to be given in terms of pure twist-3 terms upon the inspection of Eqs. (3.3a, 3.4d). Hence, after consequently applying the WW-type approximation we are left with no term. Our approximation predicts this structure function to be zero.

Instead, data from Jefferson Lab and HERMES show a small but clearly non-zero effect of the order of (2-3) % [110–115]. What may seem at first glance to be a failure of the approach is in fact in line with it. The important point is that in this case, the entire effect is due to $\bar{q}gq$-terms only. More precisely, the numerator of the asymmetry is proportional to $\bar{q}gq$-correlators, while the denominator is of course give by $f_1^a D_1^a$, i.e. in terms of qq-correlators. Therefore we may formulate this approximation as follows

$$A_{LU}^{\sin \phi_h} \quad \propto \quad \frac{\langle \bar{q}gq \rangle}{\langle \bar{q}q \rangle} \quad \overset{\exp}{=} \quad \mathcal{O}\left((2-3)\,\% \right). \tag{7.1}$$

We should keep in mind several reservations. First, the experimental result quoted in (7.1) contains also kinematic prefactors which help to reduce the value. Second, the denominator contains f_1^a and D_1^a which are the largest TMD and FF because of positivity constraints. Third, the numerator is a sum of 4 terms, so its overall smallness could also result from cancellation of different terms, rather than indicating that all 4 terms are small. Keeping these reservations cautiously in mind, we may nevertheless consider the experimental observation of a (2-3) % asymmetry $A_{LU}^{\sin \phi_h}$ [110–115] as an encouraging indication that $\bar{q}gq$-terms are smaller than $\bar{q}q$ terms, in line with the generic expectation (3.1).

To conclude, the WW-type approximation does not fail in the case of $F_{LU}^{\sin \phi}$. This is a unique observable, the only twist-3 SIDIS structure not "contaminated" by leading twist terms. Our WW-type approximation qualitatively predicts the asymmetry $A_{LU}^{\sin \phi}$ to be small which is in agreement with experiment. It is beyond our approach to make in this case a quantitative prediction. We notice that one obtains a zero result for this asymmetry also in the parton model motivated approach limited to leading twist TMDs [116].

COMPASS: https://arxiv.org/pdf/1401.6284.pdf
data: https://hepdata.net/record/ins1278730

7.2 Subleading twist $A_{LT}^{\cos\phi_S}$

In the WW-type approximation the structure function $F_{LT}^{\cos\phi_S}$ is due to $g_T^a(x, k_\perp)$ and $D_1^a(z, P_\perp)$ whose collinear counterparts are more or less well known, see Secs. 3.4 and 5.1.

We assume the Gaussian Ansatz for $g_T^a(x, k_\perp)$

$$g_T^q(x, k_\perp^2) = g_T^q(x) \frac{1}{\pi\langle k_\perp^2\rangle_{g_T}} e^{-k_\perp^2/\langle k_\perp^2\rangle_{g_T}}, \tag{7.2}$$

where $g_T^q(x)$ is calculated according to Eq. 3.2a. Notice that we could have used WW-type relation of Eq. (3.3f) to relate $g_T^q(x, k_\perp^2)$ and $g_{1T}^{\perp q}(x, k_\perp^2)$ however we choose not to do it. In fact Eq. (3.3f) suggests kinematical zero $g_T^q(x, 0) = 0$ which is not supported by the model calculations [54] and thus Eq. (3.3f) can be used only in its integrated form. The Eq. (3.3f) is not exact and is not on the same footing as WW-approximation of Eq. (3.2a), and we parametrize directly $g_T^q(x, k_\perp^2)$ using the Gaussian shape. For illustrative purpose we show "violation" of Eq. (3.3f) in Fig. 16.

$F_{LT}^{\cos\phi_S}$ structure function then reads

$$F_{LT}^{\cos\phi_S}(x, z, P_{hT}) = -\frac{2M}{Q} x^2 \sum_q e_q^2 \, g_T^q(x) \, D_1^q(z) \, \mathcal{G}(P_{hT}), \tag{7.3a}$$

$$F_{LT}^{\cos\phi_S}(x, z) = -\frac{2M}{Q} x^2 \sum_q e_q^2 \, g_T^q(x) \, D_1^q(z), \tag{7.3b}$$

with the width $\lambda = z^2\langle k_\perp^2\rangle_{g_T} + \langle P_\perp^2\rangle_{D_1}$ in the Gaussian $\mathcal{G}(P_{hT})$. We estimate $g_T^a(x)$ in terms of $g_1^a(x)$ according to Eq. (3.2a) assuming for the Gaussian width $\langle k_\perp^2\rangle_{g_T} = \langle k_\perp^2\rangle_{g_1}$.[3]

Asymmetries $A_{LT}^{\cos\phi_S} = F_{LT}^{\cos\phi_S}/F_{UU}$ for COMPASS are plotted in Fig. 15. Notice that the asymmetry scales at small transverse hadron momenta as $A_{LT}^{\cos\phi_S} \propto (P_{hT})^0$ which makes it easier to measure if longitudinally polarized lepton beams and transversely polarized targets are available.

We should include a comparison to COMPASS data [107, 109].

---

[3] Notice that one could also proceed in a different way: explore first the WW-type-relation (3.3e), and assume then the Gauss Ansatz for $g_{1T}^\perp(x, k_\perp)$ according to (6.1). Solving then the convolution integral yields a result different from (7.3a) which depends much more strongly on Gaussian model parameters. The operations of applying the WW-type approximations and employing the Gauss Ansatz do not commute in general. The solution presented in (7.3a) is preferable as it helps to minimize model dependence.
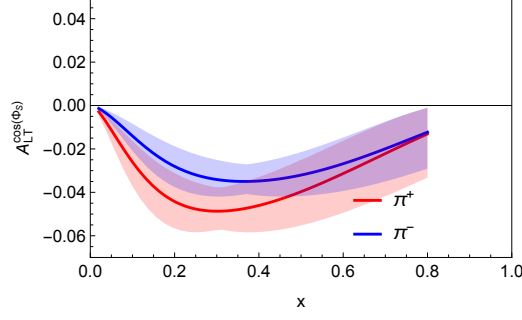
Figure 15. $A_{LT}^{\cos\phi_S}$ as a function of x.
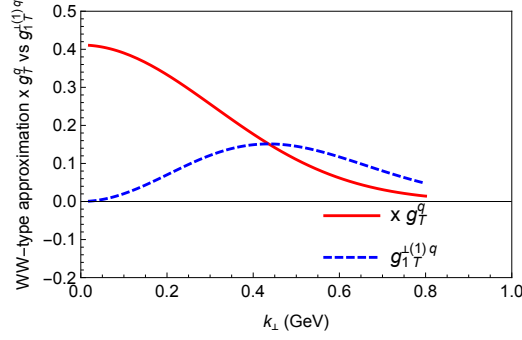
Figure 16. RHS and LHS of Eq. 3.3f.

7.3 Subleading twist $A_{LL}^{\cos\phi_h}$

The structure function $F_{UL}^{\cos\phi_h}$ reads

$$F_{LL}^{\cos\phi_h}(x, z, P_{hT}) = -\frac{2M}{Q}\, x \sum_q e_q^2\, x\, g_L^{\perp(1)q}(x)\, D_1^q(z)\, b_{\mathrm{B}}^{(1)}\left(\frac{zP_{hT}}{\lambda}\right)\mathcal{G}(P_{hT})\,, \quad (7.4\text{a})$$

$$F_{LL}^{\cos\phi_h}(x, z, \langle P_{hT}\rangle) = -\frac{2M}{Q}\, x \sum_q e_q^2\, x\, g_L^{\perp(1)q}(x)\, D_1^q(z)\, c_{\mathrm{B}}^{(1)}\left(\frac{z}{\lambda^{1/2}}\right)\,, \quad (7.4\text{b})$$

where $\lambda = z^2\langle k_\perp^2\rangle_{g_L^\perp} + \langle P_\perp^2\rangle_{D_1}$, $b_{\mathrm{B}}^{(1)} = 2M_N$, $c_{\mathrm{B}}^{(1)} = \sqrt{\pi}\, M_N$, see App. B.3. We approximate the Gaussian width $\langle k_\perp^2\rangle_{g_L^\perp} = \langle k_\perp^2\rangle_{g_1}$ and estimate $g_L^{\perp(1)a}(x)$ according to Eq. (3.3c) as

$$x\, g_L^{\perp(1)a}(x) = \frac{\langle k_\perp^2\rangle_{g_1}}{2\, M_N^2}\, g_1^a(x)\,. \quad (7.5)$$

The asymmetries $A_{LL}^{\cos\phi_S} = F_{LL}^{\cos\phi_S}/F_{UU}$ for COMPASS are plotted in Fig. 17.

We should include a comparison to COMPASS data [107, 109].
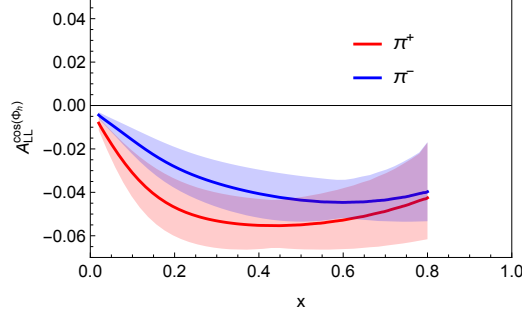
Figure 17. $A_{LL}^{\cos(\phi_h)}$ as a function of x at typical kinematics of COMPASS, $\langle x \rangle = 0.05$, $\langle z \rangle = 0.36$, $\langle Q^2 \rangle = 2.4$ GeV^2.

7.4 Subleading twist $A_{UL}^{\sin\phi_h}$

This twist-3 asymmetry has played a special role, as it was historically the first single spin asymmetry ever measured in SIDIS [117–120]. See also the recent COMPASS data [121]. This asymmetry is sizable despite being twist-3. Although it was subject to numerous phenomenological studies, this asymmetry still remains unexplained.

Retaining the only non-zero term in the WW-type approximation, and assuming for $h_L^q(x, k_\perp)$ a Gaussian Ansatz

$$h_L^q(x, k_\perp^2) = h_L^q(x) \frac{1}{\pi \langle k_\perp^2 \rangle_{h_L}} e^{-k_\perp^2/\langle k_\perp^2 \rangle_{h_L}} , \qquad (7.6)$$

we obtain for the structure function

$$F_{UL}^{\sin\phi_h}(x, z, P_{hT}) = \frac{2M}{Q} x \sum_q e_q^2 \, x \, h_L^q(x) \, H_1^{\perp(1)q}(z) \, b_A^{(1)} \left(\frac{zP_{hT}}{\lambda} \right) \mathcal{G}(P_{hT}) , \quad (7.7a)$$

$$F_{UL}^{\sin\phi_h}(x, z, \langle P_{hT} \rangle) = \frac{2M}{Q} x \sum_q e_q^2 \, x \, h_L^q(x) \, H_1^{\perp(1)q}(z) \, c_A^{(1)} \left(\frac{z}{\lambda^{1/2}} \right) \qquad (7.7b)$$

where $\lambda = z^2 \langle k_\perp^2 \rangle_{h_L} + \langle P_\perp^2 \rangle_{H_1^\perp}$ and $b_A^{(1)} = 2m_h$ and $c_A^{(1)} = \sqrt{\pi} \, m_h$, see App. B.3 for details. We now approximate $\langle k_\perp^2 \rangle_{h_L} = \langle k_\perp^2 \rangle_{h_1}$ and explore (3.3f) to estimate

$$x h_L^q(x) = -2h_{1L}^{\perp(1)q}(x) \qquad (7.8)$$

and finally express $h_{1L}^{\perp(1)q}(x)$ in terms of $h_1^a(x)$ using (3.6b). $h_{1L}^{\perp(1)q}(x)$ is shown in Fig. 10.

The asymmetries $A_{UL}^{\sin\phi_h} = F_{UL}^{\sin\phi_h}/F_{UU}$ as a function of x for COMPASS is plotted in Fig. 18 (a). We also compare our calculations to HERMES data [120] in Fig. 18 (b).
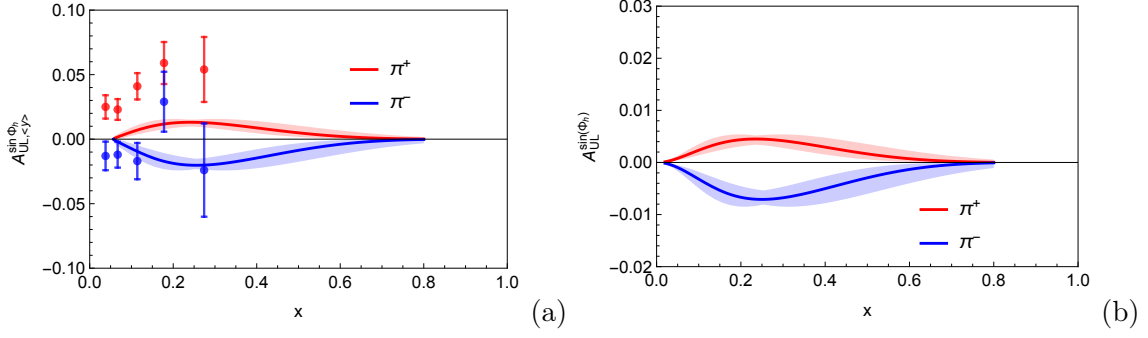
Figure 18. $A_{UL}^{\sin \phi_h}$ as a function of x , comparison to HERMES data [120] (a), and predictions for COMPASS (b).

7.5 Subleading twist $A_{LT}^{\cos(2\phi_h - \phi_S)}$

Retaining the only non-zero term in the WW-type approximation, and assuming for $g_T^{\perp a}(x, k_\perp)$ a Gaussian Ansatz

$$g_T^{\perp q}(x, k_\perp^2) = g_T^{\perp (2)q}(x) \frac{2M^4}{\pi \langle k_\perp^2 \rangle_{g_T^\perp}^3} e^{-k_\perp^2 / \langle k_\perp^2 \rangle_{g_T^\perp}} \,, \tag{7.9}$$

We estimate $\langle k_\perp^2 \rangle_{g_T^\perp} = \langle k_\perp^2 \rangle_{g_1}$ and explore the WW-type approximation (3.3d),

$$x g_T^{\perp (2)q}(x) = \frac{\langle k_\perp^2 \rangle_{g_{1T}^\perp}}{M_N^2} g_{1T}^{\perp (1)q}(x) \,, \tag{7.10}$$

where we finally express $g_{1T}^{\perp (1)q}(x)$ in terms of $g_1^q(x)$ according to Eq. (3.6a).

We obtain for the structure function

$$F_{LT}^{\cos(2\phi_h - \phi_S)}(x, z, P_{hT}) = -\frac{2M}{Q} x \sum_q e_q^2 \, x \, g_T^{\perp (2)q}(x) \, D_1^q(z) \, b_C^{(2)} \left(\frac{z P_{hT}}{\lambda} \right)^2 \mathcal{G}(P_{hT}) \tag{7.11a}$$

$$F_{LT}^{\cos(2\phi_h - \phi_S)}(x, z, \langle P_{hT} \rangle) = -\frac{2M}{Q} x \sum_q e_q^2 \, x \, g_T^{\perp (2)q}(x) \, D_1^q(z) \, c_C^{(2)} \left(\frac{z}{\lambda^{1/2}} \right)^2 \tag{7.11b}$$

where $\lambda = z^2 \langle k_\perp^2 \rangle_{g_T^\perp} + \langle P_\perp^2 \rangle_{D_1}$ and $b_C^{(2)} = c_C^{(2)} = M_N^2$, see App. B.3 for details.

The asymmetry $A_{LT}^{\cos(\phi_h - \phi_S)} = F_{LT}^{\cos(\phi_h - \phi_S)} / F_{UU}$ as a function of x and P_{hT} for COMPASS is plotted in Fig. 19.

We should include a comparison to COMPASS data [107, 109].
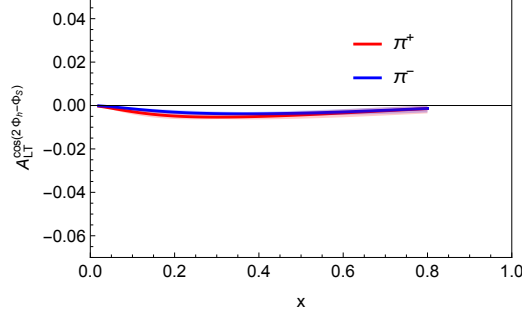
Figure 19. $A_{LT}^{\cos(2\phi_h-\phi_S)}$ as a function of x for COMPASS.

7.6 Subleading twist $A_{UT}^{\sin\phi_S}$

In the structure function $F_{UT}^{\sin\phi_S}$ we encounter 3 interesting new features. This is the first case with more than 1 contribution after applying the WW-type approximation. Assuming Gauss Ansätze for the TMDs $f_T^q(x, k_\perp)$, $h_T^{\perp q}(x, k_\perp)$, $h_T^q(x, k_\perp)$ we obtain

$$F_{UT}^{\sin\phi_S}(x, z, P_{hT}) = \frac{2M}{Q}\, x \sum_q e_q^2 \left[x\, f_T^q(x)\, D_1(z)\, \mathcal{G}(P_{hT}) \right. \tag{7.12a}$$
$$\left. - \tfrac{1}{2}\, x\, \left(h_T^{(1)q}(x) - h_T^{\perp(1)q}(x) \right) H_1^{\perp(1)q}(z)\, \frac{4z^2 m_h\, M_N}{\lambda} \left(1 - \frac{P_{hT}^2}{\lambda} \right) \mathcal{G}(P_{hT}) \right]$$

$$F_{UT}^{\sin\phi_S}(x, z) = \frac{2M}{Q}\, x \sum_q e_q^2\, x\, f_T^q(x)\, D_1(z) \tag{7.12b}$$

with respectively $\lambda = z^2 \langle k_\perp^2 \rangle_{f_T} + \langle P_\perp^2 \rangle_{D_1}$ in the first, and $\lambda = z^2 \langle k_\perp^2 \rangle_{h_T^\perp} + \langle P_\perp^2 \rangle_{H_1^\perp}$ in the second term of Eq. (7.11a) where we assumed $\langle k_\perp^2 \rangle_{h_T^\perp} = \langle k_\perp^2 \rangle_{h_T}$.

The second interesting feature not encountered before is that a contribution drops out upon integrating the structure function over P_{hT}, cf. Eq. (7.11a) vs. (7.11b). This is a property of the weight $\omega_B^{\{2\}}$, see Eq. (2.20) and App. B, which appears also in $F_{LT}^{\cos\phi_S}$, Eq. (2.19f), where it however drops out in WW-type approximation. In principle, this property could help to discriminate experimentally the terms associated with this weight.

Exploring the WW-type approximations (3.3g, 3.3h) the chiral odd twist-3 TMDs can be unambiguously related to transversity

$$- \tfrac{1}{2}\, x \left(h_T^{(1)q}(x) - h_T^{\perp(1)q}(x) \right) = h_1^{(1)q}(x) = \frac{\langle k_\perp^2 \rangle_{h_1}}{2M_N^2}\, h_1^q(x)\,. \tag{7.13a}$$

Now we encounter the third interesting feature, namely the treatment of $f_T^q(x)$ is not unambiguous. We could explore the sum rule (2.14) or employ the WW-type approximation (3.4g) to obtain

$$x\, f_T^q(x) \overset{!?}{=} \begin{cases} 0 & \text{due to sum rule (2.14),} \\ - f_{1T}^{\perp(1)q}(x) & \text{due to WW-type (3.4g),} \end{cases} \tag{7.13b}$$

We recall that the twist-3 TMD $f_T^q(x, k_\perp) \neq 0$ in general, but the collinear T-odd PDF $f_T^q(x) = 0$ due to time reversal, Eq. (2.14). This was discussed in Sec. 3.7.

Notice that in Eq. (7.11a) we really have a choice, because we strictly speaking deal with the convoluted non-zero TMD $f_T^q(x, k_\perp)$, and the Gauss model only *artificially* introduces the collinear function $f_T^q(x)$ expected to be zero. However, in Eq. (7.11b) we have no choice. Here we really deal with the collinear function $f_T^q(x)$ which must vanish due to the sum rule (2.14). How should one proceed?

If we wish to respect the sum rule (2.14), we have to describe $f_T^q(x, k_\perp)$ by a function with a node in $k_\perp$. A simple Gaussian is not adequate for that. But from phenomenological point of view, one of course could work with a superposition of Gaussians[4] with different widths,

$$
x\, f_T^q(x, k_\perp) = -\, f_{1T}^{\perp(1)q}(x)\, \sum_{i=1}^{n} a_i\, \frac{\exp(-k_\perp^2/\langle k_\perp^2\rangle_i)}{\pi \langle k_\perp^2\rangle_i}\,,
$$
$$
\sum_{i=1}^{n} a_i = 0\,,\ \ \langle k_\perp^2\rangle_i \neq \langle k_\perp^2\rangle_j\ \ \forall\, i \neq j,\ 1 \leq i, j \leq n,\ n \geq 2. \quad (7.14)
$$

The minimal choice would be $n = 2$ with $a_1 = -a_2 = 1$ and $\langle k_\perp^2\rangle_1 = \langle k_\perp^2\rangle_{f_1^\perp}$ to make maximal use of the theoretical guidance provided by the WW-type approximation (3.4g). The second Gaussian width $\langle k_\perp^2\rangle_2$ could then be chosen very small $\langle k_\perp^2\rangle_2 \ll \langle k_\perp^2\rangle_{f_1^\perp}$. Within such a Gaussian description we would have a transverse momentum dependence of $f_T^q(x, k_\perp^2)$ similar to that of $f_{1T}^{\perp(1)q}(x, k_\perp^2)$ at not too small $k_\perp$. A very small parameter $\langle k_\perp^2\rangle_2$ could be thought of as a relict, e.g. of gluonic pole contributions in the $\bar{q}gq$-term $\tilde{f}_T^q(x, k_\perp)$. It will be very interesting to follow up on this in future studies.

At this point, however, we have no guidance from phenomenology or theory to fix additional parameters and choose a pragmatic and simple solution, namely to implement the sum rule (2.14) also in Eq. (7.11a). This is a model-dependent choice and this step could be revised along the lines of the above discussion. Our final result is therefore

$$
F_{UT}^{\sin\phi_S}(x, z, P_{hT}) = \frac{2M}{Q}\, x \sum_q e_q^2\, h_1^{(1)q}(x)\, H_1^{\perp(1)q}(z)\, \frac{4z^2 m_h\, M_N}{\lambda} \left(1 - \frac{P_{hT}^2}{\lambda}\right) \mathcal{G}(P_{hT})
$$
$$
F_{UT}^{\sin\phi_S}(x, z) = 0\,. \tag{7.15}
$$

In (7.14) we recover the consistent result for the "collinear" (i.e. related to the weight $\omega^{\{0\}}$) SIDIS structure function $F_{UT}^{\sin\phi_S}(x, z)$ in WW-type approximation, see Eq. (2.21d).

The asymmetries $A_{UT}^{\sin\phi_S} = F_{UT}^{\sin\phi_S}/F_{UU}$ for Jefferson Lab 12 GeV are plotted in Fig. 20. **Compare to HERMES data [122]? Is there by now final data? Will be interesting!**

---

[4] The possibility of TMDs with nodes is not unrealistic. For instance in the covariant parton model the helicity TMDs exhibit nodes for the u and d- flavor [65]. We will have to revise our description of $g_1^q(x, k_\perp)$ in Eq. (5.6) and App. A.2 to something of the type (7.13), if this prediction is confirmed experimentally.

Figure 20. $A_{UT}^{\sin \phi_S}$ as a function of x (left panel), and as a function of P_{hT} (right panel) at typical kinematics of Jefferson Lab 12 GeV, $\langle x \rangle = 0.25$, $\langle z \rangle = 0.54$, $\langle Q^2 \rangle = 2.4$ GeV^2.

7.7 Subleading twist $A_{UU}^{\cos \phi_h}$

Historically this was the first predicted [104] and measured [123] azimuthal asymmetry in (unpolarized) SIDIS, and later explored in [73] to extract information on the Gaussian widths of $f_1^q(x, k_\perp)$ and $D_1^q(x, P_\perp)$ (under the implicit assumption of WW-type approximations).

The structure function $F_{UU}^{\cos \phi_h}$, Eq. (2.19a), contains after the WW-type approximation two contributions. Assuming Gaussian Ansätze for $h^q(x, k_\perp)$ and $f^\perp(x, P_\perp)$ we obtain

$$F_{UU}^{\cos \phi_h}(x, z, P_{hT}) = +\frac{2M}{Q} x \sum_q e_q^2 \left[x\, h^q(x)\, H_1^{\perp(1)q}(z)\, b_{\mathrm{A}}^{(1)} \left(\frac{zP_{hT}}{\lambda} \right) \mathcal{G}(P_{hT}) \right.$$

$$\left. - x\, f^{\perp(1)q}(x)\, D_1^q(z)\, b_{\mathrm{B}}^{(1)} \left(\frac{zP_{hT}}{\lambda} \right) \mathcal{G}(P_{hT}) \right] \quad (7.16a)$$

$$F_{UU}^{\cos \phi_h}(x, z, \langle P_{hT} \rangle) = +\frac{2M}{Q} x \sum_q e_q^2 \left[x\, h^q(x)\, H_1^{\perp(1)q}(z)\, c_{\mathrm{A}}^{(1)} \left(\frac{z}{\lambda^{1/2}} \right) \right.$$

$$\left. - x\, f^{\perp(1)q}(x)\, D_1^q(z)\, c_{\mathrm{B}}^{(1)} \left(\frac{z}{\lambda^{1/2}} \right) \right] \quad (7.16b)$$

with $\lambda = z^2 \langle k_\perp^2 \rangle_h + \langle P_\perp^2 \rangle_{H_1^\perp}$ in the first, and $\lambda = z^2 \langle k_\perp^2 \rangle_{f^\perp} + \langle P_\perp^2 \rangle_{D_1}$ in the second term respectively in (7.15a) and (7.15b). The coefficients $b_i^{(1)}$ and $c_i^{(1)}$ are defined in App. B.3.

The application of the WW-type approximation (3.4h) for $h^q(x)$ is subtle. Applying it literally would imply $x\, h^q(x) = -2\, h_1^{\perp(1)}(x)$ at variance with the sum rule (2.14) for the collinear T-odd twist-3 TMD $h^q(x)$. The situation is analog to the case of $f_T^q(x, k_\perp)$ discussed in Sec. 7.6. Also here one could introduce an additional Gauss parameter and use a double Gaussian to describe $h^q(x, k_\perp)$. One should keep this in mind as an interesting

possibility to be explored in future studies. However, at this point we have no guidance from theory or phenomenology to fix additional parameters. We therefore proceed analogously to Sec. 7.7, and impose (in a model-dependent step) the sum rule (2.14) by setting

$$x\, h_1^q(x) = 0\,. \tag{7.17a}$$

For $f^{\perp(1)}(x)$ we explore Eq. (3.3b) as

$$x\, f^{\perp(1)}(x) = \frac{\langle k_\perp^2 \rangle_{f_1}}{2M_N^2}\, f_1^q(x)\,, \tag{7.17b}$$

and estimate its Gaussian width as $\langle k_\perp^2 \rangle_{f^\perp} = \langle k_\perp^2 \rangle_{f_1}$. The latter means the Gaussian factors of $F_{UU}^{\cos\phi_h}$ and F_{UU} cancel out, i.e. at some point for $P_{hT} \gtrsim 1\,\text{GeV}$ we would obtain from (7.15a) an asymmetry $A_{UU}^{\cos\phi_h} = F_{UU}^{\cos\phi_h}/F_{UU}$ exceeding 100 % and violating unitarity. This is of course an artifact of our approximations, and reminds us that the WW-type approximations as well as the entire TMD formalism must be applied to small $P_{hT} \ll Q$, and in the case of $A_{UU}^{\cos\phi_h}$ preferably for $P_{hT} < 1\,\text{GeV}$, as shown in Fig. 21.
(Alexei: did you notice it [73]? How did you treat it?)

The asymmetries $A_{UU}^{\cos\phi_h}$ for Jefferson Lab 12 GeV are plotted in Fig. 21. **We should compare to EMC, or JLab [86, 124], HERMES and COMPASS [103, 125]. There is probably also newer data!**
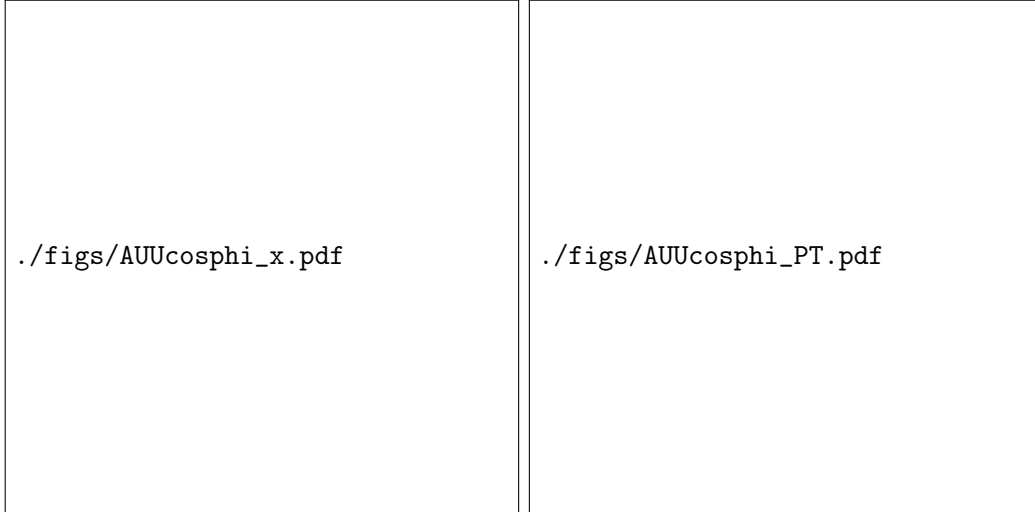
Figure 21. $A_{UU}^{\cos\phi_h}$ as a function of x (left panel), and as a function of P_{hT} (right panel) at typical kinematics of Jefferson Lab 12 GeV, $\langle x \rangle = 0.25$, $\langle z \rangle = 0.54$, $\langle Q^2 \rangle = 2.4\ \text{GeV}^2$.

We may potentially run into positivity issues also for other observables. However, I would suggest not to worry too much. We see in the pictures that the respective asymmetries are smaller than 100 % for reasonably small P_{hT} and can be happy with that! But perhaps we should include a comment somewhere?

7.8 Subleading twist $A_{UT}^{\sin(2\phi_h - \phi_S)}$

In this last asymmetry we encounter the first case with more than 1 contribution in our treatment. Assuming Gauss Ansätze for $f_T^{\perp q}(x, k_\perp)$, $h_T^{\perp q}(x, k_\perp)$, $h_T^q(x, k_\perp)$ we find

$$
F_{UT}^{\sin(2\phi_h - \phi_S)}(x, z, P_{hT}) = \frac{2M}{Q} x \sum_q e_q^2 \left[x\, f_T^{\perp(2)q}(x)\, D_1(z)\, b_{\mathrm{C}}^{(2)} \left(\frac{zP_{hT}}{\lambda} \right)^2 \mathcal{G}(P_{hT}) \right.
$$
$$
\left. + x \left(h_T^{(1)q}(x) + h_T^{\perp(1)q}(x) \right) H_1^{\perp(1)q}(z)\, \frac{b_{\mathrm{AB}}^{(2)}}{2} \left(\frac{zP_{hT}}{\lambda} \right)^2 \mathcal{G}(P_{hT}) \right]
$$
$$(7.18a)$$

$$
F_{UT}^{\sin(2\phi_h - \phi_S)}(x, z, P_{hT}) = \frac{2M}{Q} x \sum_q e_q^2 \left[x\, f_T^{\perp(2)q}(x)\, D_1(z)\, c_{\mathrm{C}}^{(2)} \left(\frac{z}{\lambda^{1/2}} \right)^2 \right.
$$
$$
\left. + x \left(h_T^{(1)q}(x) + h_T^{\perp(1)q}(x) \right) H_1^{\perp(1)q}(z)\, \frac{c_{\mathrm{AB}}^{(2)}}{2} \left(\frac{z}{\lambda^{1/2}} \right)^2 \right]
$$
$$(7.18b)$$

with respectively $\lambda = z^2 \langle k_\perp^2 \rangle_{f_T^\perp} + \langle P_\perp^2 \rangle_{D_1}$ in the first, and $\lambda = z^2 \langle k_\perp^2 \rangle_{h_T^\perp} + \langle P_\perp^2 \rangle_{H_1^\perp}$ in the second terms in Eqs. (7.17a, 7.17b). We use $\langle k_\perp^2 \rangle_{h_T^\perp} = \langle k_\perp^2 \rangle_{h_T}$. The coefficients $b_i^{(2)}$ and $c_i^{(2)}$ are defined in App. B.3. We now explore the WW-type approximations in Eqs. (3.4f, 3.3g, 3.3h) to express the twist-3 TMDs in terms of the Sivers function and pretzelosity as follows

$$
x\, f_T^{\perp(2)q}(x) = f_{1T}^{\perp(2)q}(x) \equiv \frac{\langle k_\perp^2 \rangle_{f_{1T}^\perp}}{M_N^2} f_{1T}^{\perp(1)q}(x), \qquad (7.19a)
$$

$$
-\tfrac{1}{2} x \left(h_T^{(1)q}(x) + h_T^{\perp(1)q}(x) \right) = h_{1T}^{\perp(2)q}(x). \qquad (7.19b)
$$

Figure 22. Azimuthal asymmetry $A_{UU}^{\cos\phi}$ in charged hadron production in SIDIS of $280\,\mathrm{GeV}$ muons off protons as function of z. The data from EMC [123] refer to $\langle Q \rangle = 4.8\,\mathrm{GeV}$. The theoretical curve is the "WW-type and Cahn-effect-only" approximation for this observable in the Gauss model with parameters fixed from HERMES data and neglecting evolution effects. From Ref. [76].

The asymmetries $A_{UT}^{\sin(2\phi_h-\phi_S)} = F_{UT}^{\sin(2\phi_h-\phi_S)}/F_{UU}$ for Jefferson Lab 12 GeV are plotted in Fig. 23.
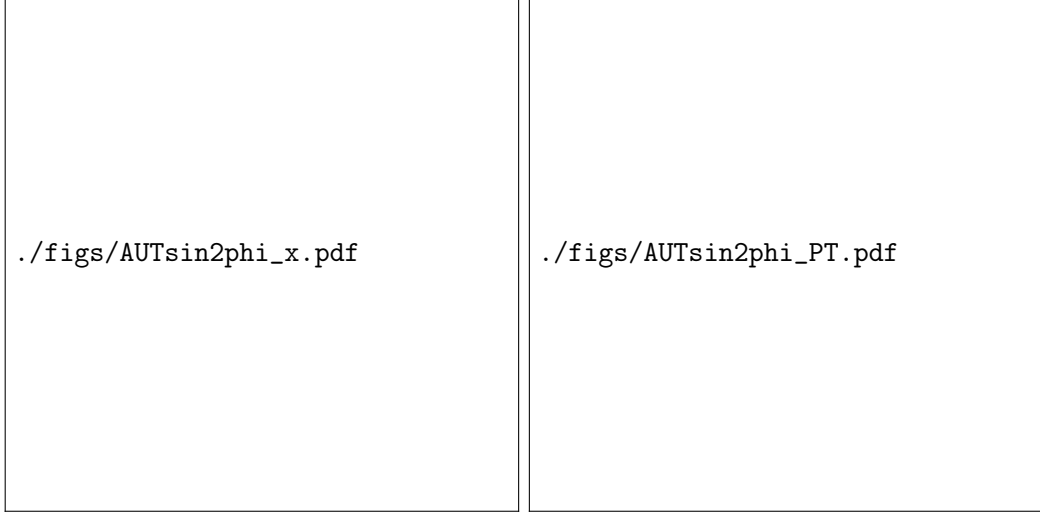
Figure 23. $A_{UT}^{\sin(2\phi_h-\phi_S)}$ as a function of x (left panel), and as a function of P_{hT} (right panel) at typical kinematics of Jefferson Lab 12 GeV, $\langle x \rangle = 0.25$, $\langle z \rangle = 0.54$, $\langle Q^2 \rangle = 2.4$ GeV^2.

8 Conclusions (0 % okay, PS)

The following is just a collections of text fragments cut out from the main text and pasted here in the hope it might be useful.

It is important to remark that the generalized parton model approach of Ref. [116] provides a description, which is largely equivalent to ours.

The results presented in this work are of importance for several reasons. First, to the best of our knowledge it is the first complete study of all SIDIS structure functions up to twist-3 in a unique approach. Second, the results are of use for experiments prepared in the near-term (Jefferson Lab 12) or proposed in the long-term (Electron Ion Collider), and provide helpful input for Montecarlo event generators [26]. Third, our predictions will help to interpret data. The quality of the approximations can only be determined experimentally. It is of importance to establish clear predictions, what we can expect to see in experiments on the basis of the WW approximation. If our predictions will be confirmed, it will mean the WW-type approximations for TMDs work well and call for theoretical explanations why. If our predictions fail, it will mean that certain $\bar{q}gq$-terms are sizable and call for theoretical studies to explain why. In any case, we are going to learn important lessons

In the dedicated study [35] it was shown that the error bars of the present data are compatible with a violation of the WW-approximation for $g_T^a(x)$ up to 40 % in certain regions of x. Rephrased in a more optimistic way, one may interpret the findings of [35] as "the WW approximation works to an accuracy of 40 % or better," and having an approximation with such a quality for TMDs would be very valuable. It would help to interpret first data, and allow us to make predictions for new experiments (JLab 12, EIC) where unknown TMDs contribute.

The aim of the presented study was to review what can be said about the quality of WW-(type-)approximations on the basis of results from theory, models, and phenomenology. In particular, we have presented a complete treatment of SIDIS observables in the WW-type-approximation. This is what we found out.

Bla, bla, bla.

9 Acknowledgments

A The "minimal basis" of TMDs and FFs

This Appendix describes the technical details of the parametrizations used in this work.

A.1 Unpolarised functions $f_1^a(x, k_\perp)$ and $D_1(z, P_\perp)$

In this work we use the leading-order parametrizations from [70] for the unpolarized PDF $f_1^a(x)$ and from [72] for the unpolarized FF $D_1^a(z)$. If not otherwise stated the parametrizations are taken at the scale $Q^2 = 2.4 \, \text{GeV}^2$ typical for many currently available SIDIS data. These parameterizations were used in [73] and other works whose extractions we adopt.

To describe the transverse momentum dependence of $f_1^a(x, k_\perp)$ and $D_1(z, P_\perp)$ we use the Gaussian Ansatz in Eqs. (5.1). All early [73–76] and some recent [77] analyses employed flavor and x- or z-independent widths $\langle k_\perp^2 \rangle$ and $\langle P_\perp^2 \rangle$. In the the analysis [78] of HERMES multiplicities flavor-independence of the widths was assumed. On long run one may anticipate that new precision data will require to relax these assumptions. However, one may also expect that the Gaussian Ansatz will remain a useful *approximation* as long as one is interested in describing data on transverse hadron momenta $P_{hT} \ll Q$.

The parameters resulting from calculations or extractions are presented in Table 1. As most extractions of TMDs that we will use are done with the choice of $\langle k_\perp^2 \rangle_{f_1} = 0.25 \, \text{GeV}^2$, $\langle P_\perp^2 \rangle_{D_1} = 0.2 \, \text{GeV}^2$, for our numerical estimates in this work we will use these fixed widths.

Some comments are in order. In [73] no attempt was made to assign an uncertainty of the best fit result. The uncertainty of the numbers from [76] includes only the statistical error, but no systematic uncertainty. For comparison lattice results from [40] are included whose range indicates flavor-dependence (first number u-flavor, second number d-flavor). Notice that this is the contribution of the flavor averaged over contributions from the respective quarks and antiquarks. Chiral theories predict significant differences in the $k_\perp$-behavior of sea and valence quarks [82]. We will comment more on the lattice results in the next section. In view of the large (and partly underestimated) uncertainties and the fact that those parameters are anti-correlated the numbers from the different approaches quoted in Table 1 can be considered to be in good agreement.

A.2 Helicity distribution $g_1^a(x, k_\perp)$

For the helicity PDF $g_1^a(x) = \int d^2 k_\perp \, g_1^a(x, k_\perp) \equiv \int d^2 k_\perp \, g_{1L}^a(x, k_\perp)$ we use in this work the leading-order parametrizations from [71]. If not otherwise stated the parametrizations are taken at the scale $Q^2 = 2.5 \, \text{GeV}^2$.

In lack of phenomenological information on the $k_\perp$-dependence of $g_1^a(x, k_\perp)$ we explore lattice QCD results from [40] to constrain the Gaussian width in Eq. (5.6). On a lattice with pion and nucleon masses $m_\pi \approx 500 \, \text{MeV}$ and $M_N = 1.291(23) \, \text{GeV}$ and with an axial coupling constant $g_A^{(3)} = 1.209(36)$ reasonably close to its physical value $1.2695(29)$ the following results were obtained for the mean square transverse parton momenta [40]. For the unpolarized TMDs it was found $\langle k_\perp^2 \rangle_{f_1^u} = (0.3741 \, \text{GeV})^2$ and $\langle k_\perp^2 \rangle_{f_1^d} = (0.3839 \, \text{GeV})^2$. For the helicity TMDs it was found $\langle k_\perp^2 \rangle_{g_1^u} = (0.327 \, \text{GeV})^2$ and $\langle k_\perp^2 \rangle_{g_1^d} = (0.385 \, \text{GeV})^2$. These values are quoted in Table 1.

study	$\langle Q^2 \rangle, \langle x \rangle, \langle z \rangle$ [GeV^2]	$\langle k_\perp^2 \rangle_{f_1}$ [GeV^2]	$\langle P_\perp^2 \rangle_{D_1}$ [GeV^2]	$\langle k_\perp^2 \rangle_{g_1}$ [GeV^2]
fit of [73]	5, 0.1, 0.3	~ 0.25	~ 0.2	–
fit of [76]	2.5, 0.1, 0.4	0.38 ± 0.06	0.16 ± 0.01	–
fit of [78]	2.4, 0.1, 0.3	0.57 ± 0.08	0.12 ± 0.01	–
fit of [77]	2.4, 0.1, 0.5	~ 0.3	~ 0.18	–
lattice [40]	4, – , –	0.14–0.15	–	0.11-0.15

Table 1. Gauss model parameters for $f_1^a(x, k_\perp)$, $D_1^a(z, P_\perp)$, $g_1^a(x, k_\perp)$ from phenomenological and lattice QCD studies. The kinematics to which the phenomenological results and the renormalization scale of the lattice results are indicated. The range of lattice values indicates flavor dependence (first number refers to u-flavor, second number to d-flavor).

The lattice values for $\langle k_\perp^2 \rangle_{f_1}$ consistently underestimate the phenomenological numbers, see Table 1. The exact reasons for that are unknown, but it is natural to think it might be related to the fact that the lattice predictions [40] do not refer to TMDs entering in SIDIS (or Drell-Yan or other process) because a different gauge link was chosen, see Sec. 3.5. Still one may expect these results to bear considerable information on QCD dynamics.[5] To make use of this information we shall assume that the lattice results [40] provide robust predictions for the *ratios* $\langle k_\perp^2 \rangle_{g_1^u} / \langle k_\perp^2 \rangle_{f_1^u} \approx 0.76$. With the phenomenological value $\langle k_\perp^2 \rangle_{f_1} = 0.25$ GeV^2 we then obtain the estimate for the width of the helicity TMD $\langle k_\perp^2 \rangle_{g_1} = 0.19$ GeV^2. In our phenomenological study we use this value for u-quarks and for simplicity also for d-quarks. Even though the lattice values indicate an interesting flavor dependence, see Table 1, for a proton target this is a very good approximation due to u-quark dominance. When precision data for deuterium and especially for ^{3}He from Jefferson Lab become available, it will be interesting to re-investigate this point in detail.

A.3   Sivers function $f_{1T}^{\perp q}(x, k_\perp)$

Sivers distribution function was studied in Refs. [93–95, 97, 116, 126–130]. We will use parametrizations from Refs. [93, 97, 116]:

$$\langle k_\perp^2 \rangle_{f_{1T}^\perp} \equiv \frac{\langle k_\perp^2 \rangle M_1^2}{\langle k_\perp^2 \rangle + M_1^2} \tag{A.1}$$

$$f_{1T}^\perp(x, k_\perp^2) = -\frac{M}{M_1} \sqrt{2e} \, \mathcal{N}_q(x) \, f_{q/p}(x, Q) \, \frac{e^{-k_\perp^2 / \langle k_\perp^2 \rangle_{f_{1T}^\perp}}}{\pi \langle k_\perp^2 \rangle}, \tag{A.2}$$

---

[5] The results [40] refer also to pion masses above the physical value. This is caveat is presumably less critical and will be overcome as lattice QCD simulations are becoming feasible at physical pion masses.

$$
\begin{array}{ccc}
N_u = 0.40 & \alpha_u = 0.35 & \beta_u = 2.6 \\
N_d = -0.97 & \alpha_d = 0.44 & \beta_d = 0.90 \\
& M_1^2 = 0.19 (\text{GeV}^2) &
\end{array}
$$

Table 2. Best values of the fit of the Sivers functions. Table from Ref. [97]

where M_1 is a mass parameter, M the proton mass and

$$
\mathcal{N}_q(x) = N_q \, x^\alpha (1-x)^\beta \, \frac{(\alpha + \beta)^{(\alpha+\beta)}}{\alpha^\alpha \beta^\beta} \tag{A.3}
$$

The first moment of Sivers function is:

$$
f_{1T}^{\perp(1)q}(x) = -\frac{\sqrt{\frac{e}{2}} \langle k_\perp^2 \rangle M_1^3}{M(\langle k_\perp^2 \rangle + M_1^2)^2} \, \mathcal{N}_q(x) f_q(x, Q) = -\sqrt{\frac{e}{2}} \frac{1}{MM_1} \frac{\langle k_\perp^2 \rangle_{f_{1T}^\perp}^2}{\langle k_\perp^2 \rangle} \, \mathcal{N}_q(x) f_q(x, Q) \tag{A.4}
$$

We can rewrite parameterizations of Sivers functions as

$$
f_{1T}^{\perp q}(x, k_\perp) = f_{1T}^{\perp(1)q}(x) \frac{2M^2}{\pi \langle k_\perp^2 \rangle_{f_{1T}^\perp}^2} e^{-k_\perp^2 / \langle k_\perp^2 \rangle_{f_{1T}^\perp}} \ . \tag{A.5}
$$

The fit the HERMES proton and COMPASS deuteron data from including only Sivers functions for u and d quarks was done in Ref. [97], corresponding to seven free parameters, and parameters are shown in Table 2.

A.4 Transversity $h_1^q(x, k_\perp)$ and Collins function $H_1^{\perp q}(x, P_\perp)$

These functions were studied in Refs. [37, 38, 98–100, 131]. The following shape was assumed for parametrizations Refs. [37, 38, 98]:

$$
h_1^q(x, k_\perp^2) = h_1^q(x) \frac{e^{-k_\perp^2 / \langle k_\perp^2 \rangle_{h_1}}}{\pi \langle k_\perp^2 \rangle_{h_1}} \ , \tag{A.6}
$$

$$
h_1^q(x) = \frac{1}{2} \mathcal{N}_q^T(x) \left[f_1(x) + g_1(x) \right] \ , \tag{A.7}
$$

$$
H_{1h/q}^\perp(z, P_\perp^2) = \frac{z m_h}{2 P_\perp} \Delta^N D_{h/q^\uparrow}(z, P_\perp^2) = \frac{z m_h}{M_C} e^{-p_\perp^2 / M_C^2} \sqrt{2e} H_{1h/q}^\perp(z) \frac{e^{-P_\perp^2 / \langle P_\perp^2 \rangle}}{\pi \langle P_\perp^2 \rangle} \ , \tag{A.8}
$$

with m_h produced hadron mass and

$$
\mathcal{N}_q^T(x) = N_q^T \, x^\alpha (1-x)^\beta \, \frac{(\alpha + \beta)^{(\alpha+\beta)}}{\alpha^\alpha \beta^\beta} \ , \tag{A.9}
$$

$$
H_{1h/q}^\perp(z) = \mathcal{N}_q^C(z) D_{h/q}(z) \, , \tag{A.10}
$$

$$
\mathcal{N}_q^C(z) = N_q^C \, z^\gamma (1-z)^\delta \, \frac{(\gamma + \delta)^{(\gamma+\delta)}}{\gamma^\gamma \delta^\delta} \, , \tag{A.11}
$$

and $-1 \leq N_q^T \leq 1$, $-1 \leq N_q^C \leq 1$. The helicity distributions $g_1(x)$ are taken from Ref. [132], parton distribution and fragmentation functions are the GRV98LO PDF set [71] and the

DSS fragmentation function set [72]. Notice that with these choices both the transversity and the Collins function automatically obey their proper positivity bounds. Note that as in Ref. [98] we use two Collins fragmentation functions, *favored* and *disfavored* ones, see Ref. [98] for details on implementation, and corresponding parameters N_a^C are then N_{fav}^C and N_{dis}^C. For numerical estimates we use parameters extracted in Ref. [98], see Table 3.

$N_u^T = 0.46^{+0.20}_{-0.14}$	$N_d^T = -1.00^{+1.17}_{-0.00}$
$\alpha = 1.11^{+0.89}_{-0.66}$	$\beta = 3.64^{+5.80}_{-3.37}$
$\langle k_\perp^2 \rangle_{h_1} = 0.25 \ (\text{GeV}^2)$	
$N_{\text{fav}}^C = 0.49^{+0.20}_{-0.18}$	$N_{\text{dis}}^C = -1.00^{+0.38}_{-0.00}$
$\gamma = 1.06^{+0.45}_{-0.32}$	$\delta = 0.07^{+0.42}_{-0.07}$
$M_C^2 = 1.50^{+2.00}_{-1.12} \ (\text{GeV}^2)$	

Table 3. Best values of the 9 free parameters fixing the u and d quark transversity distribution functions and the favored and disfavored Collins fragmentation functions. The table is from Ref. [98].

According to Eq. (B.8) we obtain the following expression for the first moment of Collins fragmentation function:

$$H_{1h/q}^{\perp(1)}(z) = \frac{H_{1h/q}^{\perp}(z)\sqrt{e/2}\langle P_\perp^2 \rangle M_C^3}{z m_h (M_C^2 + \langle P_\perp^2 \rangle)^2} \ . \tag{A.12}$$

We also define the following variable:

$$\langle P_\perp^2 \rangle_{H_1^\perp} = \frac{\langle P_\perp^2 \rangle M_C^2}{\langle P_\perp^2 \rangle + M_C^2}. \tag{A.13}$$

We can rewrite the parameterizations of Collins FF as

$$H_1^\perp(z, P_\perp) = H_1^{\perp(1)}(z)\frac{2z^2 m_h^2}{\pi \langle P_\perp^2 \rangle_{H_1^\perp}^2} e^{-P_\perp^2/\langle P_\perp^2 \rangle_{H_1^\perp}} \ . \tag{A.14}$$

A.5 Boer-Mulders function $h_1^\perp(x, k_\perp)$

The Boer-Mulders function $h_1^\perp$ [2] measures the transverse polarization asymmetry of quarks inside an unpolarized nucleon. The Boer-Mulders functions were studied phenomenologically in Refs. [102, 105, 106]

The following parameterization was used in Refs. [102]:

$$\langle k_\perp^2 \rangle_{h_1^\perp} = \frac{\langle k_\perp^2 \rangle M_{BM}^2}{\langle k_\perp^2 \rangle + M_{BM}^2} \ , \tag{A.15}$$

$$h_1^\perp(x, k_\perp^2) = -\frac{M}{M_{BM}}\sqrt{2e}\,N_q\,f_{q/p}(x, Q)\frac{e^{-k_\perp^2/\langle k_\perp^2 \rangle_{h_1^\perp}}}{\pi \langle k_\perp^2 \rangle} , \tag{A.16}$$

The first moment of Boer-Mulders function is:

$$h_1^{\perp(1)q}(x) = -\frac{\sqrt{\frac{e}{2}}\,\langle k_\perp^2\rangle M_{BM}^3}{M(\langle k_\perp^2\rangle + M_{BM}^2)^2}\,N_q f_q(x,Q) = -\sqrt{\frac{e}{2}}\frac{1}{MM_{BM}}\frac{\langle k_\perp^2\rangle_{h_1^\perp}^2}{\langle k_\perp^2\rangle}\,N_q f_q(x,Q) \qquad (A.17)$$

We can rewrite parameterization of Boer-Mulders functions as

$$h_1^{\perp q}(x,k_\perp) = h_1^{\perp(1)q}(x)\frac{2M^2}{\pi\langle k_\perp^2\rangle_{h_1^\perp}^2}e^{-k_\perp^2/\langle k_\perp^2\rangle_{h_1^\perp}}\ . \qquad (A.18)$$

N_u	$=$	-0.49 ± 0.15	N_d	$= \quad -1\pm0.2$
M_{BM}^2	$=$	0.1 ± 0.2		(GeV^2)

Table 4. Fitted parameters of Boer-Mulders quark distributions. Values are from Ref. [102]

A.6 Pretzelosity distribution $h_{1T}^\perp(x,k_\perp)$

Pretzelosity distribution function $h_{1T}^\perp$ [108] describes transversely polarized quarks inside a transversely polarized nucleon. We use the following form of $h_{1T}^{\perp a}$ [108]:

$$h_{1T}^{\perp a}(x,k_\perp^2) = \frac{M^2}{M_{TT}^2}e^{-k_\perp^2/M_{TT}^2}h_{1T}^{\perp a}(x)\frac{e^{-k_\perp^2/\langle k_\perp^2\rangle}}{\pi\langle k_\perp^2\rangle} = \frac{M^2}{M_T^2}h_{1T}^{\perp a}(x)\frac{e^{-k_\perp^2/\langle k_\perp^2\rangle_{h_{1T}^\perp}}}{\pi\langle k_\perp^2\rangle}\ , \qquad (A.19)$$

where

$$h_{1T}^{\perp a}(x) = e\,\mathcal{N}^a(x)(f_1^a(x,Q) - g_1^a(x,Q)), \qquad (A.20)$$

$$\mathcal{N}^a(x) = N^a x^\alpha(1-x)^\beta\frac{(\alpha+\beta)^{\alpha+\beta}}{\alpha^\alpha\beta^\beta}\ , \qquad (A.21)$$

$$\langle k_\perp^2\rangle_{h_{1T}^\perp} = \frac{\langle k_\perp^2\rangle M_{TT}^2}{\langle k_\perp^2\rangle + M_{TT}^2}\ , \qquad (A.22)$$

where N^a, α, β, and M_T are parameters fitted to data that can be found in Table 5.

We use Eq. (B.8) to calculate the second moment of $h_{1T}^{\perp a}(x,k_\perp^2)$ of Eq. (A.19) and obtain:

$$h_{1T}^{\perp(2)a}(x) = \frac{h_{1T}^{\perp a}(x)\langle k_\perp^2\rangle_{h_{1T}^\perp}^3}{2M^2 M_{TT}^2\langle k_\perp^2\rangle}\ . \qquad (A.23)$$

We can rewrite parametrization of pretzelosity functions as

$$h_{1T}^{\perp q}(x,k_\perp) = h_{1T}^{\perp(2)q}(x)\frac{2M^4}{\pi\langle k_\perp^2\rangle_{h_{1T}^\perp}^3}e^{-k_\perp^2/\langle k_\perp^2\rangle_{h_{1T}^\perp}}\ . \qquad (A.24)$$

α	=	2.5 ± 1.5	β	=	2 fixed
N_u	=	1 ± 1.4	N_d	=	-1 ± 1.3
M_{TT}^2	=	0.18 ± 0.7	(GeV^2)		

Table 5. Fitted parameters of the pretzelosity quark distributions. Table from Ref. [108]

B Convolution integrals and expressions in Gaussian Ansatz

In this Appendix we explain the notation for convolution integrals of TMDs and FFs and give the explicit results obtained assuming the Gaussian Ansatz.

B.1 Notation for convolution integrals

Structure functions are expressed as convolutions of TMDs and FFs in the Bjorken limit at tree level. For reference we quote the convolution integrals in "Amsterdam notation" [4]

$$\mathcal{C}\big[w f D\big] = x \sum_a e_a^2 \int d^2\boldsymbol{p}_T \, d^2\boldsymbol{k}_T \, \delta^{(2)}\big(\boldsymbol{p}_T - \boldsymbol{k}_T - \boldsymbol{P}_{h\perp}/z\big) \, w(\boldsymbol{p}_T, \boldsymbol{k}_T) \, f^a(x, p_T^2) \, D^a(z, z^2 k_T^2),$$
(B.1)

where all transverse momenta refer to the virtual photon-proton center-of-mass frame and $\hat{\boldsymbol{h}} = \boldsymbol{P}_{h\perp}/P_{h\perp}$. Hereby $\boldsymbol{p}_T$ is the transverse momentum of quark with respect to nucleon, $\boldsymbol{k}_T$ is the transverse momentum of the fragmenting quark with respect to produced hadron. The notation is not unique. The one chosen in this work, in comparison to other works, is

$$\text{transverse momentum in TMD:} \quad [\boldsymbol{k}_\perp]_{\text{our}} = [\boldsymbol{k}_\perp]_{\text{Ref.}[116]} = \quad [\boldsymbol{p}_T]_{\text{Ref.}[4]}, \tag{B.2}$$

$$\text{transverse momentum in FF:} \quad [\boldsymbol{P}_\perp]_{\text{our}} = [\boldsymbol{p}_\perp]_{\text{Ref.}[116]} = -z\,[\boldsymbol{k}_T]_{\text{Ref.}[4]}, \tag{B.3}$$

$$\text{transverse hadron momenta:} \quad [\boldsymbol{P}_{hT}]_{\text{our}} = [\boldsymbol{P}_T]_{\text{Ref.}[116]} = \quad [\boldsymbol{P}_{h\perp}]_{\text{Ref.}[4]}. \tag{B.4}$$

Notice that $[\boldsymbol{P}_\perp]_{\text{our}} = -z\,[\boldsymbol{k}_T]_{\text{Ref.}[4]}$ is the transverse momentum the hadron acquires in the fragmentation process. The normalization for unpolarized fragmentation functions is

$$D_1^a(z) = \left[\int d^2\boldsymbol{P}_\perp D_1^a(z, P_\perp^2)\right]_{\text{our}} = \left[z^2 \int d^2\boldsymbol{k}_T D_1^a(z, z^2 k_T^2)\right]_{\text{Ref. }[4]}. \tag{B.5}$$

The "Amsterdam" convolution integral (B.1) reads in our notation

$$\mathcal{C}\big[w f D\big] = x \sum_a e_a^2 \int d^2\boldsymbol{k}_\perp \, d^2\boldsymbol{P}_\perp \, \delta^{(2)}\big(z\boldsymbol{k}_\perp + \boldsymbol{P}_\perp - \boldsymbol{P}_{hT}\big) \, w\left(\boldsymbol{k}_\perp, -\frac{\boldsymbol{P}_\perp}{z}\right) f^a(x, k_\perp^2) \, D^a(z, P_\perp^2). \tag{B.6}$$

B.2 Gaussian Ansatz

For a generic TMD and FF the Gaussian Ansatz is given by

$$f^a(x, k_\perp^2) = f^a(x)\frac{\exp(-k_\perp^2/\langle k_\perp^2\rangle)}{\pi\langle k_\perp^2\rangle}, \quad D^a(z, P_\perp^2) = D^a(z)\frac{\exp(-P_\perp^2/\langle P_\perp^2\rangle)}{\pi\langle P_\perp^2\rangle} \tag{B.7}$$

where $\langle k_\perp^2\rangle$ could be x-dependent, and $\langle P_\perp^2\rangle$ z-dependent. Both could be flavor-dependent. The variable $P_\perp$ is convenient because phenomenological experience shows that $P_\perp$ in

$D_1^{q/h}(z, P_\perp^2)$ exhibits a Gaussian distribution with weakly z-dependent Gaussian width. The distribution of transverse momenta in $\left[D^a(z, z^2 k_T^2)\right]_{\text{Ref.[4]}}$ would require a strongly z-dependent Gaussian width. It is of course a matter of taste which one prefers to use.

It is convenient to work with transverse moments of TMDs and FFs which are defined, and in the Gaussian model given by

$$
\begin{aligned}
f^{(n)}(x) &= \int d^2\boldsymbol{k}_\perp \left(\frac{k_\perp^2}{2M^2}\right)^n f(x, k_\perp^2) \overset{\text{Gauss}}{=} \frac{n!\,\langle k_\perp^2\rangle^n}{2^n\,M_N^{2n}}\, f(x), \\
D^{(n)}(z) &= \int d^2\boldsymbol{P}_\perp \left(\frac{P_\perp^2}{2z^2 m_h^2}\right)^n D(z, P_\perp^2) \overset{\text{Gauss}}{=} \frac{n!\,\langle P_\perp^2\rangle^n}{2^n z^{2n}\, m_h^{2n}} D(z)\,.
\end{aligned}
\tag{B.8}
$$

It is important to keep in mind that these objects are well-defined in the Gaussian model. However, in QCD and even in simple models [54, 82] one faces issues with UV divergences and has to carefully define how to deal with them. Results of Eqs. (B.8) assume that Gaussian dependence is factorized from x or z dependence and parametrizations are made with respect to either $f(x)$ or $D(z)$. As we saw in Appendix A some TMD functions are parametrized with higher moments directly as operator product expansion of TMDs may start from higher twist matrix element instead of the usual twist-2 one. In those cases equivalent formulas to Eqs. (B.8) can be easily derived.

B.3 Convolution integrals in Gauss Ansatz

Solving the convolution integrals relevant for SIDIS in the Gaussian Ansatz yields

$$
\mathcal{C}\left[\omega^{\{0\}} f D\right] = u\,\mathcal{G}(P_{hT})
\tag{B.9a}
$$

$$
\mathcal{C}\left[\omega_{\text{A}}^{\{1\}} f D\right] = u\,\mathcal{G}(P_{hT}) \left(\frac{zP_{hT}}{m_h}\right) \frac{\langle P_\perp^2\rangle}{z^2\lambda}
\tag{B.9b}
$$

$$
\mathcal{C}\left[\omega_{\text{B}}^{\{1\}} f D\right] = -u\,\mathcal{G}(P_{hT}) \left(\frac{zP_{hT}}{M_N}\right) \frac{\langle k_\perp^2\rangle}{\lambda}
\tag{B.9c}
$$

$$
\mathcal{C}\left[\omega_{\text{A}}^{\{2\}} f D\right] = u\,\mathcal{G}(P_{hT}) \frac{\langle k_\perp^2\rangle\langle P_\perp^2\rangle}{\lambda M_N m_h} \left(-1 + \frac{2P_{hT}^2}{\lambda}\right)
\tag{B.9d}
$$

$$
\mathcal{C}\left[\omega_{\text{B}}^{\{2\}} f D\right] = u\,\mathcal{G}(P_{hT}) \frac{\langle k_\perp^2\rangle\langle P_\perp^2\rangle}{\lambda M_N m_h} \left(1 - \frac{P_{hT}^2}{\lambda}\right)
\tag{B.9e}
$$

$$
\mathcal{C}\left[\omega_{\text{AB}}^{\{2\}} f D\right] = u\,\mathcal{G}(P_{hT}) \left(\frac{zP_{hT}}{M_N}\right)\left(\frac{zP_{hT}}{M_h}\right) \frac{\langle k_\perp^2\rangle}{\lambda} \frac{\langle P_\perp^2\rangle}{z^2\lambda}
\tag{B.9f}
$$

$$
\mathcal{C}\left[\omega_{\text{C}}^{\{2\}} f D\right] = \frac{u}{2}\,\mathcal{G}(P_{hT}) \left(\frac{zP_{hT}}{M_N}\right)\left(\frac{zP_{hT}}{M_N}\right) \frac{\langle k_\perp^2\rangle}{\lambda} \frac{\langle k_\perp^2\rangle}{\lambda}
\tag{B.9g}
$$

$$
\mathcal{C}\left[\omega^{\{3\}} f D\right] = \frac{u}{2}\,\mathcal{G}(P_{hT}) \left(\frac{zP_{hT}}{M_N}\right)\left(\frac{zP_{hT}}{M_N}\right)\left(\frac{zP_{hT}}{m_h}\right) \frac{\langle k_\perp^2\rangle}{\lambda} \frac{\langle k_\perp^2\rangle}{\lambda} \frac{\langle P_\perp^2\rangle}{z^2\lambda}
\tag{B.9h}
$$

with the $\omega_i^{\{n\}}$ as defined in Eq. (2.20), and we introduced the abbreviations

$$
u = x \sum_a e_a^2 f^a(x) D^a(z)\,, \quad \mathcal{G}(P_{hT}) = \frac{\exp(-P_{hT}^2/\lambda)}{\pi\lambda}\,, \quad \lambda = z^2\langle k_\perp^2\rangle + \langle P_\perp^2\rangle\,,
\tag{B.10}
$$

with the normalization $\int d^2 P_{hT}\, \mathcal{G}(P_{hT}) = 1$. It is important to keep in mind that strictly speaking $\mathcal{G}(P_{hT}) = \mathcal{G}(P_{hT}, x, z)$ *also* depends on x and z. The "non-compact" notation in Eqs. (B.9) was chosen to display the pattern. The masses M_N or m_h in the denominators of the P_{hT} indicate the "origins" of the contributions: due to intrinsic $k_\perp$ from target, due to transverse momenta $P_\perp$ acquired during fragmentation, or both. The weight $\omega_{\mathrm{B}}^{\{2\}}$ is the only which enters cross sections and does not have a homogeneous scaling in P_{hT}.

For practical application it is convenient to absorb as many (Gauss model) parameters as possible into expressions that can be more easily fitted to data. One way to achieve this is to make use of the transverse moments (B.8). We introduce the following abbreviations

$$u_{\mathrm{A}}^{\{1\}} = x \sum_a e_a^2 f^a(x) D^{(1)a}(z)\,, \qquad u_{\mathrm{B}}^{\{1\}} = x \sum_a e_a^2 f^{(1)a}(x) D^a(z)\,, \tag{B.11}$$

$$u_{\mathrm{AB}}^{\{2\}} = x \sum_a e_a^2 f^{(1)a}(x) D^{(1)a}(z)\,, \qquad u_{\mathrm{C}}^{\{2\}} = x \sum_a e_a^2 f^{(2)a}(x) D^a(z)\,, \tag{B.12}$$

$$u_{\mathrm{C}}^{\{3\}} = x \sum_a e_a^2 f^{(2)a}(x) D^{(1)a}(z)\,. \tag{B.13}$$

In this notation the results in Eqs. (B.9) read

$$\mathcal{C}\big[\omega_{\mathrm{A}}^{\{1\}}\, f\, D\big] = u_{\mathrm{A}}^{(1)}\, \mathcal{G}(P_{hT}) \left(\frac{z P_{hT}}{m_h}\right) \frac{2m_h^2}{\lambda} \tag{B.14a}$$

$$\mathcal{C}\big[\omega_{\mathrm{B}}^{\{1\}}\, f\, D\big] = -u_{\mathrm{B}}^{(1)}\, \mathcal{G}(P_{hT}) \left(\frac{z P_{hT}}{M_N}\right) \frac{2M_N^2}{\lambda} \tag{B.14b}$$

$$\mathcal{C}\big[\omega_{\mathrm{B}}^{\{2\}}\, f\, D\big] = u_{\mathrm{B}}^{(2)}\, \mathcal{G}(P_{hT}) \frac{4z^2 m_h M_N}{\lambda} \left(1 - \frac{P_{hT}^2}{\lambda}\right) \tag{B.14c}$$

$$\mathcal{C}\big[\omega_{\mathrm{AB}}^{\{2\}}\, f\, D\big] = u_{\mathrm{AB}}^{(2)}\, \mathcal{G}(P_{hT}) \left(\frac{z P_{hT}}{M_N}\right) \left(\frac{z P_{hT}}{M_h}\right) \frac{2M_N^2}{\lambda} \frac{2m_h^2}{\lambda} \tag{B.14d}$$

$$\mathcal{C}\big[\omega_{\mathrm{C}}^{\{2\}}\, f\, D\big] = \frac{u_{\mathrm{C}}^{(2)}}{2}\, \mathcal{G}(P_{hT}) \left(\frac{z P_{hT}}{M_N}\right) \left(\frac{z P_{hT}}{M_N}\right) \frac{2M_N^2}{\lambda} \frac{2M_N^2}{\lambda} \tag{B.14e}$$

$$\mathcal{C}\big[\omega^{\{3\}}\, f\, D\big] = \frac{u^{(3)}}{2}\, \mathcal{G}(P_{hT}) \left(\frac{z P_{hT}}{M_N}\right) \left(\frac{z P_{hT}}{M_N}\right) \left(\frac{z P_{hT}}{m_h}\right) \frac{2M_N^2}{\lambda} \frac{2M_N^2}{\lambda} \frac{2m_h^2}{\lambda} \tag{B.14f}$$

In this notation the results in Eqs. (B.9) read

$$\mathcal{C}\big[\omega_i^{\{n\}}\, f\, D\big] = u_i^{(n)}\, \mathcal{G}(P_{hT}) \times \left[\delta_{n2}\, \delta_{i\mathrm{B}}\, a_{\mathrm{B}}^{(2)} + b_i^{(n)} \left(\frac{z P_{hT}}{\lambda}\right)^n\right] \tag{B.15}$$

with

$$b^{(0)} = 1\,, \tag{B.16}$$

$$b_{\mathrm{A}}^{(1)} = 2m_h\,, \qquad\qquad b_{\mathrm{B}}^{(1)} = 2M_N\,, \tag{B.17}$$

$$a_{\mathrm{B}}^{(2)} = 4M_N m_h \lambda^{-1} z^2\,, \quad b_{\mathrm{AB}}^{(2)} = -b_{\mathrm{B}}^{(2)} = 4M_N m_h\,, \quad b_{\mathrm{C}}^{(2)} = M_N^2\,, \tag{B.18}$$

$$b^{(3)} = 2M_N^2 m_h\,. \tag{B.19}$$

Finally, integrating out transverse hadron momenta yields

$$\int d^2 P_{hT}\, \mathcal{C}\big[\omega_i^{\{n\}}\, f\, D\big] = u_i^{(n)}\, c_i^{(n)} \left(\frac{z}{\lambda^{1/2}}\right)^n \tag{B.20}$$

with

$$c^{(0)} = 1 \,, \tag{B.21}$$

$$c^{(1)}_{\mathrm{A}} = \sqrt{\pi}\, m_h \,, \qquad c^{(1)}_{\mathrm{A}} = \sqrt{\pi}\, M_N \,, \tag{B.22}$$

$$c^{(2)}_{\mathrm{AB}} = 4 M_N m_h \,, \qquad c^{(2)}_{\mathrm{C}} = M_N^2 \,, \qquad c^{(2)}_{\mathrm{B}} = 0 \,, \tag{B.23}$$

$$c^{(3)} = \tfrac{3}{2} \sqrt{\pi}\, M_N^2 m_h \,. \tag{B.24}$$

References

[1] P. J. Mulders and R. D. Tangerman, *The complete tree-level result up to order 1/Q for polarized deep-inelastic leptoproduction*, Nucl. Phys. **B461** (1996) 197–237, [hep-ph/9510301].

[2] D. Boer and P. J. Mulders, *Time-reversal odd distribution functions in leptoproduction*, Phys. Rev. **D57** (1998) 5780–5786, [hep-ph/9711485].

[3] K. Goeke, A. Metz and M. Schlegel, *Parameterization of the quark-quark correlator of a spin- 1/2 hadron*, Phys. Lett. **B618** (2005) 90–96, [hep-ph/0504130].

[4] A. Bacchetta et al., *Semi-inclusive deep inelastic scattering at small transverse momentum*, JHEP **02** (2007) 093, [hep-ph/0611265].

[5] S. Arnold, A. Metz and M. Schlegel, *Dilepton production from polarized hadron hadron collisions*, 0809.2262.

[6] A. Metz and A. Vossen, *Parton Fragmentation Functions*, Prog. Part. Nucl. Phys. **91** (2016) 136–202, [1607.02521].

[7] G. A. Miller, *Densities, Parton Distributions, and Measuring the Non-Spherical Shape of the Nucleon*, Phys.Rev. **C76** (2007) 065209, [0708.2297].

[8] M. Burkardt, *Spin-orbit correlations and single-spin asymmetries*, 0709.2966.

[9] M. Burkardt, *The g(2) Structure Function*, AIP Conf.Proc. **1155** (2009) 26–34, [0905.4079].

[10] A. Bacchetta, M. Boglione, A. Henneman and P. J. Mulders, *Bounds on transverse momentum dependent distribution and fragmentation functions*, Phys. Rev. Lett. **85** (2000) 712–715, [hep-ph/9912490].

[11] S. Wandzura and F. Wilczek, *Sum Rules for Spin Dependent Electroproduction: Test of Relativistic Constituent Quarks*, Phys. Lett. **B72** (1977) 195.

[12] R. Jaffe and X.-D. Ji, *Chiral odd parton distributions and Drell-Yan processes*, Nucl.Phys. **B375** (1992) 527–560.

[13] R. Jaffe, *G(2): The Nucleon's Other Spin Dependent Structure Function*, Comments Nucl.Part.Phys. **19** (1990) 239.

[14] J. Balla, M. V. Polyakov and C. Weiss, *Nucleon matrix elements of higher twist operators from the instanton vacuum*, Nucl.Phys. **B510** (1998) 327–364, [hep-ph/9707515].

[15] B. Dressler and M. V. Polyakov, *On the twist - three contribution to h(L) in the instanton vacuum*, Phys.Rev. **D61** (2000) 097501, [hep-ph/9912376].

[16] M. Gockeler, R. Horsley, W. Kurzinger, H. Oelrich, D. Pleiter et al., *A Lattice calculation of the nucleon's spin dependent structure function g(2) revisited*, Phys.Rev. **D63** (2001) 074506, [hep-lat/0011091].

[17] M. Gockeler, R. Horsley, D. Pleiter, P. E. Rakow, A. Schafer et al., *Investigation of the second moment of the nucleon's g(1) and g(2) structure functions in two-flavor lattice QCD*, Phys.Rev. **D72** (2005) 054507, [hep-lat/0506017].

[18] E143 collaboration, K. Abe et al., *Measurements of the proton and deuteron spin structure functions g1 and g2*, Phys. Rev. **D58** (1998) 112003, [hep-ph/9802357].

[19] E155 collaboration, P. L. Anthony et al., *Precision measurement of the proton and deuteron spin structure functions g2 and asymmetries A(2)*, Phys. Lett. **B553** (2003) 18–24, [hep-ex/0204028].

[20] A. M. Kotzinian and P. J. Mulders, *Longitudinal quark polarization in transversely polarized nucleons*, Phys. Rev. **D54** (1996) 1229–1232, [hep-ph/9511420].

[21] A. M. Kotzinian and P. J. Mulders, *Probing transverse quark polarization via azimuthal asymmetries in leptoproduction*, Phys. Lett. **B406** (1997) 373–380, [hep-ph/9701330].

[22] A. Kotzinian, B. Parsamyan and A. Prokudin, *Predictions for double spin asymmetry A(LT) in semi inclusive DIS*, Phys. Rev. **D73** (2006) 114017, [hep-ph/0603194].

[23] H. Avakian et al., *Are there approximate relations among transverse momentum dependent distribution functions?*, Phys. Rev. **D77** (2008) 014023, [0709.3253].

[24] A. Metz, P. Schweitzer and T. Teckentrup, *Lorentz invariance relations between parton distributions and the Wandzura-Wilczek approximation*, Phys. Lett. **B680** (2009) 141–147, [0810.5212].

[25] T. Teckentrup, A. Metz and P. Schweitzer, *Lorentz invariance relations and Wandzura-Wilczek approximation*, Mod.Phys.Lett. **A24** (2009) 2950–2959, [0910.2567].

[26] H. Avakian, H. Matevosyan, B. Pasquini and P. Schweitzer, *Studying the information content of TMDs using Monte Carlo generators*, J. Phys. **G42** (2015) 034015.

[27] J. C. Collins, *Leading-twist single-transverse-spin asymmetries: Drell- Yan and deep-inelastic scattering*, Phys. Lett. **B536** (2002) 43–48, [hep-ph/0204004].

[28] J. P. Ralston and D. E. Soper, *Production of Dimuons from High-Energy Polarized Proton Proton Collisions*, Nucl. Phys. **B152** (1979) 109.

[29] A. Efremov and P. Schweitzer, *The Chirally odd twist 3 distribution e(a)(x)*, JHEP **0308** (2003) 006, [hep-ph/0212044].

[30] R. L. Jaffe, *Spin, twist and hadron structure in deep inelastic processes*, hep-ph/9602236.

[31] R. Tangerman and P. Mulders, *Polarized twist - three distributions g(T) and h(L) and the role of intrinsic transverse momentum*, hep-ph/9408305.

[32] E. V. Shuryak, *The Role of Instantons in Quantum Chromodynamics. 1. Physical Vacuum*, Nucl.Phys. **B203** (1982) 93.

[33] D. Diakonov and V. Y. Petrov, *Instanton Based Vacuum from Feynman Variational Principle*, Nucl.Phys. **B245** (1984) 259.

[34] D. Diakonov, M. V. Polyakov and C. Weiss, *Hadronic matrix elements of gluon operators in the instanton vacuum*, Nucl.Phys. **B461** (1996) 539–580, [hep-ph/9510232].

[35] A. Accardi, A. Bacchetta, W. Melnitchouk and M. Schlegel, *What can break the Wandzura–Wilczek relation?*, *JHEP* **11** (2009) 093, [0907.2942].

[36] A. V. Efremov, K. Goeke and P. Schweitzer, *Collins effect in semi-inclusive deeply inelastic scattering and in e+ e- annihilation*, *Phys. Rev.* **D73** (2006) 094025.

[37] M. Anselmino et al., *Transversity and Collins functions from SIDIS and e+ e- data*, *Phys. Rev.* **D75** (2007) 054032, [hep-ph/0701006].

[38] M. Anselmino et al., *Update on transversity and Collins functions from SIDIS and e+ e- data*, *Nucl. Phys. Proc. Suppl.* **191** (2009) 98–107, [0812.4366].

[39] Y. Koike, K. Tanaka and S. Yoshida, *Drell-Yan double-spin asymmetry A(LT) in polarized p anti-p collisions: Wandzura-Wilczek contribution*, *Phys.Lett.* **B668** (2008) 286–292, [0805.2289].

[40] P. Hagler, B. U. Musch, J. W. Negele and A. Schafer, *Intrinsic quark transverse momentum in the nucleon from lattice QCD*, *Europhys. Lett.* **88** (2009) 61001, [0908.1283].

[41] B. U. Musch, P. Hagler, J. W. Negele and A. Schafer, *Exploring quark transverse momentum distributions with lattice QCD*, *Phys. Rev.* **D83** (2011) 094507, [1011.1213].

[42] B. Yoon, T. Bhattacharya, M. Engelhardt, J. Green, R. Gupta, P. Hägler et al., *Lattice QCD calculations of nucleon transverse momentum-dependent parton distributions using clover and domain wall fermions*, in *Proceedings, 33rd International Symposium on Lattice Field Theory (Lattice 2015): Kobe, Japan, July 14-18, 2015*, SISSA, SISSA, 2015. 1601.05717.

[43] M. Engelhardt, P. Hägler, B. Musch, J. Negele and A. Schäfer, *Lattice QCD study of the Boer-Mulders effect in a pion*, *Phys. Rev.* **D93** (2016) 054501, [1506.07826].

[44] X. Ji, P. Sun, X. Xiong and F. Yuan, *Soft factor subtraction and transverse momentum dependent parton distributions on the lattice*, *Phys. Rev.* **D91** (2015) 074009, [1405.7640].

[45] B. U. Musch, P. Hagler, M. Engelhardt, J. W. Negele and A. Schafer, *Sivers and Boer-Mulders observables from lattice QCD*, *Phys. Rev.* **D85** (2012) 094510, [1111.4249].

[46] M. Engelhardt, *to be published*, .

[47] LHPC collaboration, LHPC et al., *Transverse structure of nucleon parton distributions from lattice QCD*, *Phys. Rev. Lett.* **93** (2004) 112001, [hep-lat/0312014].

[48] LHPC Collaborations collaboration, P. Hagler et al., *Nucleon Generalized Parton Distributions from Full Lattice QCD*, *Phys.Rev.* **D77** (2008) 094502, [0705.4295].

[49] QCDSF collaboration, M. Gockeler et al., *Quark helicity flip generalized parton distributions from two-flavor lattice QCD*, *Phys. Lett.* **B627** (2005) 113–123, [hep-lat/0507001].

[50] M. Burkardt and Y. Koike, *Violation of sum rules for twist three parton distributions in QCD*, *Nucl.Phys.* **B632** (2002) 311–329, [hep-ph/0111343].

[51] S. D. Bass, *Fixed poles, polarized glue and nucleon spin structure*, *Acta Phys.Polon.* **B34** (2003) 5893–5926, [hep-ph/0311174].

[52] M. Stratmann, *Bag model predictions for polarized structure functions and their Q**2 evolutions*, *Z.Phys.* **C60** (1993) 763–772.

[53] A. Signal, *Calculations of higher twist distribution functions in the MIT bag model*, *Nucl.Phys.* **B497** (1997) 415–434, [hep-ph/9610480].

[54] H. Avakian, A. Efremov, P. Schweitzer and F. Yuan, *The transverse momentum dependent distribution functions in the bag model*, *Phys.Rev.* **D81** (2010) 074035, [1001.5467].

[55] R. Jakob, P. Mulders and J. Rodrigues, *Modeling quark distribution and fragmentation functions*, *Nucl.Phys.* **A626** (1997) 937–965, [hep-ph/9704335].

[56] M. Wakamatsu, *Polarized structure functions g(2)(x) in the chiral quark soliton model*, *Phys.Lett.* **B487** (2000) 118–124, [hep-ph/0006212].

[57] B. Pasquini, S. Cazzaniga and S. Boffi, *Transverse momentum dependent parton distributions in a light-cone quark model*, *Phys.Rev.* **D78** (2008) 034025, [0806.2298].

[58] C. Lorce, B. Pasquini and M. Vanderhaeghen, *Unified framework for generalized and transverse-momentum dependent parton distributions within a 3Q light-cone picture of the nucleon*, *JHEP* **1105** (2011) 041, [1102.4704].

[59] R. Kundu and A. Metz, *Higher twist and transverse momentum dependent parton distributions: A Light front Hamiltonian approach*, *Phys.Rev.* **D65** (2002) 014009, [hep-ph/0107073].

[60] M. Schlegel and A. Metz, *On the validity of Lorentz invariance relations between parton distributions*, hep-ph/0406289.

[61] K. Goeke, A. Metz, P. Pobylitsa and M. Polyakov, *Lorentz invariance relations among parton distributions revisited*, *Phys.Lett.* **B567** (2003) 27–30, [hep-ph/0302028].

[62] C. Lorcé, B. Pasquini and P. Schweitzer, *Unpolarized transverse momentum dependent parton distribution functions beyond leading twist in quark models*, *JHEP* **01** (2015) 103, [1411.2550].

[63] C. Lorcé, B. Pasquini and P. Schweitzer, *Transverse pion structure beyond leading twist in constituent models*, *Eur. Phys. J.* **C76** (2016) 415, [1605.00815].

[64] P. Zavada, *The Structure functions and parton momenta distribution in the hadron rest system*, *Phys.Rev.* **D55** (1997) 4290–4299, [hep-ph/9609372].

[65] A. V. Efremov, P. Schweitzer, O. V. Teryaev and P. Zavada, *The relation between TMDs and PDFs in the covariant parton model approach*, *Phys. Rev.* **D83** (2011) 054025, [1012.5296].

[66] A. V. Efremov, P. Schweitzer, O. V. Teryaev and P. Zavada, *Transverse momentum dependent distribution functions in a covariant parton model approach with quark orbital motion*, *Phys. Rev.* **D80** (2009) 014021, [0903.3490].

[67] S. Meissner, A. Metz and K. Goeke, *Relations between generalized and transverse momentum dependent parton distributions*, *Phys.Rev.* **D76** (2007) 034002, [hep-ph/0703176].

[68] A. Mukherjee, *Twist Three Distribution e(x): Sum Rules and Equation of Motion Relations*, *Phys.Lett.* **B687** (2010) 180–183, [0912.1446].

[69] A. Harindranath and W.-M. Zhang, *Examination of Wandzura-Wilczek relation for g2 (x, q**2) in pQCD*, *Phys.Lett.* **B408** (1997) 347–356, [hep-ph/9706419].

[70] A. D. Martin, W. J. Stirling, R. S. Thorne and G. Watt, *Parton distributions for the LHC*, *Eur. Phys. J.* **C63** (2009) 189–285, [0901.0002].

[71] M. Gluck, E. Reya and A. Vogt, *Dynamical parton distributions revisited*, *Eur. Phys. J.* **C5** (1998) 461–470, [hep-ph/9806404].

[72] D. de Florian, R. Sassot and M. Stratmann, *Global analysis of fragmentation functions for pions and kaons and their uncertainties*, Phys. Rev. **D75** (2007) 114010, [hep-ph/0703242].

[73] M. Anselmino et al., *The role of Cahn and Sivers effects in deep inelastic scattering*, Phys. Rev. **D71** (2005) 074006, [hep-ph/0501196].

[74] J. C. Collins et al., *Sivers effect in semi-inclusive deeply inelastic scattering*, Phys. Rev. **D73** (2006) 014021, [hep-ph/0509076].

[75] U. D'Alesio and F. Murgia, *Azimuthal and Single Spin Asymmetries in Hard Scattering Processes*, Prog. Part. Nucl. Phys. 61 **2008** (2008) 394–454, [0712.4328].

[76] P. Schweitzer, T. Teckentrup and A. Metz, *Intrinsic transverse parton momenta in deeply inelastic reactions*, Phys.Rev. **D81** (2010) 094019, [1003.2190].

[77] A. Signori, A. Bacchetta, M. Radici and G. Schnell, *Investigations into the flavor dependence of partonic transverse momentum*, JHEP **11** (2013) 194, [1309.3507].

[78] M. Anselmino, M. Boglione, J. O. Gonzalez Hernandez, S. Melis and A. Prokudin, *Unpolarised Transverse Momentum Dependent Distribution and Fragmentation Functions from SIDIS Multiplicities*, JHEP **04** (2014) 005, [1312.6261].

[79] A. Bacchetta, D. Boer, M. Diehl and P. J. Mulders, *Matches and mismatches in the descriptions of semi- inclusive processes at low and high transverse momentum*, JHEP **08** (2008) 023, [0803.0227].

[80] S. M. Aybat and T. C. Rogers, *TMD Parton Distribution and Fragmentation Functions with QCD Evolution*, Phys.Rev. **D83** (2011) 114042, [1101.5057].

[81] F. Landry, R. Brock, P. M. Nadolsky and C. Yuan, *Tevatron Run-1 Z boson data and Collins-Soper-Sterman resummation formalism*, Phys.Rev. **D67** (2003) 073016, [hep-ph/0212159].

[82] P. Schweitzer, M. Strikman and C. Weiss, *Intrinsic transverse momentum and parton correlations from dynamical chiral symmetry breaking*, JHEP **01** (2013) 163, [1210.1267].

[83] J. Collins, L. Gamberg, A. Prokudin, T. C. Rogers, N. Sato and B. Wang, *Relating Transverse Momentum Dependent and Collinear Factorization Theorems in a Generalized Formalism*, Phys. Rev. **D94** (2016) 034014, [1605.00671].

[84] HERMES collaboration, A. Airapetian et al., *Multiplicities of charged pions and kaons from semi-inclusive deep-inelastic scattering by the proton and the deuteron*, Phys. Rev. **D87** (2013) 074029, [1212.5407].

[85] COMPASS collaboration, M. Aghasyan et al., *Transverse-momentum-dependent Multiplicities of Charged Hadrons in Muon-Deuteron Deep Inelastic Scattering*, 1709.07374.

[86] CLAS COLLABORATION collaboration, M. Osipenko et al., *Measurement of unpolarized semi-inclusive pi+ electroproduction off the proton*, Phys.Rev. **D80** (2009) 032004, [0809.1153].

[87] CLAS collaboration, H. Avakian et al., *Measurement of Single and Double Spin Asymmetries in Deep Inelastic Pion Electroproduction with a Longitudinally Polarized Target*, Phys. Rev. Lett. **105** (2010) 262002, [1003.4549].

[88] D. W. Sivers, *Single spin production asymmetries from the hard scattering of point - like constituents*, Phys. Rev. **D41** (1990) 83.

[89] M. Anselmino, M. Boglione, U. D'Alesio, S. Melis, F. Murgia and A. Prokudin, *New insight on the Sivers transverse momentum dependent distribution function*, J. Phys. Conf. Ser. **295** (2011) 012062, [1012.3565].

[90] M. Anselmino et al., *Extracting the sivers function from polarized sidis data and making predictions*, Phys. Rev. **D72** (2005) 094007, [hep-ph/0507181].

[91] M. Anselmino et al., *Comparing extractions of Sivers functions*, hep-ph/0511017.

[92] W. Vogelsang and F. Yuan, *Single-transverse spin asymmetries: From dis to hadronic collisions*, Phys. Rev. **D72** (2005) 054028.

[93] M. Anselmino et al., *Sivers Effect for Pion and Kaon Production in Semi- Inclusive Deep Inelastic Scattering*, Eur. Phys. J. **A39** (2009) 89–100, [0805.2677].

[94] A. Bacchetta and M. Radici, *Constraining quark angular momentum through semi-inclusive measurements*, Phys. Rev. Lett. **107** (2011) 212001, [1107.5755].

[95] M. G. Echevarria, A. Idilbi, Z.-B. Kang and I. Vitev, *QCD Evolution of the Sivers Asymmetry*, Phys. Rev. **D89** (2014) 074013, [1401.5078].

[96] HERMES collaboration, A. Airapetian et al., *Observation of the Naive-T-odd Sivers Effect in Deep-Inelastic Scattering*, Phys. Rev. Lett. **103** (2009) 152002, [0906.3918].

[97] M. Anselmino, M. Boglione, U. D'Alesio, S. Melis, F. Murgia and A. Prokudin, *Sivers Distribution Functions and the Latest SIDIS Data*, in *19th International Workshop on Deep-Inelastic Scattering and Related Subjects (DIS 2011) Newport News, Virginia, April 11-15, 2011*, 2011. 1107.4446.

[98] M. Anselmino, M. Boglione, U. D'Alesio, S. Melis, F. Murgia and A. Prokudin, *Simultaneous extraction of transversity and Collins functions from new SIDIS and e+e-data*, Phys. Rev. **D87** (2013) 094019, [1303.3822].

[99] Z.-B. Kang, A. Prokudin, P. Sun and F. Yuan, *Nucleon tensor charge from Collins azimuthal asymmetry measurements*, Phys. Rev. **D91** (2015) 071501, [1410.4877].

[100] M. Anselmino, M. Boglione, U. D'Alesio, J. O. Gonzalez Hernandez, S. Melis, F. Murgia et al., *Collins functions for pions from SIDIS and new e^+e^- data: a first glance at their transverse momentum dependence*, Phys. Rev. **D92** (2015) 114023, [1510.05389].

[101] HERMES collaboration, A. Airapetian et al., *Effects of transversity in deep-inelastic scattering by polarized protons*, Phys. Lett. **B693** (2010) 11–16, [1006.4221].

[102] V. Barone, M. Boglione, J. O. Gonzalez Hernandez and S. Melis, *Phenomenological analysis of azimuthal asymmetries in unpolarized semi-inclusive deep inelastic scattering*, Phys. Rev. **D91** (2015) 074019, [1502.04214].

[103] HERMES COLLABORATION collaboration, F. Giordano and R. Lamb, *Measurement of azimuthal asymmetries of the unpolarized cross section at HERMES*, AIP Conf.Proc. **1149** (2009) 423–426, [0901.2438].

[104] R. N. Cahn, *Azimuthal Dependence in Leptoproduction: A Simple Parton Model Calculation*, Phys.Lett. **B78** (1978) 269.

[105] V. Barone, S. Melis and A. Prokudin, *The Boer-Mulders effect in unpolarized SIDIS: An Analysis of the COMPASS and HERMES data on the cos 2 phi asymmetry*, Phys. Rev. **D81** (2010) 114026, [0912.5194].

[106] V. Barone, S. Melis and A. Prokudin, *Azimuthal asymmetries in unpolarized Drell-Yan processes and the Boer-Mulders distributions of antiquarks*, *Phys. Rev.* **D82** (2010) 114025, [1009.3423].

[107] B. Parsamyan, *Transverse spin dependent azimuthal asymmetries at COMPASS*, *J.Phys.Conf.Ser.* **295** (2011) 012046, [1012.0155].

[108] C. Lefky and A. Prokudin, *Extraction of the distribution function $h_{1T}^{\perp}$ from experimental data*, *Phys. Rev.* **D91** (2015) 034010, [1411.0580].

[109] COMPASS COLLABORATION collaboration, A. Kotzinian, *Beyond Collins and Sivers: Further measurements of the target transverse spin-dependent azimuthal asymmetries in semi-inclusive DIS from COMPASS*, 0705.2402.

[110] CLAS Collaboration collaboration, H. Avakian et al., *Measurement of beam-spin asymmetries for pi + electroproduction above the baryon resonance region*, *Phys.Rev.* **D69** (2004) 112004, [hep-ex/0301005].

[111] HERMES Collaboration collaboration, A. Airapetian et al., *Beam-Spin Asymmetries in the Azimuthal Distribution of Pion Electroproduction*, *Phys.Lett.* **B648** (2007) 164–170, [hep-ex/0612059].

[112] W. Gohn, H. Avakian, K. Joo and M. Ungaro, *Beam spin asymmetries from semi-inclusive pion electroproduction in deep inelastic scattering*, *AIP Conf.Proc.* **1149** (2009) 461–464.

[113] M. Aghasyan, H. Avakian, P. Rossi, E. De Sanctis, D. Hasch et al., *Precise Measurements of Beam Spin Asymmetries in Semi-Inclusive π^0 production*, *Phys.Lett.* **B704** (2011) 397–402, [1106.2293].

[114] COMPASS collaboration, C. Adolph et al., *Measurement of azimuthal hadron asymmetries in semi-inclusive deep inelastic scattering off unpolarised nucleons*, *Nucl. Phys.* **B886** (2014) 1046–1077, [1401.6284].

[115] CLAS collaboration, W. Gohn et al., *Beam-spin asymmetries from semi-inclusive pion electroproduction*, *Phys. Rev.* **D89** (2014) 072011, [1402.4097].

[116] M. Anselmino, M. Boglione, U. D'Alesio, S. Melis, F. Murgia et al., *General Helicity Formalism for Polarized Semi-Inclusive Deep Inelastic Scattering*, *Phys.Rev.* **D83** (2011) 114019, [1101.1011].

[117] HERMES Collaboration collaboration, A. Airapetian et al., *Observation of a single spin azimuthal asymmetry in semiinclusive pion electro production*, *Phys.Rev.Lett.* **84** (2000) 4047–4051, [hep-ex/9910062].

[118] HERMES Collaboration collaboration, A. Airapetian et al., *Single spin azimuthal asymmetries in electroproduction of neutral pions in semiinclusive deep inelastic scattering*, *Phys.Rev.* **D64** (2001) 097101, [hep-ex/0104005].

[119] HERMES Collaboration collaboration, A. Airapetian et al., *Measurement of single spin azimuthal asymmetries in semiinclusive electroproduction of pions and kaons on a longitudinally polarized deuterium target*, *Phys.Lett.* **B562** (2003) 182–192, [hep-ex/0212039].

[120] HERMES Collaboration collaboration, A. Airapetian et al., *Subleading-twist effects in single-spin asymmetries in semi-inclusive deep-inelastic scattering on a longitudinally polarized hydrogen target*, *Phys.Lett.* **B622** (2005) 14–22, [hep-ex/0505042].

[121] M. Alekseev, V. Y. Alexakhin, Y. Alexandrov, G. Alexeev, A. Amoroso et al., *Azimuthal asymmetries of charged hadrons produced by high-energy muons scattered off longitudinally polarised deuterons*, Eur.Phys.J. **C70** (2010) 39–49, [1007.1562].

[122] HERMES COLLABORATION collaboration, G. Schnell, *The Sivers and other semi-inclusive single-spin asymmetries at HERMES*, PoS **DIS2010** (2010) 247.

[123] EUROPEAN MUON COLLABORATION collaboration, J. Aubert et al., *MEASUREMENT OF HADRONIC AZIMUTHAL DISTRIBUTIONS IN DEEP INELASTIC MUON PROTON SCATTERING*, Phys.Lett. **B130** (1983) 118.

[124] H. Mkrtchyan, P. Bosted, G. Adams, A. Ahmidouch, T. Angelescu et al., *Transverse momentum dependence of semi-inclusive pion production*, Phys.Lett. **B665** (2008) 20–25, [0709.3020].

[125] COMPASS COLLABORATION collaboration, R. Joosten, *Unpolarized azimuthal asymmetries from the COMPASS experiment at CERN*, AIP Conf.Proc. **1182** (2009) 585–588.

[126] A. V. Efremov, K. Goeke, S. Menzel, A. Metz and P. Schweitzer, *Sivers effect in semi-inclusive DIS and in the Drell-Yan process*, Phys. Lett. **B612** (2005) 233–244, [hep-ph/0412353].

[127] S. M. Aybat, J. C. Collins, J.-W. Qiu and T. C. Rogers, *The QCD Evolution of the Sivers Function*, Phys. Rev. **D85** (2012) 034043, [1110.6428].

[128] L. Gamberg, Z.-B. Kang and A. Prokudin, *Indication on the process-dependence of the Sivers effect*, Phys. Rev. Lett. **110** (2013) 232301, [1302.3218].

[129] M. Anselmino, M. Boglione and S. Melis, *A Strategy towards the extraction of the Sivers function with TMD evolution*, Phys. Rev. **D86** (2012) 014028, [1204.1239].

[130] P. Sun and F. Yuan, *Energy Evolution for the Sivers Asymmetries in Hard Processes*, Phys. Rev. **D88** (2013) 034016, [1304.5037].

[131] Z.-B. Kang, A. Prokudin, P. Sun and F. Yuan, *Extraction of Quark Transversity Distribution and Collins Fragmentation Functions with QCD Evolution*, Phys. Rev. **D93** (2016) 014009, [1505.05589].

[132] M. Gluck, E. Reya, M. Stratmann and W. Vogelsang, *Models for the polarized parton distributions of the nucleon*, Phys. Rev. **D63** (2001) 094005, [hep-ph/0011215].

Remarks & Corrections in version 00r (PS)

- I reshuffled some subsections with good intentions. Please, see whether you like it.
  AP good for me

- Introduced a new procedure: first assume Gauss Ansatz, then evaluate convolution integrals, finally use WW. This gives **different** results from Saman & Alexei.
  Advantages:
  1. The results can be written in a compact way.
  2. There is less model dependence due to the simpler expressions.
  3. In the new expressions it is more natural to incorporate the sum rules (2.14) for T-odd twist-3 functions. AP good for me, we need to expand a little on differences with the previous version.

- The numerical results are obtained with DSS'07 and GRV'00 and GRSV'98. DSS is 10 years old. GRSV is from last millennium. I agree that DSS is acceptable (if we do not touch kaons). However, we should use a more modern input for $f_1^q(x)$ and $g_1^q(x)$ (even though I know and understand that it does not matter). AP good for me, I implemented MRSTW instead.

- I introduced \begin{subequations} … \end{subequations}. Notice that it comes before equations arrays start and after they end, and it can contain text in-between.
  AP good for me

- notation: in all(?) formulas {\bf …} changed to {\bm …}
  $\boldsymbol{\xi}_T$ changed to $\boldsymbol{\xi}_\perp$ in Eqs. (2.11, 2.15) (Fourier variables of $\boldsymbol{k}_\perp$, $\boldsymbol{p}_\perp$)
  In Eq. (2.15) the integration is over ξ^+ (not ξ^-), and $(-\infty) \to (+\infty)$. AP good for me

- more serious: in Eq. (2.15) replacement $\boldsymbol{p}_\perp = \boldsymbol{P}_\perp$ was wrong. Correct: $\boldsymbol{p}_\perp = -\boldsymbol{P}_\perp/z$.
  Because of that we have corrections $P_\perp^k \to -P_\perp^k/z$ in (2.16b, 2.16d, 2.16e, 3.7d).
  Luckily no influence on numerical results. Please, double check (2.16a-2.16e)! AP have no time, anybody?

- in several places correction $D_q^h(z) \to D_1^q(z)$,
  correction $H^\perp(z, P_\perp^2) \to H(z, P_\perp^2)$ in (3.7d) AP good for me

- after Eq. (2.12i) changed $\epsilon_T^{ij} \equiv \epsilon^{-+ij}$ to $\epsilon^{ij} \equiv \epsilon^{-+ij}$ (we use throughout ϵ^{ij}) AP good for me

- corrected sign of term with $f_T^\perp$ in (2.12f). Should be negative. Compare to [4]. AP good for me, thank you

- corrected sign typos in Eq. (2.19e) (term with $\tilde{D}^\perp$) and Eq. (2.19h) (term with $\tilde{G}^\perp$) Both drop out in WW, so no consequence. AP good for me

- the figure names
  `ALLcosPhi_x.pdf,` `ALLcosPhi_PT.pdf,`
  `ALTcos2Phi_x.pdf,` `ALTcos2Phi_PT.pdf,`
  `AULsinPhi_x.pdf,` `AULsinPhi_PT.pdf`
  were spelled incorrectly (in latex source: `Phi`. Name of file `phi`).
  Fixed in latex file, names of figures are unchanged. AP good for me

- We should not show predictions for JLab 12, but compare to available data. Often we will have huge error bars. Then we can say that JLab 12 will resolve the situation. AP good for me, I change that

- Often we write M or M_N and mean the nucleon mass. I would prefer M_N but writing M everywhere would be less work. We write sometimes $H^\perp(z, P_\perp^2)$ and sometimes $H^\perp(z, P_\perp)$, etc. We have to agree on a common notation. I propose without square. AP good for me, I prefer $H^\perp(z, P_\perp^2)$